

AD-A145 419

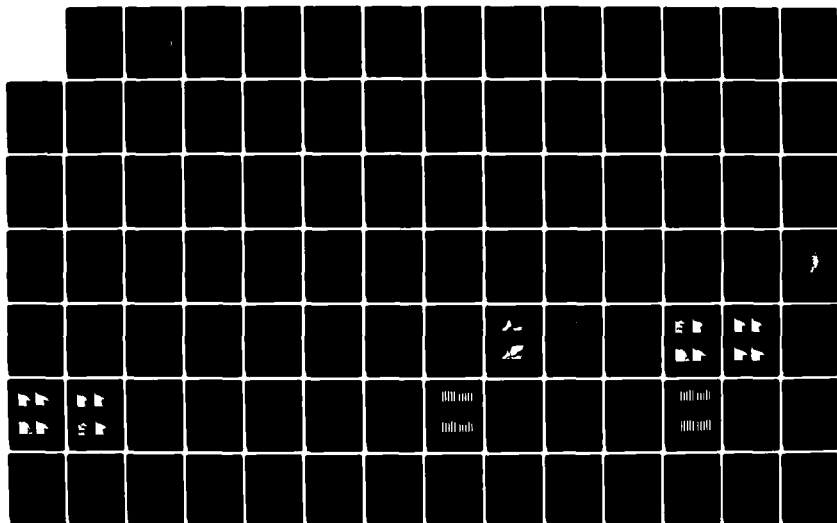
MULTISPECTRAL PASSIVE MICROWAVE CORRELATIONS WITH AN
ANTECEDENT PRECIPITA..(U) AIR FORCE INST OF TECH
WRIGHT-PATTERSON AFB OH G D WILKE AUG 84
AFIT/C1/NR-84-61T F/G 14/2

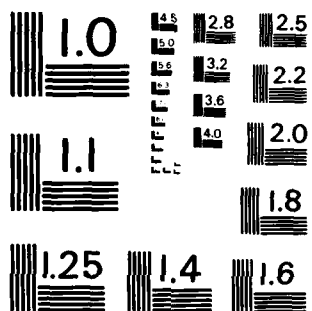
1/2

UNCLASSIFIED

F/G 14/2

N1





MICROCOPY RESOLUTION TEST CHART
NATIONAL BUREAU OF STANDARDS-1963-A

UNCLASS

SECURITY CLASSIFICATION OF THIS PAGE (When Data Entered)

REPORT DOCUMENTATION PAGE		READ INSTRUCTIONS BEFORE COMPLETING FORM
1. REPORT NUMBER AFIT/CI/NR 84-61T	2. GOVT ACCESSION NO.	3. RECIPIENT'S CATALOG NUMBER
4. TITLE (and Subtitle) Multispectral Passive Microwave Correlations With An Antecedent Precipitation Index Using The Nimbus 7 SMMR		5. TYPE OF REPORT & PERIOD COVERED THESIS/DISSERTATION
7. AUTHOR(s) Gregory Delfin Wilke		6. PERFORMING ORG. REPORT NUMBER
9. PERFORMING ORGANIZATION NAME AND ADDRESS AFIT STUDENT AT: Texas A&M University		8. CONTRACT OR GRANT NUMBER(s)
11. CONTROLLING OFFICE NAME AND ADDRESS AFIT/NR WPAFB OH 45433		10. PROGRAM ELEMENT, PROJECT, TASK AREA & WORK UNIT NUMBERS
14. MONITORING AGENCY NAME & ADDRESS (if different from Controlling Office)		12. REPORT DATE Aug 1984
		13. NUMBER OF PAGES 126
		15. SECURITY CLASS. (of this report) UNCLASS
		15a. DECLASSIFICATION DOWNGRADING SCHEDULE

AD-A145 419

UTION STATEMENT (of this Report)

) FOR PUBLIC RELEASE; DISTRIBUTION UNLIMITED

UTION STATEMENT (of the abstract entered in Block 20, if different from Report)

DTIC
ELECTE
SEP 13 1984

B

EMENTARY NOTES

D FOR PUBLIC RELEASE: IAW AFR 190-17

Lyn E. Wolaver
LYNN E. WOLAVER
Dean for Research and
Professional Development
AFIT, Wright-Patterson AFB OH

19. KEY WORDS (Continue on reverse side if necessary and identify by block number)

20. ABSTRACT (Continue on reverse side if necessary and identify by block number)

ATTACHED

DTIC FILE COPY

DD FORM 1473
1 JAN 73

EDITION OF 1 NOV 65 IS OBSOLETE

UNCLASS

84 09 13 025

SECURITY CLASSIFICATION OF THIS PAGE (When Data Entered)

ABSTRACT

Multispectral Passive Microwave Correlations with an Antecedent
Precipitation Index using the Nimbus 7 SMMR. (August 1984)

Gregory Delfin Wilke, B.G.S., University of Nebraska Omaha

M.S., University of Nebraska Omaha

Chairman of Advisory Committee: John F. Griffiths

Analysis of the passive microwave brightness temperatures from the Scanning Multichannel Microwave Radiometer (SMMR) aboard Nimbus 7 can infer soil moisture through an Antecedent Precipitation Index (API). This investigation involves correlation analysis between five passive microwave brightness temperature wavelengths (0.81, 1.36, 1.66, 2.80, and 4.54 cm) in two polarizations spanning a one year period. Data analysis was done by a temporal and areal approach, for both the normalized brightness temperatures and the differences in the polarized channels, for all five SMMR wavelengths. Three transformations of the polarized brightness temperatures were used to evaluate the ability of the microwave data to infer soil moisture through correlations with the API. These transformations included the horizontally polarized normalized brightness temperature, the difference between the polarized channels, and the normalized difference between the polarized channels. It was evident that all three indices had very high correlations with API, however the correlation coefficient for the normalized brightness temperature data consistently

202

→ was slightly higher than the values for the other two indices. The conclusion is that polarized data can infer soil moisture through the API without the use of surface data.

Accession For	
NTIS GRA&I	<input checked="" type="checkbox"/>
DTIC TAB	<input type="checkbox"/>
Unannounced	<input type="checkbox"/>
Justification	
By	
Distribution/	
Availability Codes	
Dist	Avail and/or Special
A-1	



AFIT RESEARCH ASSESSMENT

The purpose of this questionnaire is to ascertain the value and/or contribution of research accomplished by students or faculty of the Air Force Institute of Technology (AU). It would be greatly appreciated if you would complete the following questionnaire and return it to:

AFIT/NR
Wright-Patterson AFB OH 45433

RESEARCH TITLE: Multispectral Passive Microwave Correlations With An Antecedent
Precipitation Index Using The Nimbus 7 SMMR

AUTHOR: Gregory Delfin Wilke

RESEARCH ASSESSMENT QUESTIONS:

1. Did this research contribute to a current Air Force project?

☐ a. YES

☐ b. NO

2. Do you believe this research topic is significant enough that it would have been researched (or contracted) by your organization or another agency if AFIT had not?

☐ a. YES

☐ b. NO

3. The benefits of AFIT research can often be expressed by the equivalent value that your agency achieved/received by virtue of AFIT performing the research. Can you estimate what this research would have cost if it had been accomplished under contract or if it had been done in-house in terms of manpower and/or dollars?

☐ a. MAN-YEARS _____

☐ b. \$ _____

4. Often it is not possible to attach equivalent dollar values to research, although the results of the research may, in fact, be important. Whether or not you were able to establish an equivalent value for this research (3. above), what is your estimate of its significance?

☐ a. HIGHLY
SIGNIFICANT

☐ b. SIGNIFICANT

☐ c. SLIGHTLY
SIGNIFICANT

☐ d. OF NO
SIGNIFICANCE

5. AFIT welcomes any further comments you may have on the above questions, or any additional details concerning the current application, future potential, or other value of this research. Please use the bottom part of this questionnaire for your statement(s).

NAME _____

GRADE _____

POSITION _____

ORGANIZATION _____

LOCATION _____

STATEMENT(s): _____

MULTISPECTRAL PASSIVE MICROWAVE CORRELATIONS WITH AN
ANTECEDENT PRECIPITATION INDEX USING THE NIMBUS 7 SMMR

A THESIS

by

GREGORY DELFIN WILKE

Submitted to the Graduate College of
Texas A&M University
in partial fulfillment of the requirements for the degree of
MASTER OF SCIENCE

August 1984

Major Subject: Meteorology

84 . 09 13 025

MULTISPECTRAL PASSIVE MICROWAVE CORRELATIONS WITH AN
ANTECEDENT PRECIPITATION INDEX USING THE NIMBUS 7 SMMR


A Thesis


by

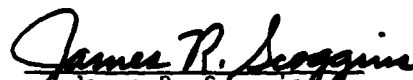
GREGORY DELFIN WILKE

Approved as to style and content by:


John F. Griffiths
(Chairman of Committee)


George L. Huebner, Jr.
(Member)


Marshall J. McFarland
(Member)


James R. Scoggins
(Head of Department)

August 1984

ACKNOWLEDGEMENTS

I wish to express my appreciation and gratitude to Prof. John F. Griffiths, the chairman of my advisory committee. His advice and encouragement were warmly received at crucial points in the research. I am also deeply indebted to the other members of my advisory committee, Dr. Marshall Joe McFarland, who directed the research, and Dr. George L. Huebner, who provided technical expertise.

I would like to thank the staff members of the Remote Sensing Center, Texas A&M University, for both their technical advice and administrative assistance. Dr. Richard W. Newton provided an office and an excellent work environment. Billy V. Clark provided considerable help and advice on the VAX computer system, Diana Thomas spent numerous hours preparing this manuscript, and Rose Kress provided advice and editorial comments. Dr. Paul H. Harder deserves my sincere appreciation for his extensive assistance in computer programming and technical advice involving this research.

This research was partially funded by the NASA Johnson Space Center by Grant no. NAS9-16822.

Finally, my greatest appreciation and deepest thanks belong to my wife, Nancy. Her support and encouragement through 12 years of marriage provided the driving force needed to finally achieve this goal. The completion of this manuscript is as much her accomplishment as it is mine.

TABLE OF CONTENTS

	Page
ABSTRACT	iii
ACKNOWLEDGEMENTS	v
TABLE OF CONTENTS	vi
LIST OF TABLES	ix
LIST OF FIGURES	xi
CHAPTER I. INTRODUCTION	1
Purpose	1
Need for Soil Moisture Information	1
Passive Microwave Indication of Soil Moisture	2
Ground Observations	3
Analytical Approach	4
CHAPTER II. LITERATURE REVIEW	6
Passive Microwave Remote Sensing of Soil Moisture	6
Formula for Passive Microwave Emission	7
Radiative Transfer Models	11
Simplified Soil Emission Models	12
Noise	13
Soil Moisture Models	16
Estimation of Evapotranspiration	16
API Model	18
Other Models	21

Surface and Aircraft Microwave Investigations	22
Surface Emission	22
Investigations Involving Polarized Data	22
Normalized Brightness Temperatures	24
Satellite Passive Microwave Investigations	25
Satellite Sensors	25
Resolution	29
Statistical Analysis Techniques	29
Investigative Results	30
CHAPTER III. MATERIALS AND METHODS	33
Data	33
Primary	33
Secondary	34
Organization	34
Study Area	34
Primary Database	37
Secondary Database	40
Analysis Methods	41
Temporal Analysis	41
Areal Analysis	42
CHAPTER IV. ANALYSIS AND DISCUSSION	44
Qualitative Analysis Methods	44
Temporal Analysis	44
Areal Analysis	44

Quantitative Temporal Analysis	55
Verification of the API Effective Precipitation Exponent	56
Correlation Analysis on Transforms	59
Comparison of Transforms and Multiple Linear Regression	65
Comparison of Case Study Grid Cells	67
Supporting Data	80
CHAPTER V. SUMMARY AND CONCLUSIONS	82
Summary	82
Conclusions	82
Recommendations for Further Research.	85
REFERENCES	87
APPENDIX A. AREAL MAPS OF SMMR, CLIMATIC, AND API DATA . .	93
APPENDIX B. MONTHLY CORRELATION COEFFICIENTS	110
APPENDIX C. BI-MONTHLY AND ANNUAL CORRELATION COEFFICIENTS	119
VITA	126

LIST OF TABLES

TABLE	Page
1 CHRONOLOGY OF SATELLITE PASSIVE MICROWAVE RADIOMETRY	26
2 CASE STUDY GRID CELLS WITH APPROXIMATE CROP PERCENTAGE OF COUNTY	36
3 OKLAHOMA CROP CALENDAR	61
B-1 CORRELATION COEFFICIENT (x1000) BETWEEN THE 1.66 CM TRANSFORMS AND API FOR ROW 15 COL 29 BETWEEN 25 OCT 1978 AND 10 NOV 1979	111
B-2 CORRELATION COEFFICIENT (x1000) BETWEEN ALL TRANSFORMS AND API FOR ROW 03 COL 27 BETWEEN 25 OCT 1978 AND 10 NOV 1979	112
B-3 CORRELATION COEFFICIENT (x1000) BETWEEN ALL TRANSFORMS AND API FOR ROW 09 COL 21 BETWEEN 25 OCT 1978 AND 10 NOV 1979	113
B-4 CORRELATION COEFFICIENT (x1000) BETWEEN ALL TRANSFORMS AND API FOR ROW 09 COL 29 BETWEEN 25 OCT 1978 AND 10 NOV 1979	114
B-5 CORRELATION COEFFICIENT (x1000) BETWEEN ALL TRANSFORMS AND API FOR ROW 15 COL 29 BETWEEN 25 OCT 1978 AND 10 NOV 1979	115
B-6 CORRELATION COEFFICIENT (x1000) BETWEEN ALL TRANSFORMS AND API FOR ROW 18 COL 27 BETWEEN 25 OCT 1978 AND 10 NOV 1979	116
B-7 CORRELATION COEFFICIENT (x1000) BETWEEN ALL TRANSFORMS AND API FOR ROW 21 COL 14 BETWEEN 25 OCT 1978 AND 10 NOV 1979	117
B-8 CORRELATION COEFFICIENT (x1000) BETWEEN ALL TRANSFORMS AND API FOR ROW 29 COL 22 BETWEEN 25 OCT 1978 AND 10 NOV 1979	118
C-1 BRIGHTNESS TEMPERATURE CORRELATION COEFFICIENT MATRIX FOR ROW 15 COL 29 BETWEEN 25 OCT 1978 AND 10 NOV 1979	120
C-2 NORMALIZED BRIGHTNESS TEMPERATURE CORRELATION COEFFICIENT MATRIX FOR ROW 15 COL 29 BETWEEN 25 OCT 1978 AND 10 NOV 1979	121

TABLE	Page
C-3 CORRELATION COEFFICIENT (x1000) BETWEEN THE HORIZONTALLY POLARIZED NORMALIZED BRIGHTNESS TEMPERATURE AND API BETWEEN 25 OCT 1978 AND 10 NOV 1979	122
C-4 CORRELATION COEFFICIENT (x1000) BETWEEN THE VERTICALLY POLARIZED NORMALIZED BRIGHTNESS TEMPERATURE AND API BETWEEN 25 OCT 1978 AND 10 NOV 1979	123
C-5 CORRELATION COEFFICIENT (x1000) BETWEEN THE 1.66 CM TRANSFORMS AND API FOR A JAN-FEB SERIES BETWEEN 25 OCT 1978 AND 10 NOV 1979	124
C-6 CORRELATION COEFFICIENT (x1000) BETWEEN THE 1.66 CM TRANSFORMS AND API FOR A FEB-MAR SERIES BETWEEN 25 OCT 1978 AND 10 NOV 1979	125

LIST OF FIGURES

Figure	Page
1 Angular dependence of the polarized brightness temperature	14
2 Study area with case study grid cells	35
3 Percentage of 1980 county acreage planted in dryland winter wheat for Kansas, Oklahoma, and Northwest Texas	38
4a GOES satellite image valid 0701Z, 10 May 1979 . . .	47
4b GOES satellite image (MB enhancement) valid 0631Z, 10 May 1979	47
5 NWS weather radar summary chart valid 0635Z, 10 May 1979	48
6 Atmospheric attenuation of microwave radiation from water vapor and oxygen	48
7 SMMR brightness temperature images for 0.81 and 1.66 cm horizontal and vertical polarizations for 10 May 1979 for the study area	50
8 SMMR brightness temperature images for 2.80 and 4.54 cm horizontal and vertical polarizations for 10 May 1979 for the study area	51
9 SMMR brightness temperature images for 0.81, 1.66, 2.80, and 4.54 cm horizontal polarizations for 10 May 1979 for the study area	53
10 SMMR brightness temperature images for 0.81, 1.66, 2.80, and 4.54 cm vertical polarization for 10 May 1979 for the study area	54
11a Comparison of the 1.66 cm wavelength correlation coefficients between the horizontally polarized normalized brightness temperature and four API effective precipitation exponents for March through July 1979	57
11b Comparison of the 1.66 cm wavelength correlation coefficients between the horizontally polarized normalized brightness temperature and four API effective precipitation exponents for August through November 1979 and all months combined . .	57

Figure	Page
12 Comparison of the correlation coefficients between the horizontally polarized normalized brightness temperature and API	60
13 Comparison of the correlation coefficients between the polarization difference transform and API . .	60
14 Comparison of the correlation coefficients between the normalized polarization difference transform and API	64
15 Comparison of the correlation coefficients between multiple linear regression on all three transforms and API	64
16a Comparison of the April correlation coefficients between the three transforms and multiple linear regression (mlr) on all three transforms, and API	66
16b Comparison of the September correlation coefficients between the three transforms and multiple linear regression (mlr) on all three transforms, and API	66
17a Comparison of the correlation coefficients between the horizontally polarized normalized brightness temperature and API for row 15 col 29	68
17b Comparison of the correlation coefficients between the horizontally polarized normalized brightness temperature and API for row 09 col 29	68
18a Time series plots of API for row 15 col 29 between 23 Oct 1978 and 12 Jan 1979	69
18b Time series plots of API for row 15 col 29 between 12 Jan 1979 and 01 Apr 1979	70
18c Time series plots of API for row 15 col 29 between 01 Apr 1979 and 20 Jun 1979	71
18d Time series plots of API for row 15 col 29 between 20 Jun 1979 and 08 Sep 1979	72
18e Time series plots of API for row 15 col 29 between 08 Sep 1979 and 10 Nov 1979	73
19a Time series plots of API for row 09 col 29 between 23 Oct 1978 and 12 Jan 1979	75

Figure	Page
19b Time series plots of API for row 09 col 29 between 12 Jan 1979 and 01 Apr 1979	76
19c Time series plots of API for row 09 col 29 between 01 Apr 1979 and 20 Jun 1979	77
19d Time series plots of API for row 09 col 29 between 20 Jun 1979 and 08 Sep 1979	78
19e Time series plots of API for row 09 col 29 between 08 Sep 1979 and 10 Nov 1979	79
A-1 Areal map of the 10 May 1979 SMMR brightness temperatures (K) for the study area for the 0.81 cm horizontally polarized wavelength	94
A-2 Areal map of the 10 May 1979 SMMR brightness temperatures (K) for the study area for the 0.81 cm vertically polarized wavelength	95
A-3 Areal map of the 10 May 1979 SMMR brightness temperatures (K) for the study area for the 1.36 cm horizontally polarized wavelength	96
A-4 Areal map of the 10 May 1979 SMMR brightness temperatures (K) for the study area for the 1.36 cm vertically polarized wavelength	97
A-5 Areal map of the 10 May 1979 SMMR brightness temperatures (K) for the study area for the 1.66 cm horizontally polarized wavelength	98
A-6 Areal map of the 10 May 1979 SMMR brightness temperatures (K) for the study area for the 1.66 cm vertically polarized wavelength	99
A-7 Areal map of the 10 May 1979 SMMR brightness temperatures (K) for the study area for the 2.80 cm horizontally polarized wavelength	100
A-8 Areal map of the 10 May 1979 SMMR brightness temperatures (K) for the study area for the 2.80 cm vertically polarized wavelength	101
A-9 Areal map of the 10 May 1979 SMMR brightness temperatures (K) for the study area for the 4.54 cm horizontally polarized wavelength	102

Figure	Page
A-10 Areal map of the 10 May 1979 SMMR brightness temperatures (K) for the study area for the 4.54 cm vertically polarized wavelength	103
A-11 Areal map of the 10 May 1979 maximum temperatures (C) for the study area	104
A-12 Areal map of the 10 May 1979 minimum temperatures (C) for the study area	105
A-13 Areal map of the 10 May 1979 precipitation (mm) for the study area	106
A-14 Areal map of the 10 May 1979 snowfall (cm) for the study area	107
A-15 Areal map of the 10 May 1979 snowdepth (cm) for the study area	108
A-16 Areal map of the 10 May 1979 Antecedent Precipitation Index values (mm) for the study area	109

CHAPTER I

INTRODUCTION

Purpose

The purpose of the research is to determine the relationship between multispectral dual polarized satellite passive microwave brightness temperatures and the Antecedent Precipitation Index (API) over uniform agricultural areas in the Southern Great Plains of the United States. The API is calculated from actual precipitation observations and simulates soil moisture, therefore, soil moisture content can be inferred through knowledge of the API (Blanchard *et al.*, 1980). The specific instrument used to obtain the data was the Scanning Multi-channel Microwave Radiometer (SMMR) aboard the Nimbus 7 satellite. Specific objectives included the investigation of three transformations of both the vertical and horizontal brightness temperatures to determine the applicability of both normalized brightness temperature and polarized channel data to infer soil moisture.

Need for Soil Moisture Information

Knowledge of large-scale patterns of soil moisture is needed to evaluate the condition of the soil or crop and is essential to the disciplines of agriculture, hydrology, and meteorology. In the field

This report follows the style and format of the Journal of Climate and Applied Meteorology.

of agriculture Idso et al. (1975a) described the need for soil moisture information for many diverse applications, including improved crop yield forecasting and irrigation scheduling. In fact, knowledge of the moisture condition of the soil is needed before undertaking any agricultural activity from planting to harvesting.

Remote sensing has been used to evaluate or monitor numerous hydrologic parameters. Burgy (1974) cites thirteen hydrologic parameters which can be measured or inferred through remote sensing. These are surface temperature, cloud cover, atmospheric liquid water content, snow cover, water equivalent of snowpack, vegetation, land use, soil moisture, short wave radiation in the radiation budget, long wave radiation in the radiation budget, water body configuration, soil types, and basin area. Knowledge of the moisture content of the soil surface layer is necessary for separating rainfall into its runoff and infiltration components. This knowledge is needed for both soil moisture modeling and flood forecasting.

In meteorology, soil moisture determines the division of net radiation into its latent and sensible heat components. An estimation of evaporation or evapotranspiration requires input of current soil moisture conditions. Most radiation, water budget, or global circulation models need an estimate of these parameters as initial input.

Passive Microwave Indication of Soil Moisture

Emitted radiation at microwave frequencies is a function of the moisture content of the emitting soil layer. This relationship has

been demonstrated by investigations by Cihlar and Ulaby (1975), Schmugge (1977), Schmugge et al. (1974, 1976, and 1978), and Newton (1977). Basically, this relationship is a function of the extremely high dielectric constant of water, and the relatively low values for air and dry soil. Since the dielectric constant inversely determines the soil emissivity, an increase in volumetric water content causes a decrease in the emissivity. The brightness temperature, or radiation received at the sensor antenna, is equal to the emissivity times the temperature of the emitting layer. It is possible to estimate the emissivity and therefore the soil moisture content by measuring the brightness temperature and estimating the soil surface temperature from meteorological observations. Meneely (1977) attempted to show this by using 1.55 cm passive microwave data from the Nimbus 5 sensor, however he did not get particularly encouraging results. Later work by McFarland and Blanchard (1977), Theis (1979), and Blanchard et al. (1980, 1981) involving 1.55 cm passive microwave data, indicated a strong linear correlation with rainfall history and inferred soil moisture for essentially bare agricultural soils through a time series analysis of brightness temperatures. Harder (1984) found similar correlations using Nimbus 7 passive microwave data at the 1.66 cm wavelength.

Ground Observations

One of the largest problems confronting all researchers is obtaining accurate and reliable ground observations (Harder, 1984). In

satellite remote sensing the vast area sensed presents an even greater problem in acquiring accurate ground observations. There are many conventional ways to measure soil moisture over limited areas, but a practical method for measuring soil moisture over an area consisting of several thousands of square kilometers has not been developed. Therefore this investigation will use the Antecedent Precipitation Index (API) to infer the ground observations needed to estimate soil moisture. This index represents soil moisture as a first order Markov chain through input of effective precipitation (Harder, 1984).

Analytical Approach

This investigation involved both a qualitative and quantitative approach. Initially, the data were analyzed qualitatively to determine all patterns or trends. The qualitative analysis consisted of a temporal analysis of SMMR brightness temperature data between 25 Oct 1978 and 10 Nov 1979, areal analysis on one case study grid cell, and image processor files for all grid cells in the study area. One day was chosen from the time series to be used as a case study. Areal maps of passive microwave brightness temperatures over the study area were used as input to create various image processor files. The visual patterns evident on the image processor files were then simultaneously compared to determine which microwave channel had the best qualitative relationship to surface soil moisture conditions. By knowing the actual surface moisture condition through supplementary data, one can determine qualitatively which channel of microwave data has the best visual relationship to the surface moisture condition.

The quantitative approach involved regression analysis relating the passive microwave data, along with various combinations of the passive microwave brightness temperatures, with the API. The microwave data was analyzed separately in terms of polarization and monthly, bi-monthly, and annual response. This analysis will determine which wavelength and polarization combination gives the best indication of the soil moisture, as inferred by the API.

CHAPTER II

LITERATURE REVIEW

Passive Microwave Remote Sensing of Soil Moisture

There are numerous methods using microwave measurements to estimate soil moisture. These methods are summarized by Idso et al. (1975a, 1975b), Jackson et al. (1978), Schmugge et al. (1976, 1980), Schmugge (1978, 1980a, 1980b), Schmugge and Choudhury (1981), Newton (1980), and Theis et al. (1982). The microwave methods, both active and passive, deal with the 1-50 cm wavelength region. These methods rely on the dielectric properties of the soil and water mixture. Since the dielectric properties of the substance determine the electromagnetic wave propagation characteristics within the substance, these properties will also affect the surface emissive and reflective properties. The microwave emission and reflection are then a direct function of the soil moisture and can be measured by active (radar) scatterometers or passive radiometers. Active microwave methods are discussed extensively in Ulaby et al. (1974), Ulaby (1974), Ulaby and Batlivala (1974), Batlivala and Ulaby (1977), Ulaby et al. (1977, 1978) and Schmugge et al. (1979).

Passive microwave radiometers measure the surface thermal emission. In the microwave region, the Rayleigh-Jeans' approximation shows that the intensity of the observed emission, called brightness temperature, is essentially proportional to the product of the surface temperature and the emissivity. Advantages of passive microwave approaches

include the ability to penetrate non-precipitating clouds and light vegetation. A few disadvantages are the sensor response only involves the top 0-2 cm of the soil, and relatively coarse data resolution (>10 km), as a function of the altitude and diameter of the antenna of the radiometer. The formula for the brightness temperature involves the physics of passive microwave remote sensing. Since the main emphasis of this investigation will involve the passive microwave region, the remote sensing characteristics of this region will be discussed more thoroughly in the next section.

Formula for Passive Microwave Emission

According to Lintz and Simonett (1976), microwave emission from an object can be described best by the concept of a theoretical blackbody, a non-reflecting opaque object. Planck's law gives an expression for the spectral radiant emittance as a function of the wavelength for black-body radiation at a given temperature. The formula is

$$M_{\lambda} = \frac{2\pi c^2 h}{\lambda^5} \left[\exp \frac{hc}{\lambda kT} - 1 \right]^{-1} \quad (1)$$

where

M_{λ} = spectral radiance of power emitted (watts $\text{cm}^{-2} \mu\text{m}^{-1}$)

h = Planck's constant (6.626×10^{-34} J sec)

k = Boltzman's constant (1.380×10^{-23} JK $^{-1}$)

λ = wavelength (m)

T = blackbody temperature (K)

c = velocity of light (2.998×10^8 m sec $^{-1}$)

Planck's law for an ideal blackbody in the microwave region is given by the Rayleigh-Jeans' approximation of Planck's radiation formula. This approximation can be derived by first taking a Maclaurin series expansion of the bracketed quantity in (1). A general form for this expansion is

$$e^x = 1 + x + \frac{x^2}{2!} + \frac{x^3}{3!} + \dots \quad (2)$$

Expanding the exponent in this manner yields

$$e^{\frac{hc}{\lambda kT}} = 1 + \frac{hc}{\lambda kT} + \frac{hc^2/\lambda kT}{2!} + \frac{hc^3/\lambda kT}{3!} + \dots \quad (3)$$

At microwave frequencies $hc \ll kT$, therefore, we can neglect the second and all successive terms in (3). This equation then reduces to the Rayleigh-Jeans' approximation.

$$M_{\lambda} = \frac{2cT}{\lambda^2} \quad (4)$$

This gives the total spectral radiance. The polarized radiance, where each plane of polarization contains one-half of the total radiance, would be given by

$$M_p = \frac{cT}{\lambda^2} = \epsilon \sigma T^4 \text{ (for non-microwave regions)} \quad (5)$$

where ϵ is the emissivity and σ is the Stefan-Boltzmann constant, $5.67 \times 10^{-12} \text{ W cm}^{-2} \text{ K}^{-4}$.

At microwave wavelengths, the spectral radiance is linearly proportional to the temperature of the emitting layer. At shorter wavelengths, the spectral radiance is proportional to the fourth power of the temperature. This linear relationship has led to the expression of the spectral radiance as a brightness temperature. For non-blackbodies, the brightness temperature is equal to the product of the emissivity and the temperature of the emitting layer. The radiance of an equivalent blackbody is multiplied by a relative efficiency factor called the emissivity. Equation (5) can be rearranged to get the polarized brightness temperature (T_b), defined by

$$T_b = \left(\frac{\lambda}{C}\right)^2 M_p \quad (6)$$

which reduces to

$$T_b = \epsilon T \quad (7)$$

where ϵ is the emissivity and T is the graybody temperature.

The T_b measured by a satellite radiometer is given by Schmugge (1980a) as

$$T_b = T_r[rT_{sky} + (1-r)T_{soil}] + T_{atm} \quad (8)$$

where T_r is the atmospheric transmission and r is the surface reflectivity. This formula separates the T_b into its three components. These are the reflected sky brightness temperature (T_{sky}), the thermal soil emission or, under conditions of non-transmittance and

thermal equilibrium, emissivity (ϵ , since $\epsilon = 1-r$), and the contribution due to the intervening atmosphere (T_{atm}). The reflected sky brightness temperature is the product of the downwelling brightness temperature and the surface reflectivity, minus the loss due to the intervening atmosphere. The sky radiation or sky brightness temperature consists of the 4K celestial background emission plus downwelling atmospheric radiation.

Weger (1960) computed the sky brightness temperature for numerous sky conditions for wavelengths between 0.43 and 3.00 cm. Sky brightness values for a representative wavelength of 1.80 cm at a viewing angle of 50 degrees, were about 10 K for clear skies, 15 K for moderate cloud, and 30 K for uniform moderate precipitation. Under clear skies, the atmospheric transmission will be close to 1.0. With a high surface reflectivity (90%), the total contribution will be close to 9 K. Under precipitating conditions, the atmospheric transmission and surface reflectivity will decrease. With an atmospheric transmission of 80% and a surface reflectivity of 30%, the contribution will be 7.2 K. This shows that the maximum component of the T_b due to the reflected sky brightness temperature could be as large as 9 K.

The thermal emission from the soil is generated within the soil layer. The amount of energy generated at a particular point depends on the soil temperature at that point and the volumetric dielectric properties. As the energy propagates from the point of origin, it is modified by the dielectric gradient it encounters. Numerous radiative transfer models have been developed to account for these energy exchanges. Some of these models are described in Wang and Schmugge

(1978, 1980), Burke et al. (1979), and Schmugge and Choudhury (1981).

Radiative Transfer Models

Most of the radiative transfer models require a fairly detailed knowledge about the soil medium and some knowledge about the surface parameters. One very significant result from these models was given by Wilheit (1978). Wilheit defined thermal and reflective sampling depths and showed that the thermal depth is on the order of one wavelength, while the reflective depth was on the order of a few tenths of a wavelength. The thermal sampling depth referred to the layer whose effective temperature determined the amount of energy available for emission. The reflective sampling depth referred to the layer whose moisture content determined the emissivity of the soil. Wang et al. (1980a) used the empirical model of Wang and Schmugge (1980) to determine the emission from the soil surface. They computed the expected normalized brightness temperature or effective emissivity, for both 6 and 21 cm wavelengths, of a soil surface covered by different types of vegetation. While both observations and predictions showed a general decrease of sensitivity with increasing vegetation, as theory suggests, they did notice some discrepancies between measurements and theory. They suggested that the discrepancies may be explained by roughness, which was not specifically accounted for in the model.

The effects due to the intervening atmosphere fall into two categories, the direct radiation from the atmosphere incident upon the sensor, and the atmospheric attenuation of reflected or emitted surface radiation. At long wavelengths these effects are minimal when compared

to the effects from the other components and can be neglected in a first approximation of soil moisture.

Simplified Soil Emission Models

The radiative transfer models described in the literature often require extensive knowledge of the soil structure, surface roughness, vegetation, and a wide continuum of meteorological elements. These detailed data are extremely difficult to obtain over the large areas normally covered by low-resolution satellites. Most simplified models represent the soil as a single emitting layer. This makes the models well suited for using data from satellite-based passive microwave radiometers whose depth of penetration is only a few centimeters.

These models rely on the strong dependence of the soil dielectric properties on the soil moisture content. The magnitude of this dependence is so great that it overshadows all other components of the complex radiative transfer models. These secondary components can therefore be estimated or even neglected making a simplified model applicable to satellite remote sensing. One of the most important results from one of these simplified models was given by Newton (1977). Newton presented model results showing that brightness temperature was a nearly linear function of soil moisture content throughout the moisture content range, except near the dry end. The lack of a linear relationship at the dry end was explained by the tight molecular bond between the water and soil molecules in this moisture range. He also observed that when the viewing angle was increased from nadir to 40 degrees, the vertically polarized brightness temperature component increased and the

horizontally polarized brightness temperature component decreased. He stated that the mean of the two polarized components was nearly independent of viewing angle. This is shown by Fig. 1.

Wang and Schmugge (1978, 1980) used a simple empirical model of the dielectric behavior of soil-water mixtures. This was a two-layer model with an adjustable lower layer. They determined that the dielectric constant of a soil was not very responsive to soil moisture below a certain transition moisture value, and that this transition value was a simple linear function of the permanent wilting point of the soil. Since the transition moisture value was dependent on soil texture, soil texture maps would be useful in predicting the soil dielectric behavior. Wang (1980) expanded on this observation when he stated that wavelengths shorter than 30 cm have a moisture response that depends on soil texture, while longer wavelengths have no such dependence.

Noise

The relationship between the soil moisture signal and the sensor response is affected by various noise factors. These noise factors include vegetation, roughness, and instrument errors. The most significant noise factors in the passive microwave region are vegetation and roughness. The passive microwave response will be a composite of the emission from the total area sensed. This response even over "bare" agricultural soils will contain vegetative effects resulting from trees, pastures, or roadside ditches. The manner in which roughness and vegetation affect the soil moisture signal is different but the result is the same. Both factors decrease the soil moisture signal

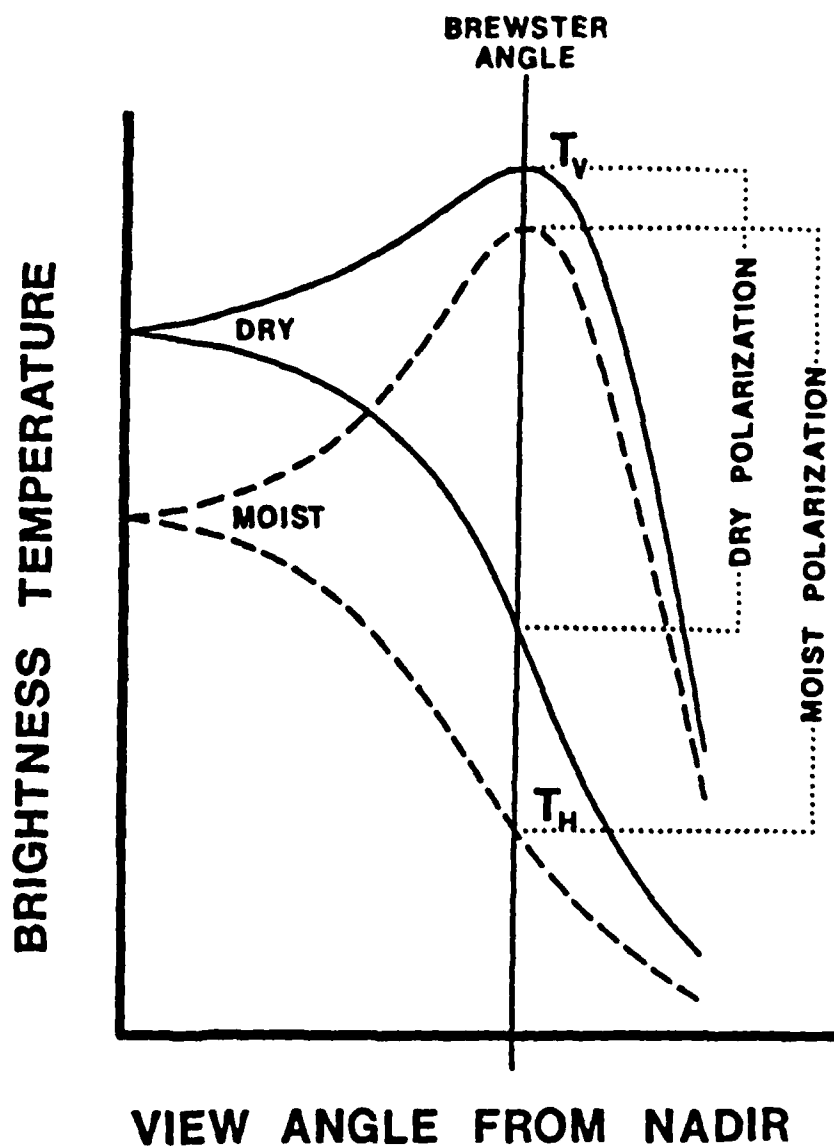


Figure 1. Angular dependence of the polarized brightness temperature. A schematic representation of the effect of soil moisture on brightness temperature and polarization (adapted from Harder, 1984).

detectable at the sensor. Poe and Edgerton (1971) investigated responses from airborne microwave radiometers at wavelengths of 0.32, 0.81, 1.55, 6.0, and 21 cm. They concluded that the shortest three wavelengths were too strongly influenced by noise, particularly roughness, to be of much use in soil moisture estimation. The longest two wavelengths were consistently sensitive to soil moisture even in the presence of a vegetative canopy. Choudhury et al. (1979) presented model calculations which agreed with previous experimental results, and concluded roughness effects were greatest for wet soils. Wang et al. (1980b) found that vegetation degrades soil moisture sensitivity at both 6 and 21 cm wavelengths by an amount related to the amount of biomass and/or moisture content of the vegetation. Wang and Choudhury (1981) developed a microwave emission model that had a two-parameter representation of soil surface roughness. They suggested both the polarization mixing parameter and the roughness height parameter could be estimated empirically by a time series analysis of transformations of polarized passive microwave brightness temperatures. McFarland (1982) suggested that when vegetation obscures the soil moisture signal, the observed brightness temperature would indicate crop temperature. This crop temperature could be compared to the ambient temperature to give an indication of crop stress. Inferred values of crop stress could then be used to infer qualitatively soil moisture content in the root zone.

Instrument errors including calibration cause an additional source of noise in the passive microwave brightness temperature measurements. All instruments have an associated error with their measurements,

however this error is greatly reduced by routine calibration. If the sensor is not calibrated and checked for consistency, the data becomes suspect. While there is an error range associated with the measurements from these instruments, it is very small when compared to the other sources of error such as vegetation and roughness, and the intervening atmosphere.

McFarland and Blanchard (1977) and Blanchard et al. (1981) reported data interpretation problems due to the cross-track scan pattern of the Nimbus 5-ESMR sensor which resulted in a non-uniform viewing angle and a degrading resolution cell as the viewing angle increased. Even though the Nimbus 7 SMMR has a constant viewing angle, the data still suffer from a degrading resolution cell, like the Nimbus 5-ESMR data, as the wavelength increases. While the magnitude of the instrument errors from the Nimbus 5-ESMR was significant, effects of vegetation and roughness will totally mask any discernible errors from the Nimbus 7 SMMR sensor.

Soil Moisture Models

Numerous soil moisture models are available in the literature ranging from extremely complex models requiring considerable meteorological input along with detailed soil and vegetation parameters, to relatively simple models which can utilize low-resolution satellite data.

Estimation of Evapotranspiration

One of the largest problems encountered in developing a soil

moisture model is the method used to estimate evaporation or evapotranspiration. Penman (1956) gave some interesting quotes on this subject from previous authors. Symons laid the groundwork for future studies in this area when he said in 1867 "evaporation is the most desperate branch of the desperate science of meteorology." Maluschitski followed this example by stating in 1900 that "no correlation can be established between the evaporation from a water surface and that for a cultivated soil, and still less in the case of a soil covered with plants." Cleveland Abbe continued this trend in 1905 when he said "of course (we) need to know the loss of water by evaporation but in nature this is so much mixed up with seepage, leakage and consumption by ... plants that our meteorological data are of comparatively little importance." We have progressed forward since these statements were made, however a unique method for estimating evaporation or evapotranspiration still has not been developed.

According to Schmugge (1978) some of the major differences in the models involve the method of computation or estimation of potential evaporation, how infiltration or runoff is computed, the way precipitation or evaporative demand is defined, the method of computing soil evaporation and plant transpiration, the number of soil layers to use and whether they are saturated or unsaturated layers, and the way the thermal properties of the soil system are accounted for. The major advantage of using a model is to provide timely point or areal estimates of soil moisture over areas where these estimates are not readily available. The major disadvantage is the inherent inaccuracy of the estimate.

Chang (1968) classified the various methods to estimate evaporation or evapotranspiration into five major classes. These are direct measurements, aerodynamic methods, energy balance approaches, empirical methods, and evaporation pans or atmometers. The input to soil moisture models normally involves one of the numerous empirical methods by using an empirical moisture depletion coefficient. If this coefficient is fixed, then the model is applicable only to areas with similar environments to the one in which it was developed. Often the model will have only limited qualitative usefulness due to inherent errors, even over similar regions. There seems to be a model in the literature for nearly every possible situation, therefore only a few representative soil moisture models will be discussed here.

API Model

The API is a very simple soil moisture model that can rely predominantly on passive microwave data. The resultant soil moisture values are much coarser than detailed models due to the low-resolution input data and the greatly simplified physics of the model. Since the problem of obtaining an accurate and unique model for estimating evaporation or evapotranspiration has not been solved, this method may prove to be a viable alternative.

Saxton and Lenz (1967) used a modified API which they termed an antecedent retention index. They used an estimate of the potential evaporation to deplete moisture during the constant rate stage of drying, and an exponential depletion rate in the falling rate stage.

An excellent description of these drying stages is given by Derendinger (1971).

According to Linsley et al. (1975) the most common soil moisture index used for storm runoff models is the API in the form used by Kohler and Linsley (1951). This form of the API was

$$I_t = I_0 K \quad (9)$$

where I_0 is the initial value, K is the depletion coefficient, less than one, and t is the time in days. They stated that the depletion coefficient or recession factor should be a function of potential evaporation or season. They suggested a seasonal value could be used since it would be strongly related to potential evapotranspiration. They noted also that initialization errors disappear after a few weeks since the errors decayed logarithmically.

Choudhury and Blanchard (1981) used a water balance approach taken from Global Climate Models to derive several forms of the API as a first-order Markov chain. Their formula for the recession factor was

$$k = \exp [-E/Z(FC-WP)] \quad (10)$$

where E is the daily total potential evapotranspiration (PET) for the previous day, Z is the soil thickness, FC is the field capacity of the soil, and WP is the permanent wilting point. They noted that a first approximation of the recession factor could be obtained from soil texture information and a climatological estimate of PET.

The form of the API used by McFarland and Harder (1982) and Harder (1984) for use with passive microwave studies was

$$API(i) = API(i-1) * k + P(i) \quad (11)$$

where $API(i)$ is the API value for day i , $API(i-1)$ is the previous day's value, k is a depletion coefficient less than one, and $P(i)$ is the effective precipitation for day i . The months of February and August were chosen to make the depletion coefficient a simple sinusoidal model which approximated the annual temperature minimum and maximum values. McFarland (1976) initially used satellite measurements to infer soil moisture through correlations between these measurements and API. He used a constant k value of 0.9 for the June and August correlations with the L-band (21 cm) brightness temperatures from the Skylab mission. McFarland and Blanchard (1977) used a varying k factor as a function of season in order to remove the seasonal temperature trend effects from the three month period of record. Blanchard et al. (1980) stated that the general form of a curve which represented inverted mean daily temperature, represented seasonal changes in k . This curve of inverted mean daily temperature was found to be remarkably similar to the inverse of a curve of the mean monthly potential evapotranspiration, calculated by the Penman equation. Making the depletion coefficient a function of season agreed with previous work by Kohler and Linsley (1951). The effective precipitation was computed by raising precipitation to a power of 0.891 as suggested by Blanchard et al. (1980). McFarland and Harder (1982) applied this model by using simple linear regression to correlate the API with passive microwave emissivity values. The emissivities were computed from the ratio of the microwave brightness temperatures to the air temperature.

Other Models

Baier and Robertson (1966) developed a multi-layered Versatile Budget (VB) model similar to the API model, but with a more detailed depletion coefficient. This coefficient was computed from the product of the potential evapotranspiration, an adjustment for a specific drying curve, and a soil-plant characteristic coefficient. The previous day's soil moisture value was then multiplied by the depletion coefficient to get the effective precipitation to be added to the infiltration amount.

Van Bavel and Lascano (1980) developed a model called CONSERVB that calculated soil moisture and temperature profiles from weather observations. This energy balance approach required either hourly or daily observations of global radiation, wind speed, air temperature, humidity, and precipitation amount and duration. These are the same parameters required for the widely-used Penman potential evapotranspiration equation. Smith and Newton (1983) modified the CONSERVB model to accept microwave radiometer data instead of meteorological observations. They used data simulation for both 6 and 21 cm wavelengths to compare to the original CONSERVB model. The resulting soil moisture predictions were nearly identical to the original model. This experiment shows that microwave data can be substituted for actual meteorological observations with an insignificant loss of predictive capability.

Surface and Aircraft Microwave Investigations

Surface Emission

Edgerton et al. (1971) measured the passive microwave emission from several substances including soils, sediments, sea ice, snow, and snowpacks. Combinations of viewing angle and wavelength were used to examine different types of soil texture. They concluded that the brightness temperature was a function of radiometer polarization and wavelength, thermodynamic temperature, soil density, surface roughness, vegetative cover, and soil moisture content. The variation of brightness temperature with soil texture and viewing angle was inherently accounted for in the experimental design. They found that the 2.2 cm wavelength response was related strongly to both soil moisture and the soil temperature of the top centimeter.

Kirdyashev et al. (1979) undertook a similar study when they investigated the sensitivity of the microwave emission under varying types and amounts of vegetation. They analyzed the radiometric response at several viewing angles at wavelengths ranging from 0.8 to 30 cm. They found that the sensitivity of the microwave emission decreased as the amount of vegetation increased, and presented quantitative models of the vegetation attenuation effects. They suggested the possibility of using microwave data to estimate biomass, plant height, and water content.

Investigations Involving Polarized Data

Newton (1977) showed that increasing the sensor's viewing angle

from nadir to near 50 degrees caused an increase in the vertically polarized brightness temperature component and a decrease in the horizontally polarized brightness temperature component. He showed that the mean of the two polarized components was nearly independent of viewing angle. When discussing the effects of vegetation and surface roughness, Newton showed that the effect of both of these parameters was to decrease the sensitivity of the emitted brightness temperature to soil moisture. He concluded that the difference between the L-band vertically polarized component of the brightness temperature and the L-band horizontally polarized component at a viewing angle of 35 degrees could be used to estimate surface roughness.

Burke and Paris (1975) and Burke et al. (1979) also examined a combination of the polarized components of the brightness temperatures. They investigated the sensitivity of the dual polarized microwave response to soil moisture at wavelengths of 2.8 and 21 cm. They compared values of the first two Stokes' parameters, $P = 0.5(T_v + T_h)$, and $Q = (T_v - T_h)$, and found they could identify both soil moisture and surface roughness effects. Q was found to be very sensitive to soil moisture at gravimetric moisture contents less than 15 percent, while P was more sensitive at moisture contents greater than 15 percent. Q was more closely related with surface roughness and nearly invariant with temperature, while P was found to be nearly invariant with viewing angle.

Burke (1980) continued the evaluation of the Stokes' parameters using aircraft data at the Ku, X, and L-band wavelengths. She found that the first Stokes' parameter, $P = 0.5(T_v + T_h)$, was more sensitive to

soil moisture than either of the individual components of the polarized brightness temperature. The second Stokes' parameter, $Q = (T_v - T_h)$, showed considerable scatter when related to surface roughness. This disagreed with her previous work, where Q had been found to be more closely related with surface roughness than P . She agreed with previous observations that vegetation completely obscured any response to soil moisture from the shorter wavelengths, and that the L-band wavelength was relatively insensitive to vegetation. She concluded that multi-spectral, multi-temporal microwave observations could indicate shallow subsurface moisture profiles.

Wang et al. (1981) took the ratio of the two Stokes' parameters and defined it as a polarization factor (P), where $P = [T_v - T_h / 0.5 (T_v + T_h)]$. They used this factor to evaluate the results of ground-based measurements of brightness temperatures at wavelengths of 6 (C-band) and 21 (L-band) cm. They found that the ratio of C-band to L-band brightness temperatures could discriminate between bare and vegetated fields. In addition they found that P could indicate biomass, with high values of P corresponding to bare fields or dry corn fields.

Normalized Brightness Temperatures

Mo et al. (1980) and Mo and Choudhury (1980) showed that soil moisture was related to an emissivity or a normalized brightness temperature (T_b), where T_b was defined as brightness temperature divided by the effective temperature of the emitting layer. They showed that the effective temperature was approximately equal to the surface

temperature for short-wavelength sensors, but that the entire thermal sampling depth must be considered for long-wavelength sensors. Wang et al. (1981) used this definition for normalized brightness temperatures when they analyzed microwave data obtained at wavelengths of 2.8, 6.0, 21, and 50 cm. They defined the emitting layer as the soil layer, whose moisture content was being measured, with a sampling depth equal to about one tenth of a wavelength. They found that the wavelength with the greatest moisture sensitivity was 6.0 cm for bare soil, 21 cm for alfalfa, and 50 cm for grass.

Njoku and O'Neill (1982) also used a normalized brightness temperature in an investigation of the relationship of the volumetric soil moisture content of the top 2 cm with ground-based passive microwave data. The radiometric wavelength bands tested were 2.8, 21.4, and a 33 to 50 cm variable UHF band. They concluded that L-band sensors would give the best indication of volumetric soil moisture in the top 2 cm, while UHF sensors would give the best indication in the top 4 cm.

Satellite Passive Microwave Investigations

Satellite Sensors

The first satellite that carried a passive microwave sensor useful for soil moisture experiments was launched in 1972. Since then, four additional satellites have been launched, with a future planned launch in mid-1985. Table 1 gives a chronology of satellite passive microwave radiometry.

Nimbus 5, launched in Dec 1972, was placed in a circular, sun-synchronous orbit at an altitude of 1112 km. The passive microwave

TABLE 1
CHRONOLOGY OF SATELLITE PASSIVE MICROWAVE RADIOMETRY

Data Acquisition	Spacecraft	Orbital Characteristics	Instrument Acronym	Wavelength- Polarization (cm)	Swath Width of Scan (km)	Smallest Resolution (km)	Principal Parameters Measured or Inferred
Dec 1972-late 1975	Nimbus 5	Circular Sun-synchronous 1112 km	ESMR	1.55	1570	25x25	Atmosphere: rain rate over ocean. Surface: sea-ice concentration, ice classification.
May 1973-Feb 1974	Skylab	Circular 438 km	S-193 S-194	2.16 21.4	180 -	16 115	Surface: oceanic winds & precipitation. (Hurricane & tropical storm monitoring) Surface: soil moisture.
Jun 1975-late 1976	Nimbus 6	Circular Sun-synchronous 1100 km	ESMR	0.81-V&H	1200	20x43	Atmosphere: rain rate over ocean. Surface: sea-ice concentration, ice classification, snow cover.
Jun 1978-Oct 1978	Seasat	Circular Near-polar 800 km	SMR	0.81-V&H 1.36-V&H 1.66-V&H 2.80-V&H 4.54-V&H	600	18x28	Atmosphere: water vapor content, liquid water content, rain rate. Surface: sea-temperature, wind speed, sea-ice concentration, ice classification, snow cover, soil moisture.
Oct 1978-current	Nimbus 7	Circular Sun-synchronous 955 km	SMR	(see above)	822	22x35	(see above)
Mid-1985 launch	DMSP	Near-polar Sun-synchronous 833 km	SSM/1	0.36-V&H 0.81-V&H 1.35-V 1.55-V&H	1390	15	Atmosphere: rain rate. Surface: rainfall location & amount, soil moisture, oceanic wind speed, sea-ice concentration, ice classification.

instrument aboard was the Electrically Scanning Microwave Radiometer (ESMR). The sensor scanned in a cross-track direction with a viewing angle ranging from nadir to 50 degrees. The radiometer had a single wavelength of 1.55 cm and a resolution element of 25 km at nadir. Its primary objective was to map surface features of the earth, particularly the distribution of polar ice and precipitating clouds over the ocean. The ESMR sensor provided about three years of passive microwave data.

Skylab was the next in the series, launched in May 1973. This was the first sensor to have a primary objective of sensing soil moisture. Skylab had a circular orbit at an altitude of 438 km. The satellite carried two passive microwave instruments useful in soil moisture experiments. The S-193 instrument mechanically scanned in a parabola at a wavelength of 2.16 cm. The smallest resolution element was 16 km. The S-194 instrument was a non-scanning sensor with a wavelength of 21.4 cm. The smallest resolution element of this L-band sensor, 115 km, was considerably larger than the smallest resolution element of the S-193 instrument. All soil moisture experiments aboard Skylab were accomplished between May 1973 and February 1974.

Nimbus 6 was launched in June 1975 with an ESMR sensor aboard. It had a circular sun-synchronous orbit at an altitude of 1100 km. This sensor differed from the Nimbus 5 ESMR in that it had a 0.81 cm dual polarized sensor which had a conical scan at a constant angle of 45 degrees with respect to the earth's surface. The change in wavelength from ESMR-5 to ESMR-6 effectively tripled the instrument's sensitivity to water droplets while retaining essentially the same sensitivity to

water vapor. Most of the studies involving ESMR-6 dealt with parameters over the ocean, such as rainfall rate or wind speed. Unfortunately the sensor was operational only for approximately two years.

Both Seasat and Nimbus 7 were launched in 1978. The sensor aboard Seasat obtained data between June 1978 and October 1978. It was placed in a circular near-polar orbit at an altitude of 800 km. Nimbus 7 replaced Seasat in Oct 1978 and is currently operational in a circular sun-synchronous orbit at an altitude of 955 km. Each satellite carried a dual polarized Scanning Multichannel Microwave Radiometer (SMMR) which operated in five wavelengths, 0.81, 1.36, 1.66, 2.80, and 4.54 cm. The sensor scanned in a conical pattern at a nearly constant angle of about 50 degrees to the earth's surface. One of the principal parameters to be measured or inferred by the SMMR sensor was soil moisture.

The Defense Meteorological Satellite Program (DMSP) satellite with a planned launch in mid-1985 will have a passive microwave radiometer aboard. The satellite will be placed in a near-polar sun-synchronous orbit at an altitude of 833 km. This DMSP satellite will carry a Special Sensor Microwave Imager (SSM/I) described in detail by Hollinger and Lo (1983). This sensor will have a conical scan at a constant angle of 53.1 degrees to the earth's surface and will operate at wavelengths of 0.36, 0.81, 1.35, and 1.55 cm. All four wavelengths will have a horizontally polarized brightness temperature component, and all but the 1.35 cm band will have a vertically polarized component. The resolution will range from about 15 km for the 0.36 cm channel to about 55 km for the 1.55 cm channel.

Resolution

Several studies have indicated that the lower resolution data from satellite-based sensors is sufficient to infer soil moisture amounts. Hardy et al. (1981) noted that operational soil moisture models used in government agencies used meteorological data which had a resolution on the order of 100 km. Newton et al. (1982) simulated the effect of degrading the resolution from a passive microwave sensor for X, C, and L-band wavelengths. They found the sensitivity to soil moisture actually increased as the simulated resolution was degraded. The optimum resolution was found to be 20 km with the sensitivity of a 60 km resolution cell being equal to that of a 5 km cell. McFarland and Harder (1982) simulated a degradation of resolution of Nimbus 5 ESMR data from 25 km to 50 km. They found the 50 km correlations between emissivity and API were as good as or better than the original 25 km resolution data.

Statistical Analysis Techniques

The most common method found in the literature to analyze passive microwave data statistically for soil moisture information was simple linear regression. Several researchers extended their analysis of simply correlating the microwave data with a measure of soil moisture by using additional techniques such as multiple linear regression or stepwise linear regression. Simple linear regression was used to analyze the data in many of the Skylab and Nimbus 5 experiments, while studies involving Nimbus 7 data tended to include additional

techniques. This current trend has been assisted by technological advances such as improved parameterization of the variables involved in the analysis scheme resulting in reduced overall error, the advent of higher resolution dual polarization multi-frequency microwave data, and the increasing availability of advanced computerized statistical packages.

Rodgers and Siddalingaiah (1983) initially analyzed three wavelengths of dual polarized Nimbus 7 SMMR data using simple linear regression to delineate rainfall areas over land. They extended the statistical analysis with a Fisher linear discriminant classification. This was analogous to their earlier work where they used Nimbus 6 ESMR data to determine rainfall over land (Rodgers et al., 1979).

Pandey and Kakar (1983) used a multiple linear regression model for retrieval of geophysical parameters from SMMR data. Spencer et al. (1983) applied a step-wise multiple linear regression approach which used Nimbus 7 SMMR data to infer rainfall rates over land. Burke and Ho (1981) used the Statistical Parameter Inversion Method (SPIM) to infer soil moisture from dual polarized 2.8 and 21 cm microwave data. The SPIM algorithm, according to Hollinger and Lo (1983), will be used in the analysis of future DMSP SSM/I data.

Investigative Results

The first available satellite sensor to be used in investigations to determine the relationship between satellite passive microwave brightness temperatures and soil moisture was the 1972 Nimbus 5-ESMR sensor. The launch of Nimbus 6 marked the first time a dual polarized sensor could be used to determine this relationship, however the early

demise of the ESMR sensor limited its investigative usefulness. The majority of investigations into this relationship currently found in the literature involved single polarized Skylab data and dual polarized Nimbus 5-ESMR data.

Stucky (1975) used simple linear regression to determine the correlation between Skylab S-193 brightness temperatures and a 10-day API. This API model used a constant depletion coefficient of 0.9. He reported a correlation of -0.9 which decreased nearly linearly to -0.2 as the viewing angle was increased to 40 degrees. He found also that correlations for viewing angles less than 25 degrees were higher for a 10-day API than a 6-day model.

McFarland (1976) used simple linear regression to determine the relationship between Skylab S-194 brightness temperatures and an 11-day API. He reported a correlation of -0.97 for June 1973 data and -0.73 for August 1973 data. He suggested the decrease in the correlation was due to increased surface roughness. Eagleman and Lin (1976) related Skylab S-194 data with actual soil moisture field samples collected near the satellite overpass times with correlations similar to those of McFarland (1976).

Schmugge et al. (1977) reported a linear correlation between Nimbus 5-ESMR data and antecedent rainfall totals over bare agricultural soils. McFarland and Blanchard (1977), Theis (1979), Blanchard et al. (1981), and McFarland and Harder (1982, 1983) reported linear correlations between a normalized brightness temperature and API. The normalized brightness temperature was computed by dividing the brightness temperature by the daily maximum air temperature. They called

this result an emissivity or a normalized emissivity. The highest correlation coefficients were found with essentially bare agricultural soils. McFarland and Harder (1983) noted that emissivities over frozen or snow-covered soil were distinctly different than those over bare unfrozen soil. They also suggested that soil moisture conditions could be inferred from a stressed crop canopy since the vegetative response was related to the underlying soil moisture conditions. Harder (1984) found that correlations using combinations of Nimbus 7 SMMR polarized brightness temperatures and API gave similar results to correlations between emissivities and API. He reported that seasonal segments of either the emissivity or various transformations of polarized brightness temperatures had higher correlation coefficients with API than annual models, however annual models were more reliable due to a larger sample size.

CHAPTER III

MATERIALS AND METHODS

Data

Primary

The primary data used in this investigation involved passive microwave data from the Nimbus 7 Scanning Multichannel Microwave Radiometer (SMMR), climatic data from the National Climatic Data Center, and computed Antecedent Precipitation Index (API) values which were used as ground observations.

NASA's Goddard Space Flight Center provided computer tapes with Nimbus 7 SMMR data from 25 Oct 1978 to 10 Nov 1979. The orbit of Nimbus 7 provided repetitive coverage every 2 or 3 days over the selected study area. The local observation time varied by about an hour with average overpass times of about 0100L and 1100L (0600Z and 1600Z), for night and day passes respectively. The data tapes included the nominal latitude and longitude of each wavelength's instantaneous field of view (IFOV). These coordinates were assumed accurate and used to align the SMMR data. This investigation utilized all 10 available SMMR data channels, which included both vertical and horizontal polarized brightness temperatures in five wavelengths: 0.81, 1.36, 1.66, 2.80, and 4.54 cm.

Computer tapes containing weather observations from over 500 stations in the cooperative observing network were purchased from the National Climatic Data Center. Daily observations of maximum and

minimum temperature, total precipitation, snowfall, and snowdepth, were extracted from these tapes for use in the analysis.

The API was used as ground observations in this investigation due to the lack of available large-scale soil moisture measurements over the study area. Observed precipitation values from the climatic data were used to calculate daily values of the API.

Secondary

Secondary data were used to obtain additional information about the study area. Images from the geostationary meteorological satellite (GOES) were used in delineating clouds for areal case study analysis. National Weather Service (NWS) weather radar summary charts were used to locate precipitating clouds. United States Geological Survey (USGS) topographic and land-use maps along with reported crop production statistics, were used to select and evaluate grid cells for a temporal case study analyses.

Organization

Study Area

The study area as shown in Fig. 2, included most of Kansas, Oklahoma, and the Panhandle of Texas, along with small portions of Colorado, New Mexico, and Missouri. The base map was generated locally in a polar stereographic map projection true at 37 degrees latitude and 100 degrees longitude. An analysis grid, which consisted of 35 rows and 40 columns of 20 x 20 kilometer cells, was overlaid onto the study area, with each county averaging between 2 and 4 grid cells. The cells

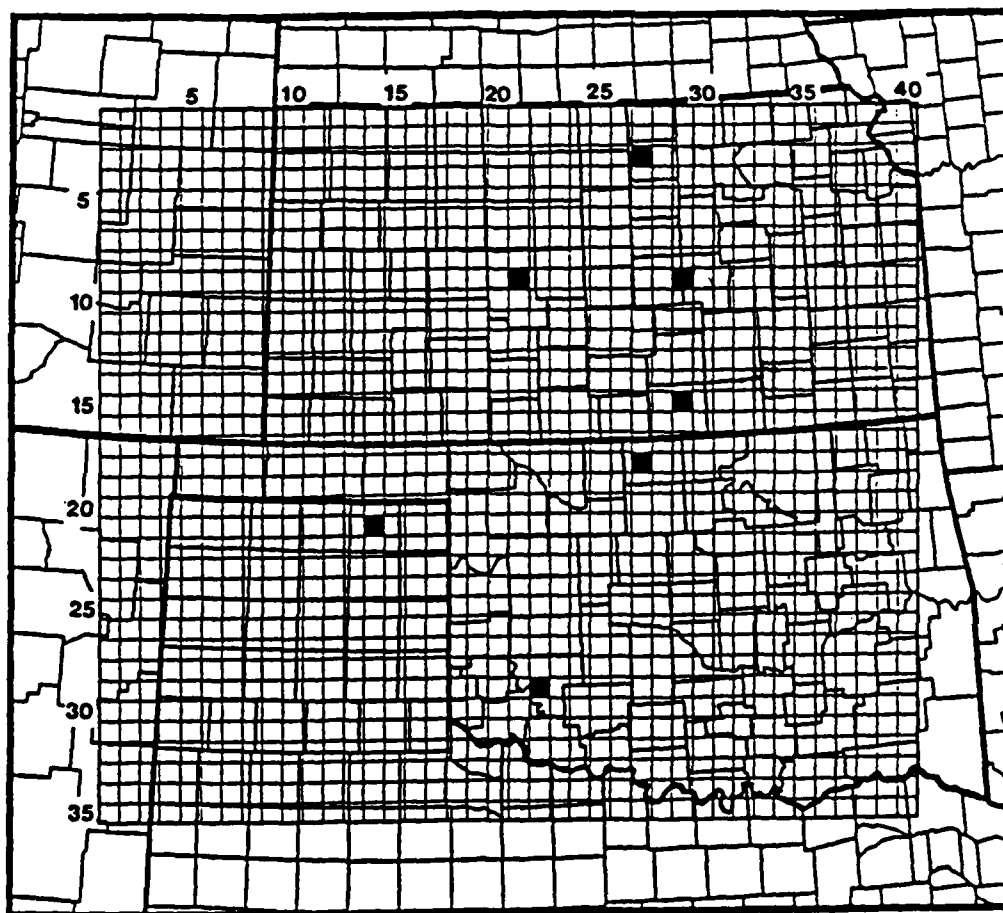


Figure 2. Study area with case study grid cells.

were numbered starting from the top left-hand corner cell. Areal analysis included the complete study area, while temporal analysis was performed on selected case study grid cells.

The case study grid cells with the approximate crop percentage of the county selected for this investigation are listed in Table 2. The crop categories listed in this table are the percentage of the total county acreage that was planted in the specified non-irrigated crop. These percentages were computed from the county size and crop acreage statistics reported in the county agricultural statistics, published annually by the State Crop and Livestock Reporting Services. The case study grid cells were chosen on the basis of a predominantly agricultural land-use with a high percentage of non-irrigated acreage planted in winter wheat.

TABLE 2
CASE STUDY GRID CELLS WITH APPROXIMATE CROP PERCENTAGE OF COUNTY

ROW	COLUMN	COUNTY	STATE	WHEAT (%)	SORGHUM (%)	CORN (%)	COTTON (%)	HAY (%)	TOTAL IRRIGATED ACREAGE (%)
03	27	CLOUD	KS	36	15	4	0	5	2
09	21	RUSH	KS	36	8	1	0	4	2
09	29	MCPHERSON	KS	45	18	2	0	4	4
15	29	SUMNER	KS	66	5	0	0	3	0
18	27	GRANT	OK	65	21	0	0	3	0
21	14	OCHILTREE	TX	42	9	0	0	0	17
29	22	KIOWA	OK	41	2	0	9	3	1

Crop categories not listed comprised < 1.5% of the total county acreage.

Figure 3 lists the 1980 dryland winter wheat acreage by county for the study area. The grid cells surrounding the selected cells were also examined using this criteria, since the SMMR IFOV of the longer wavelengths covered more than one grid cell. A minimum of 2 grid cells between selected case study grid cells was necessary due to the size of the microwave footprint.

Primary Database

The primary database consisted of SMMR, climatic, and API values. The SMMR and climatic data were analyzed objectively to the 35 x 40 grid using an exponential weighting function similar to that used by McFarland and Blanchard (1977). All observations within a specified radius-of-influence surrounding the grid cell were assigned weights based on distance in order to assign a value at the center of the cell. The radius-of-influence for brightness temperature, maximum and minimum air temperature, and precipitation were selected on the basis of density of reporting stations or available SMMR data. This analysis algorithm has been reported in detail by Harder and McFarland (1984).

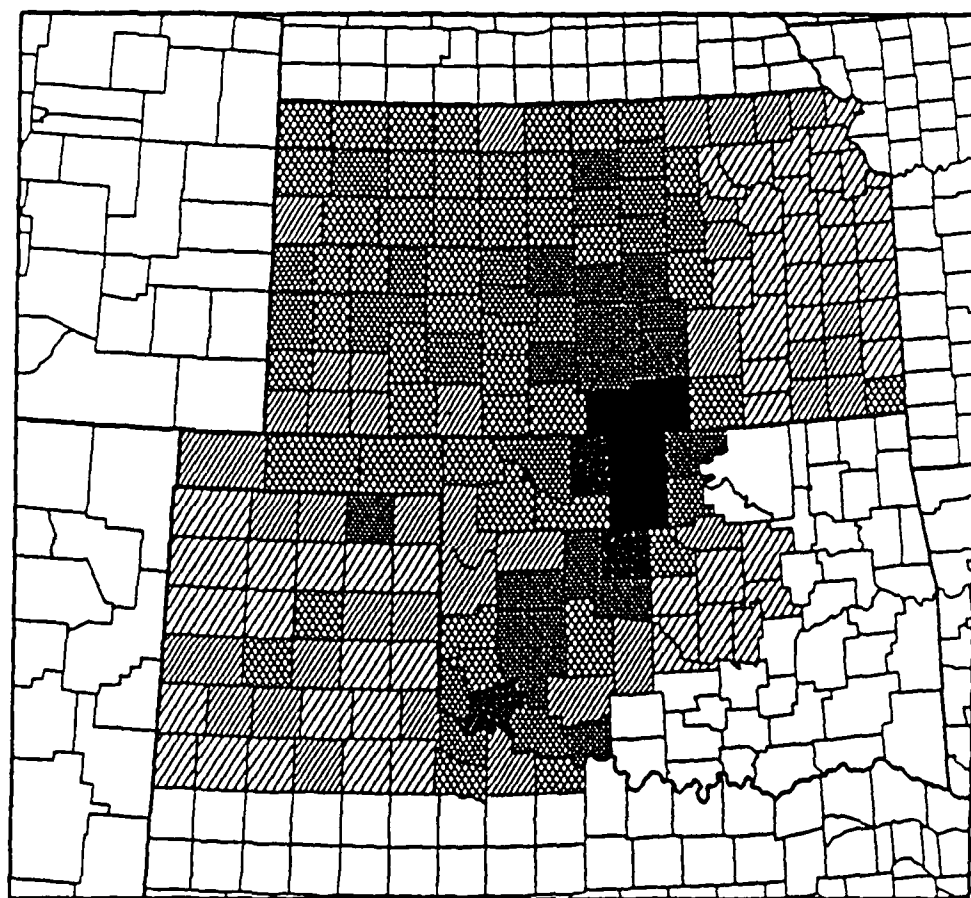
The API used in this investigation was computed using an algorithm from McFarland and Harder (1982). This form was defined as:

$$API(i) = API(i-1) * k + P(i) \quad (12)$$

where k = depletion coefficient

P = effective precipitation

The depletion coefficient was selected in a manner consistent with McFarland and Blanchard (1977) and Harder (1984). It was defined as a



LEGEND: RESP 0 1 2 3
 4 5 6 7

Figure 3. Percentage of 1980 county acreage planted in dryland winter wheat for Kansas, Oklahoma, and Northwest Texas (adapted from Harder, 1984).

sinusoidal curve with a maximum value of 0.92 on 1 February and a minimum value of 0.70 on 1 August. This forces the depletion coefficient to be a function of season, which is related to potential evapotranspiration. The effective precipitation was computed by raising the precipitation, in millimeters, to a power of 0.891. The exponent was initially suggested by Blanchard et al. (1980) in a study involving runoff for watersheds near Chickasha, Oklahoma.

Snowdepth was included in the climatic database to account for accumulated precipitation in the form of snow which would not immediately contribute to the soil moisture content. Once a positive snowdepth had been reported, the API was held constant, and all subsequent precipitation was assumed to occur as snow until the reported snowdepth reached zero. Once the reported snowdepth reached zero, all accumulated precipitation was added to the API computation as effective precipitation.

The 10 channels of interpolated SMMR brightness temperatures were placed in SMMR map files, one file for each day's data. Each file contained 350 records, one record for each of the 35 rows in each of the 10 channels of brightness temperature data. Each record represented one row, which contained 40 bytes of data. The record length was set at 40 bytes since there were 40 brightness temperature values, one per grid cell, in each row. The brightness temperatures were expressed in degrees Kelvin minus 180, and represented an integer between -128 and 127, with -128 reserved for missing data.

The interpolated climatic data values were placed in climatic map files similar to the SMMR map files, with one file per day. Each file

contained 5 channels of data: maximum air temperature, minimum air temperature, precipitation, snowfall, and snowdepth. Like the SMMR files, each byte contained one integer value. The climatic data had to be converted to a form compatible with the computer's numeric range of -128 to 127. Therefore, the temperature data were expressed in degrees Celsius times 2.5, precipitation as millimeters minus 126, and both snowfall and snowdepth as centimeters minus 126. Once again, -128 was reserved for missing values.

The calculated API values between 1 July 1978 and 10 November 1979 were placed in daily API map files similar to the SMMR and climatic map files.

Image processor files were created from SMMR, climatic, API, and GOES data. The GOES image was initially digitized to create numeric intensity values. The numeric values from these four data sources were assigned an intensity level by the image processor, and displayed as a visual image. The numeric values of the input data sources could be manipulated in a variety of ways to display combinations or transformations of the input data to emphasize qualitatively a certain feature.

Secondary Database

The secondary data consisted of geostationary meteorological satellite (GOES) images, National Weather Service (NWS) weather radar summary charts, United States Geological Survey (USGS) topographic and land-use maps, and reported crop production statistics. The first two sources of secondary data gave an indication of the amount of moisture present in the intervening atmosphere between the object sensed and the

radiometer, which would attenuate the brightness temperature signal. The last two data sources gave an indication of the surface roughness and vegetation cover.

Analysis Methods

Temporal Analysis

A computer program was written to prepare individual grid-cell time series files of the daily 10 SMMR brightness temperature values, daily values of the 5 climatic data, and the computed daily API values. The program was structured to compute and print normalized brightness temperature (emissivity) values in lieu of brightness temperature values. Normalized brightness temperature (emissivity) for night coverage, was defined as the ratio of the brightness temperature to the minimum air temperature. For day passes, it was the ratio of the brightness temperature to the maximum air temperature. This normalization of the brightness temperature has the major function of removing seasonal and shorter period temperature trends from the data, but also was assumed to approximate the emitting-layer temperature, following work by Theis (1979). This program would also plot any series of data for a particular grid cell in order to identify monthly, bi-monthly, or annual trends.

Another computer program was written to analyze statistically any combination of two of these 16 available channels, for any specified period of time. The methodology used involved simple and multiple linear regression, following previous work by Rodgers and Siddalingaiah

(1983) and Harder (1984).

Harder (1984) investigated the relationship between API and the response from 54 combinations of 1.66 cm wavelength passive microwave brightness temperature, surface temperature, and/or a sinusoidal function of the day of the year. He found that three of these indices accounted for most of the variance in the linear regression model.

A computer program was written to use data from any of the 5 SMMR wavelengths to compute these three indices: horizontally polarized normalized brightness temperature (T_h/T), polarization difference ($T_v - T_h$), and normalized polarization difference $[T_v - T_h / 0.5(T_v + T_h)]$. The program would also compute statistics using these indices on either a monthly, bi-monthly, or annual basis. The bi-monthly analysis could be accomplished by using either the Jan-Feb series Harder used, or a Feb-Mar series, which was thought to be a better representation for the winter wheat calendar during the fall months, over this study area.

Areal Analysis

The areal analysis utilized numeric map files spanning the entire study area for any one particular day. These map files contained all 10 channels of SMMR brightness temperature data, the 5-channel climatic data, and the 1-channel computed API. An example of these files for one selected case study day, 10 May 1979, is given in Appendix A, Figures A-1 through A-16. These numeric files were processed into visual images which were used for qualitative comparisons between data sources and selected channels within data sources. These image processor files were combined numerically in a variety of ways to illustrate

and help identify patterns not readily discernible on the initial numeric map files.

The numeric map files, image processor files, GOES imagery, and NWS radar summary charts, were used in the selection of specific case study days. Once these days were chosen, the USGS topographic and land-use maps, and the reported crop statistics, provided additional insight into identifying the observed patterns.

CHAPTER IV

ANALYSIS AND DISCUSSION

Qualitative Analysis Methods

Temporal Analysis

The initial analysis consisted of a qualitative screening of a grid cell 16-channel time series file. The first step in the selection process to determine which grid cell to select, involved the use of the USGS topographic and land-use maps for the location of a relatively flat agricultural area near the center of the study area. The reported crop and county statistics from the State Crop and Livestock Reporting Service were then examined to identify a county with a large percentage of winter wheat acreage. Sumner County, Kansas, located near the center of the study area, was chosen since it had the highest reported county percentage of winter wheat acreage of the entire study area. The grid cell selected, row 15, column 29, was located in the center of the northern half of Sumner County. Similar criteria were used to select six more agricultural case study grid cells spread across the entire study area.

Areal Analysis

The 16-channel time series files extending from 1 July 1978 to 10 Nov 1979 for these case study grid cells were examined to identify individual case study days to be used in an areal analysis. Selection criteria consisted of 5 or more consecutive days with no reported

precipitation, so the observed microwave response would not be unduly biased from a recent rainfall. The location and amount of precipitation were taken from the reported climatic data, and through analysis of the NWS weather radar summary charts. The existence of clouds over the study area was determined through an examination of the GOES imagery taken near the SMMR overpass times. Case study days selected for analysis consisted of: days with no precipitation, days with isolated convective cells resulting in patchy areas of precipitation, and one day with overcast conditions including a line of thunderstorm cells which covered approximately half the study area. This day, 10 May 1979, was selected as the dominant case study day for an areal analysis due to the diverse atmospheric conditions.

Images of all 10 SMMR brightness temperature channels for 10 May 1979 were created through an image processor. Photographs were taken of these images to provide a qualitative comparison of the actual brightness temperature response in these various wavelengths and polarizations. The brightness temperature ranged from approximately 230 K to near 270 K between the 10 channels, with the shorter wavelengths recording the coldest temperatures. The horizontal channels consistently exhibited a larger temperature range for a particular wavelength, which allowed better pattern recognition. The varying resolutions of the SMMR wavelengths were obvious on the images ranging from high resolution on the shorter wavelength imagery to rather low resolution of the longer wavelength imagery. Each individual 20 x 20 km grid cell was evident on the 0.81 cm wavelength imagery, while up to 12 grid

cells indicated nearly identical temperatures on the 4.54 cm wavelength imagery.

Figure 4a is a reproduction of the GOES imagery acquired near the SMMR overpass time. This image shows the cloud cover present when the brightness temperature data was collected, with circular thunderstorm cells indicated along the squall line. Figure 4b is an MB or thunderstorm enhancement of the GOES image, which indicates the presence of thunderstorms over most of the western half of the study area. The NWS weather radar summary chart depicted in Fig. 5, indicated a squall line with associated areas of heavy precipitation located northeast-southwest, just east of the center of the study area. The area of maximum precipitation indicated by the climatic data, was located along the squall line, with a secondary maximum running from the southwestern corner of Kansas, northeast to the center of the northern border of Kansas. The recorded precipitation amount was greatest near the top of the study area, near the Kansas border. These two isolated areas of heavy precipitation made this day a rather unique and very informative case study day.

Images created from the actual numeric brightness temperature values greatly enhanced the visual patterns indicated by both polarizations of the five wavelengths of the SMMR brightness temperatures. Specific patterns were evident on each of the different wavelength map files of the SMMR brightness temperatures. An explanation of the identifiable patterns seen on the various wavelength files can be provided by Fig. 6, which gives the atmospheric water vapor and oxygen attenuation curves. The actual SMMR wavelengths are given to assist in



Figure 4a. GOES satellite image valid 0701Z, 10 May 1979.



Figure 4b. GOES satellite image (MB enhancement) valid 0631Z, 10 May 1979.

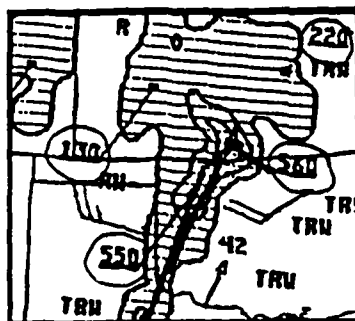


Figure 5. NMS weather radar summary chart valid 0635Z, 10 May 1979.

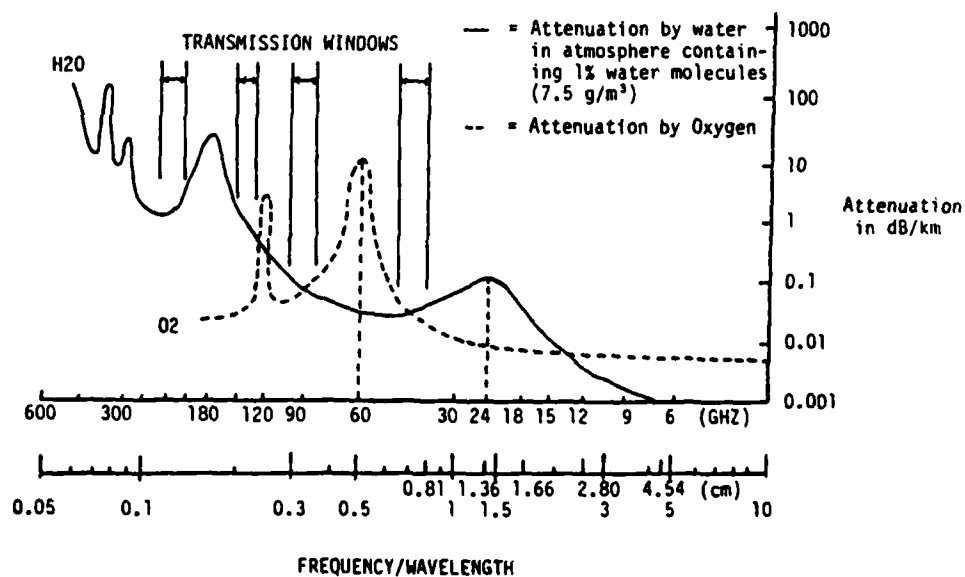


Figure 6. Atmospheric attenuation of microwave radiation from water vapor and oxygen (adapted from Lintz and Simonett, 1976).

evaluating the influence of the intervening atmosphere on the response from each specific wavelength. A comparison of both polarizations of the 0.81 and 1.66 cm wavelength imagery is provided by Fig. 7. The brightness temperature pattern seen on both the horizontal and vertical polarization photographs of each wavelength illustrates the varying response of the brightness temperature resulting from the effects of the intervening atmosphere. This pattern is more pronounced on the horizontal polarization photographs, illustrating the opportunity to extract more information from horizontally polarized brightness temperature data in a qualitative soil moisture analysis.

The patterns on both polarizations of the 2.80 and 4.54 cm wavelength imagery illustrated by Fig. 8, show the coldest temperatures near the top center of the study area close to the Kansas border. This was near the area of the maximum recorded precipitation for the secondary area, and most probably the area of overall maximum surface rainfall at the time of the SMMR overpass. Since this pattern becomes more evident at the longer wavelengths, an explanation based on theory involves the observation that the longer wavelengths are least affected by atmospheric water vapor, while the effect of the intervening atmosphere remains clearly evident of the 1.66 cm and shorter wavelengths. This hypothesis suggests that the optimum wavelength to use to sense surface precipitation or surface soil moisture without significant loss of resolution, would be the 2.80 cm wavelength. While the patterns on the 2.80 and 4.54 cm imagery were very similar, the degraded resolution of the 4.54 cm imagery was quite pronounced. This significantly

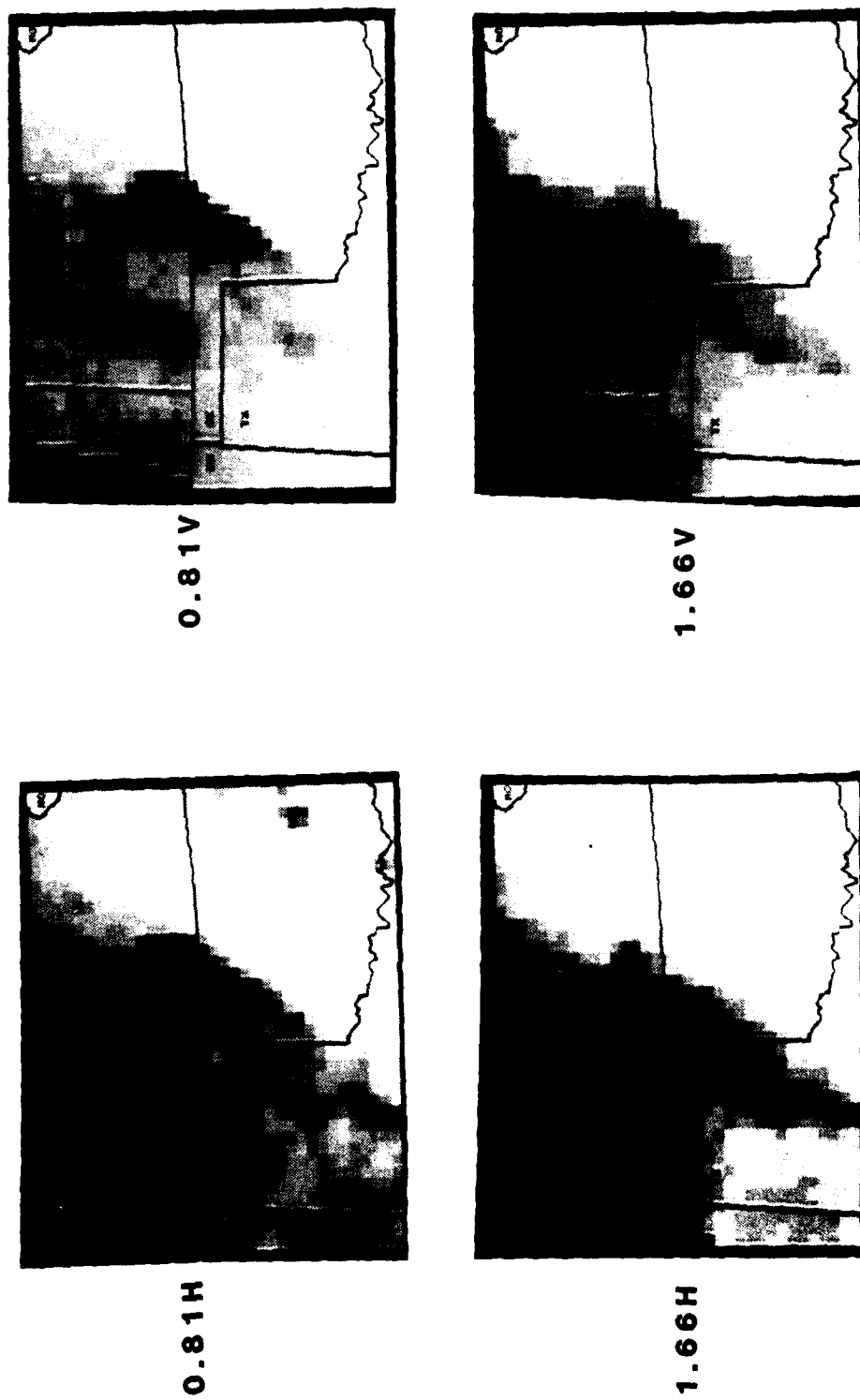


Figure 7. SMMR brightness temperature images for 0.81 and 1.66 cm horizontal and vertical polarizations for 10 May 1979 for the study area.

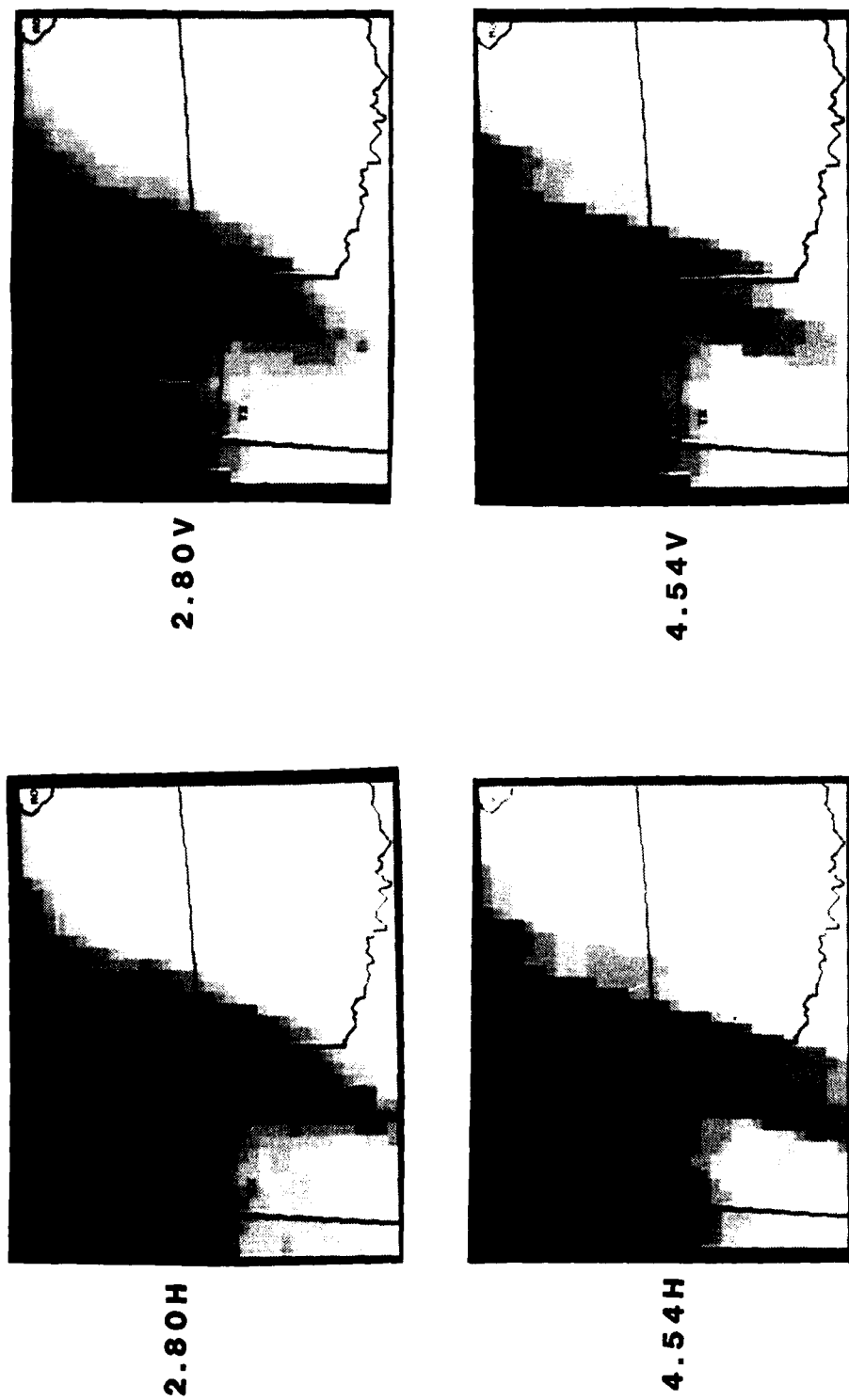


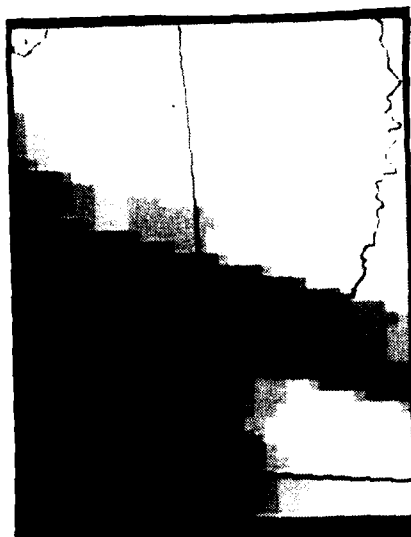
Figure 8. SMMR brightness temperature images for 2.80 and 4.54 cm horizontal and vertical polarizations for 10 May 1979 for the study area.

reduced resolution emphasizes the usefulness of the shorter wavelength imagery when examining large scale patterns.

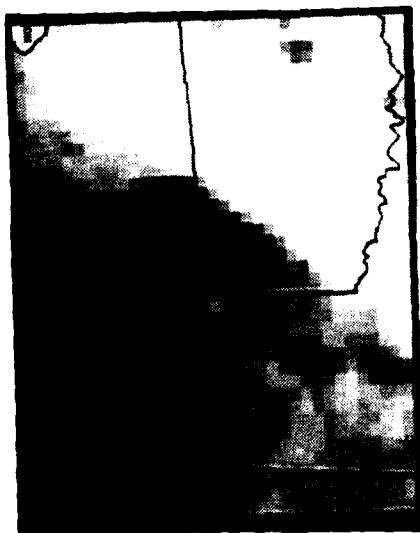
The pattern on the 0.81 cm wavelength imagery shown on Figs. 9 and 10, identified the area of maximum radar backscatter along the squall line, which indicated the maximum area of precipitating clouds. A secondary nearly circular area in southwestern Kansas was also evident on the imagery. This area was covered by precipitating clouds, but received approximately one-fourth the total rainfall amount of the area near the squall line. A likely explanation of the observed phenomena is that the 0.81 cm wavelength signal was strongly attenuated in both cases by the precipitating clouds. The area of maximum radar backscatter along the squall line was clearly discernable only on the 0.81 cm wavelength imagery. The pattern on the 1.36 cm wavelength imagery gave little indication of lower temperature over the area of maximum precipitating clouds, but indicated the area of secondary precipitation in southwestern Kansas. This wavelength is in an atmospheric water vapor attenuation region shown by Fig. 6, which explains the relatively uniform pattern indicated by this imagery. This wavelength is of great usefulness in detecting the presence of atmospheric water vapor, but is of limited usefulness for an investigation into the relationship between passive microwave brightness temperatures and API, or soil moisture. Since this wavelength had the smallest temperature range of all 5 wavelengths, which caused the relatively uniform pattern across the image, it was excluded from the figures provided in this study. The secondary area of maximum precipitation detectable on the 1.36 cm wavelength imagery was defined more vividly on the 1.66 cm



1.66H



4.54H



0.81H



2.80H

Figure 9. SMR brightness temperature images for 0.81, 1.66, 2.80, and 4.54 cm horizontal polarizations for 10 May 1979 for the study area.

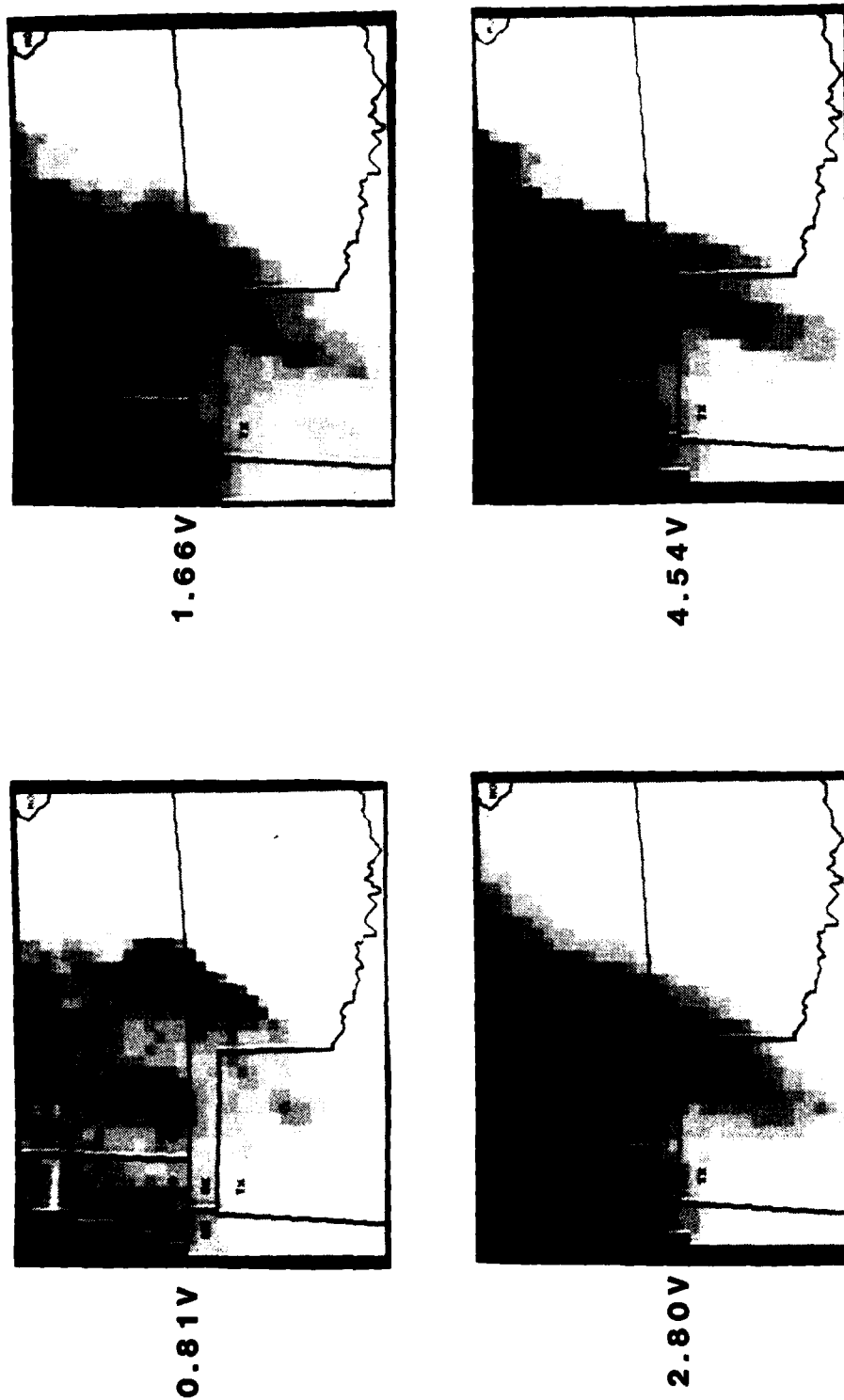


Figure 10. SMR brightness temperature images for 0.81, 1.66, 2.80, and 4.54 cm vertical polarization for 10 May 1979 for the study area.

wavelength imagery without a noticeable loss of resolution. A suggested explanation for this observation is that the brightness temperatures from the 0.81 cm imagery were strongly attenuated by the precipitating clouds, while the 1.36 cm and longer wavelengths provided a better indication of the actual surface moisture conditions. This explanation was weighted by the fact that the reported rainfall indicated by the climatic data was a 24 hour total, while the passive microwave imagery provided an instantaneous response at the time of the SMMR overpass.

Quantitative Temporal Analysis

The quantitative temporal analysis involved correlating various transformations of the SMMR brightness temperatures with the API. The correlation coefficients were compared using the Fisher's Z' transformation described by Brooks and Carruthers (1951). The equation is

$$Z' = 0.5 \ln (1+r/1-r) \quad (13)$$

where r is any correlation coefficient. This Z' statistic has a nearly normal distribution and a standard error independent of the Z' value. The standard error is given by

$$S.E.Z' = 1 / \sqrt{n-3} \quad (14)$$

where n is the number of observations involved in computing the

correlation coefficient. The calculated value of Z' can be used to test the statistical significance of the correlation coefficients. To accomplish this, the $S.E.Z'$ is multiplied by the value of the standard deviation for the selected significance level (i.e. 1.96 for a 0.05 significance level). This result is added to or subtracted from the Z' value to obtain the upper and lower Z' bounds. These Z' bounds can then be converted to correlation coefficient bounds at a particular significance level, by using the inverse of equation (13).

Verification of the API Effective Precipitation Exponent

The effective precipitation exponent used to convert precipitation to effective precipitation in the calculation of the API was 0.891. This partitions rainfall into the soil moisture component (effective rainfall) and runoff. The greater the rainfall, the greater the runoff as a function of the value of the exponent. The significance of this exponent for use in this investigation was evaluated by varying the exponent between 0.85 and 0.95 on a monthly basis for the 1.66 cm wavelength data for row 15 column 29. These data are presented in Appendix B, Table B-1. The monthly variation in the correlation coefficient between the 1.66 cm horizontally polarized normalized brightness temperature and API, shown in Figs. 11a and 11b, was found to be dependent on the amount and type of the observed monthly precipitation. During the months when the precipitation was very high, between March and May, the correlation coefficient remained equally high between all four variations of the effective precipitation exponent. When the rainfall became convective and decreased in total amount, between May

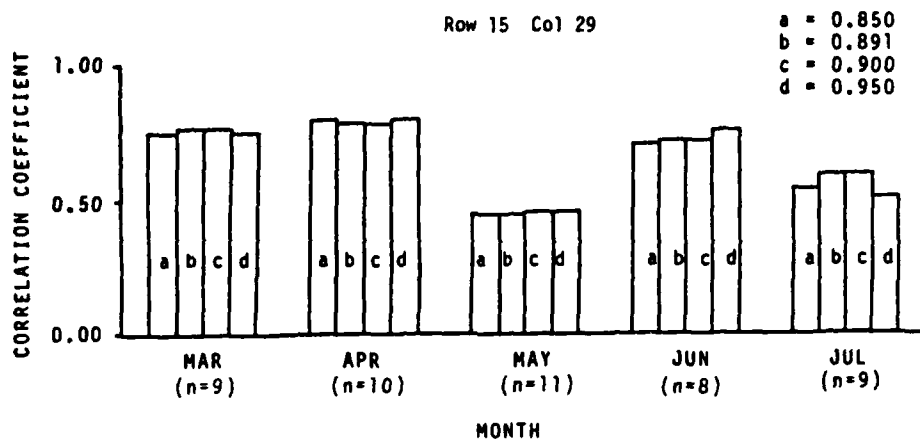


Figure 11a. Comparison of the 1.66 cm wavelength correlation coefficients between the horizontally polarized normalized brightness temperature and four API effective precipitation exponents for March through July 1979.

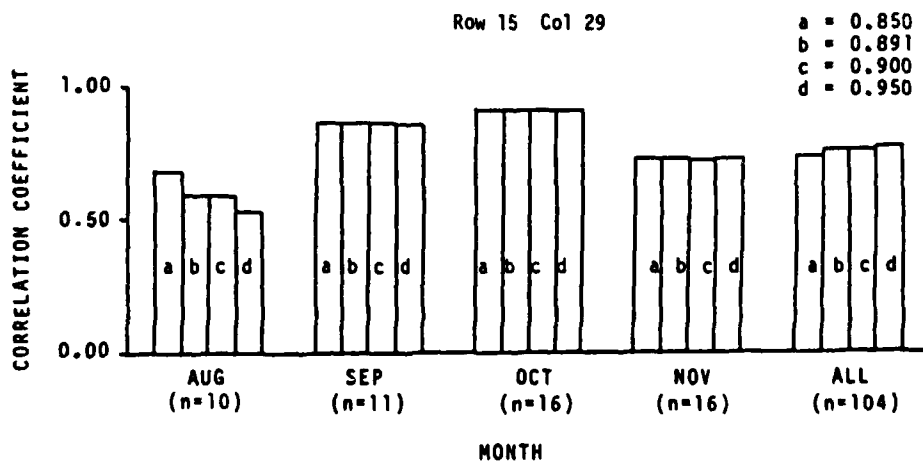


Figure 11b. Comparison of the 1.66 cm wavelength correlation coefficients between the horizontally polarized normalized brightness temperature and four API effective precipitation exponents for August through November 1979 and all months combined.

and August, the difference in the correlation coefficient between the four examples greatly increased. Months with relatively high convective rainfall benefited from the larger effective precipitation exponent, while months with low convective precipitation benefited from the lower exponent. With convective precipitation, large amounts of rainfall often occur over a small area during a short period of time. Often, much of this rainfall contributes to high rates of surface runoff, therefore, the larger effective precipitation exponent would better account for the occurrence of this type of precipitation. Little difference in the correlation coefficient was observed between September and November when precipitation was low. During light rainfall periods, little difference in the way the precipitation was reduced to effective precipitation should be evident since the initial values are minimal. The conclusion is that an effective precipitation exponent of 0.891 is a good exponent to use if one number had to be chosen for the entire year, although a value of 0.90 appears to be equally effective. A better approach would be to vary the exponent monthly based on a climatological and topographic grid cell analysis.

The correlation coefficients for the four effective precipitation exponents were compared using the Fisher's Z' transformation. July and August had the greatest range in correlation coefficients, however no significant difference was found between the correlation coefficients for any of the four effective precipitation exponents for either month, at the 0.05 significance level. The differences in the correlation coefficients between the months were greater than within months, with some months such as April and May being significantly different.

Correlation Analysis on Transforms

The quantitative temporal analysis involved correlating three transforms of the SMMR brightness temperatures with the API. These transforms were the horizontally polarized normalized brightness temperature (T_h/T), the polarized difference transform ($T_v - T_h$), and the normalized polarization difference transform $[T_v - T_h / 0.5(T_v + T_h)]$. The data used to calculate these correlations are given in Appendix B, Tables B-2 to B-8.

Figure 12 provides a comparison between the average correlation coefficient between the horizontally polarized normalized brightness temperature (T_h/T) and the API for the months of April and September 1979. The correlation coefficient is the average of all case study grid cells except Ochiltree County, Texas, (row 21, column 14) due to the presence of a large amount of irrigated acreage. This grid cell was excluded since irrigated soil would contaminate the SMMR brightness temperature correlation with API since the brightness temperatures would indicate a substantial recent rainfall, which would not be evident on the calculated API. April and September were selected since they represent months of predominantly bare soil, which is shown by the Oklahoma Crop Calendar given in Table 3. The best correlation between the SMMR brightness temperature transforms and API should occur under these conditions since the percentage of bare soil and intensity of the precipitation represent the primary influences of the correlation between the SMMR brightness temperature and API. The amount and intensity of precipitation affect the correlation coefficient since the

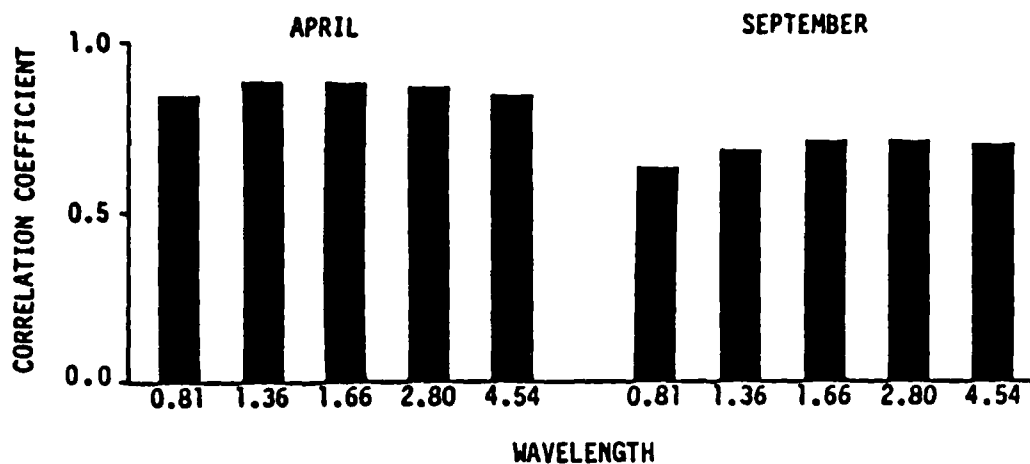


Figure 12. Comparison of the correlation coefficients between the horizontally polarized normalized brightness temperature and API. The correlation coefficients are the average of six grid cells for all SMMR wavelengths for April (n=57) and September (n=65).

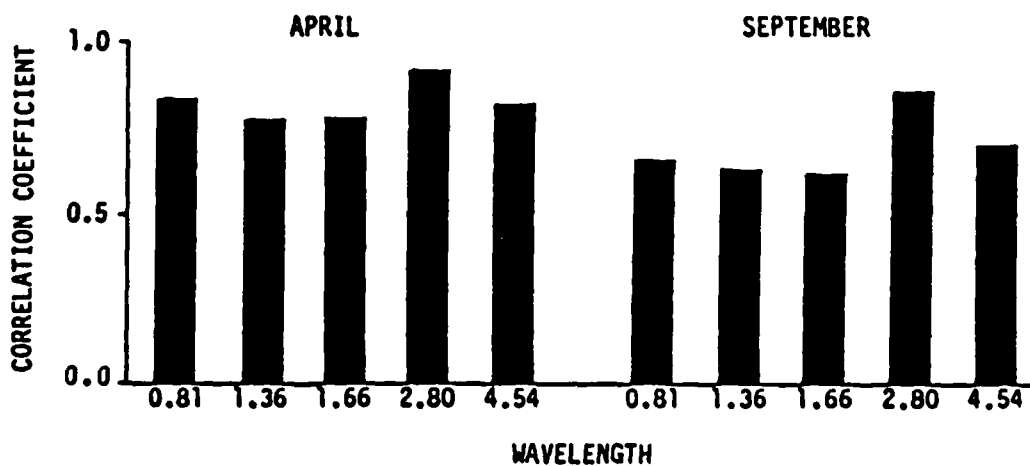


Figure 13. Comparison of the correlation coefficients between the polarization difference transform and API. The correlation coefficients are the average of six grid cells for all SMMR wavelengths for April (n=57) and September (n=65).

TABLE 3
OKLAHOMA CROP CALENDAR

	JAN	FEB	MAR	APR	MAY	JUN	JUL	AUG	SEP	OCT	NOV	DEC
Frost Free				FFFF	FFFF	FFFF	FFFF	FFFF	FFFF			
Growing period												
Winter Wheat						HHH			PPPPPPPPPP			
Barley		PPPPPPPPPP				HHH			PPPPPPPPPP			
Oats		PPPPPPPPPP				HHH			PPPPPPPPPP			
Sorghum				PPPPPPPPPP					HHHHHHHHHH			
Corn				PPPPPPPPPP					HHHHHHHHHH			
Cotton				PPPPPPPPPP					HHHHHHHHHH			
Peanuts				PPPPPPPPPP					HHHHHHHHHH			
Soybeans				PPPPPPPPPP					HHHHHHHHHH			
Alfalfa Hay				HHHHHHHHHH	HHHHHHHHHH	HHHHHHHHHH	HHHHHHHHHH	HHHHHHHHHH	HHHHHHHHHH	HHHHHHHHHH		

AVERAGE PERIOD: FFFF = No Frosts PPPP = Planting HHHH = Harvest

Note: Indicated periods relate to when 5 to 95% of the crop is planted or harvested.
(Adapted from Oklahoma Crop-Weather Bulletin)

sinusoidal moisture depletion is best suited under conditions of high amounts of uniform non-convective rainfall. Under dry conditions, the evapotranspiration curve becomes more linear causing a decrease in the correlation between the API and soil moisture. The correlation coefficients were very high for these months, ranging between 0.84 and 0.90 for April, and between 0.64 and 0.72 for September. The 1.66 cm wavelength correlation coefficient was the highest among all five wavelengths for both months, but not significantly different from the rest of the correlation coefficients, at the 0.05 level. Since the effective precipitation exponent was developed using 1.55 cm wavelength passive microwave data, the 1.66 cm wavelength would be expected to have the highest correlation with API from the five SMMR wavelengths, while a different effective precipitation exponent may work better for another wavelength. All wavelengths of the horizontally polarized normalized brightness temperature had a correlation coefficient near 0.90 over bare ground for all 6 case study grid cells.

Figure 13 gives the same comparisons as Fig. 12, but with the polarization difference ($T_v - T_h$) transform. The correlation coefficients for April range between 0.77 and 0.91, and between 0.61 and 0.87 for September. The correlation coefficients from the 1.36 and 1.66 cm wavelength data decreased considerably, particularly in September, between this transform and the horizontally polarized normalized brightness temperature. The correlation coefficients were compared with each other using the Fisher's Z' transformation. For the month of April, the 2.80 cm correlation coefficient was the highest, but it was not significantly different from either the 0.81 or 4.54 cm wavelength

correlation coefficient, at the 0.05 level. The 1.36 cm wavelength had the lowest correlation coefficient, but not significantly different from the 1.66 cm correlation coefficient. For September, the 2.80 cm wavelength correlation coefficient was significantly higher than any other coefficient, while the remaining four coefficients did not significantly differ from each other. A comparison between wavelengths of the polarization difference transform showed that the correlation coefficients from these wavelengths were nearly identical to those of the *normalized polarization difference transform*.

The correlation coefficients for the normalized polarization difference $[T_v - T_h / 0.5(T_v + T_h)]$ transform, shown by Fig. 14, ranged between 0.73 and 0.91 for April, and between 0.60 and 0.87 for September. The correlation coefficients were compared with each other using the Fisher's Z' transformation. For the month of April, the 2.80 cm correlation coefficient was the highest, but it was not significantly different from either the 0.81 or 4.54 cm wavelength correlation coefficient, at the 0.05 level. The 1.36 cm wavelength had the lowest correlation coefficient, but not significantly different from either the 0.81 or the 1.66 cm correlation coefficient. For September, the 2.80 cm wavelength correlation coefficient was significantly higher than any other coefficient, while the remaining four coefficients did not significantly differ from each other.

Figure 15 is the correlation coefficient from the multiple linear regression on all three transforms. These correlation coefficients ranged between 0.88 and 0.93 for April, and between 0.78 and 0.92 for September. While the 2.80 cm wavelength again had the highest

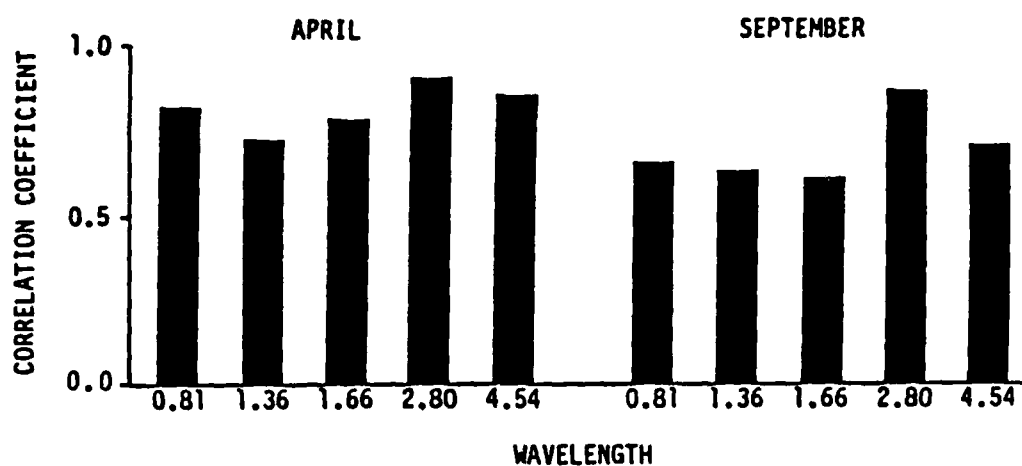


Figure 14. Comparison of the correlation coefficients between the normalized polarization difference transform and API. The correlation coefficients are the average of six grid cells for all SMMR wavelengths for April (n=57) and September (n=65).

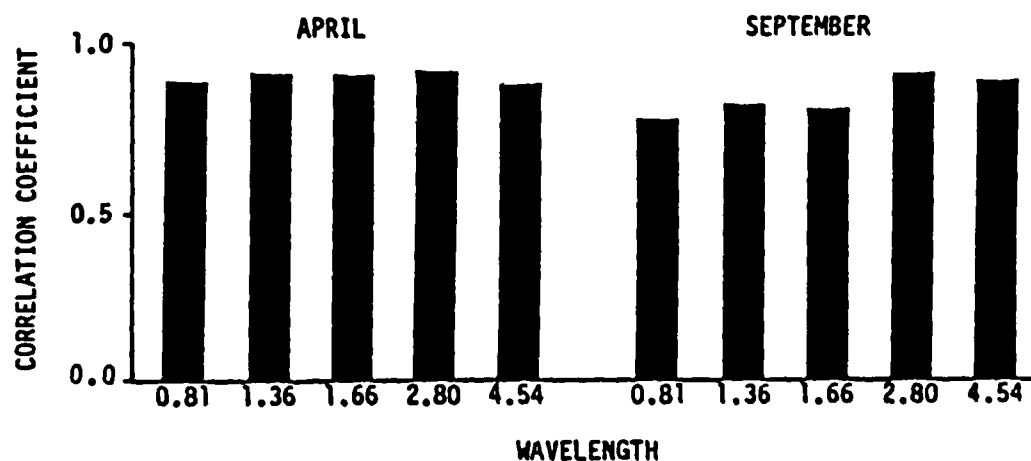


Figure 15. Comparison of the correlation coefficients between multiple linear regression on all three transforms and API. The correlation coefficients are the average of six grid cells for all SMMR wavelengths for April (n=57) and September (n=65).

correlation coefficient for the month of April, it was not significantly higher than any of the other correlation coefficients, at the 0.05 level. For September, the 2.80 cm wavelength correlation coefficient was significantly higher than all other wavelengths, except the 4.54 cm. No significant difference was found between the 0.81, 1.36, and 1.66 cm wavelength correlation coefficients. While the 2.80 cm wavelength correlation coefficient was the highest for both months, the magnitude of this coefficient for both the polarization difference and the normalized polarization difference transforms was approximately equal. This indicates that either one of these transforms of the SMMR brightness temperatures can be used independently to estimate the API over bare soil without the need of an estimate of the surface temperature.

Comparison of Transforms and Multiple Linear Regression

Figures 16a and 16b compare the correlation coefficient for each of the three transforms and the multiple linear regression on all three transforms for all five wavelengths for both April and September respectively. The relative value of each transform indicated by the magnitude of its correlation coefficient is immediately apparent, illustrating the apparent superiority of the 2.80 cm wavelength. An explanation for this observation deals with the atmospheric attenuation of each wavelength and the degrading resolution as the wavelength increases. The 0.81 cm wavelength is attenuated by both atmospheric water vapor and oxygen, thereby correlating better with precipitating clouds rather than API or soil moisture. The 1.36 cm wavelength is in

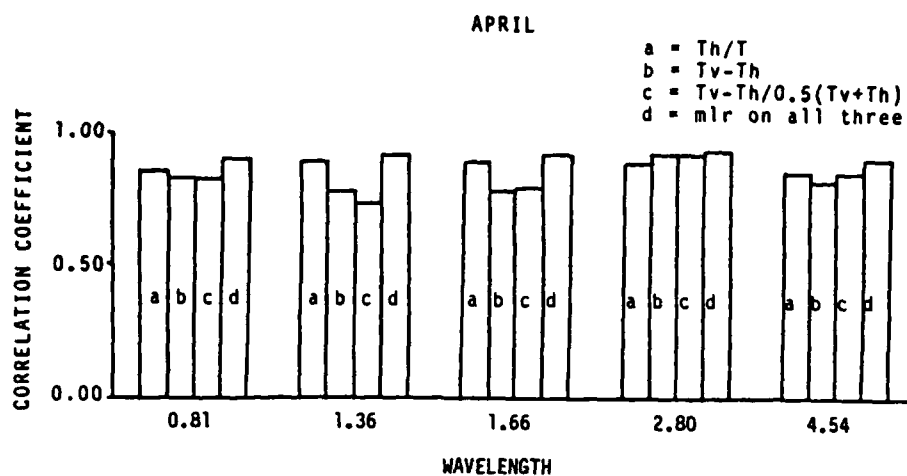


Figure 16a. Comparison of the April correlation coefficients between the three transforms and multiple linear regression (mlr) on all three transforms, and API. The correlation coefficients are the average of six grid cells ($n=57$) for all SMMR wavelengths.

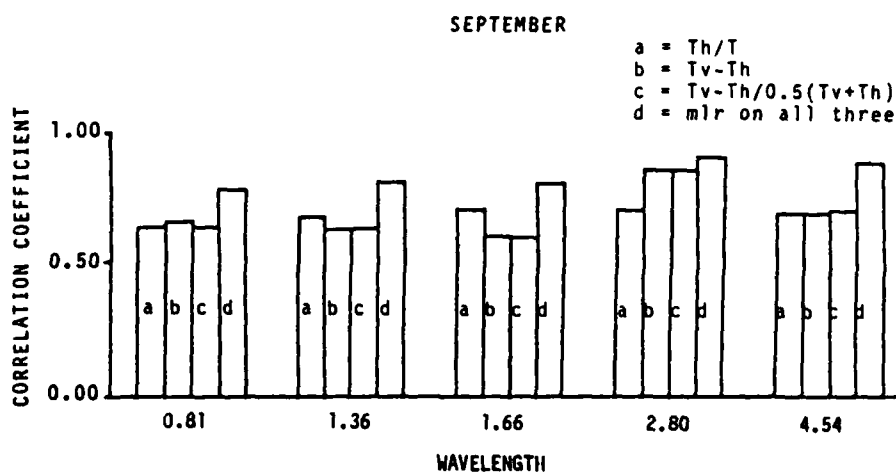


Figure 16b. Comparison of the September correlation coefficients between the three transforms and multiple linear regression (mlr) on all three transforms, and API. The correlation coefficients are the average of six grid cells ($n=65$) for all SMMR wavelengths.

the center of a water attenuation region and therefore would be expected to indicate the observed lower correlation with API. The 1.66 cm wavelength still has a rather high amount of atmospheric water vapor attenuation, but slightly lower than the 1.36 cm band. Therefore, the correlation coefficient between the 1.66 cm wavelength and API should be, and was found to be, slightly higher than the 1.36 cm correlation coefficient. Both the 2.80 and 4.54 cm wavelengths are at the lower end of both the atmospheric water vapor and oxygen attenuation curves (see Fig. 6), and should correlate well with API. The extremely high correlation coefficient from the 2.80 cm wavelength was consistently observed with all case study grid cells throughout the entire year. The correlation coefficient from the 4.54 cm wavelength was lower than that derived when using the 2.80 cm band, which is attributed to the reduced resolution of the longer wavelength, which will dilute the individual grid cell response.

Comparison of Case Study Grid Cells

The monthly correlation coefficient between the horizontally polarized normalized brightness temperature and API for the 1.66 and 2.80 cm wavelengths for the predominantly wheat grid cell, row 15 column 29, is shown in Fig. 17a. Figures 18a-e give the annual API trace, which represents soil moisture, for this grid cell. The monthly variations in the correlation coefficient are primarily the result of changes in amount of both vegetation and rainfall. The actual correlation coefficient remained between 0.75 and 0.90 for the months of March and April as a function of the large rainfall and developing wheat

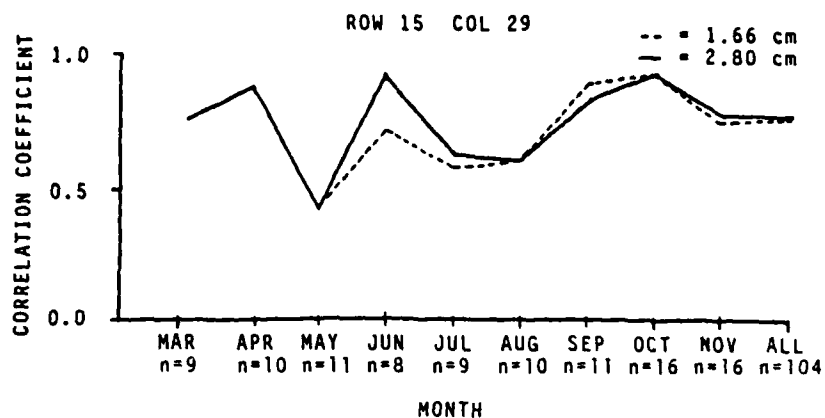


Figure 17a. Comparison of the correlation coefficients between the horizontally polarized normalized brightness temperature and API for row 15 col 29. The correlation coefficients are for both the 1.66 and 2.80 cm SMMR wavelengths.

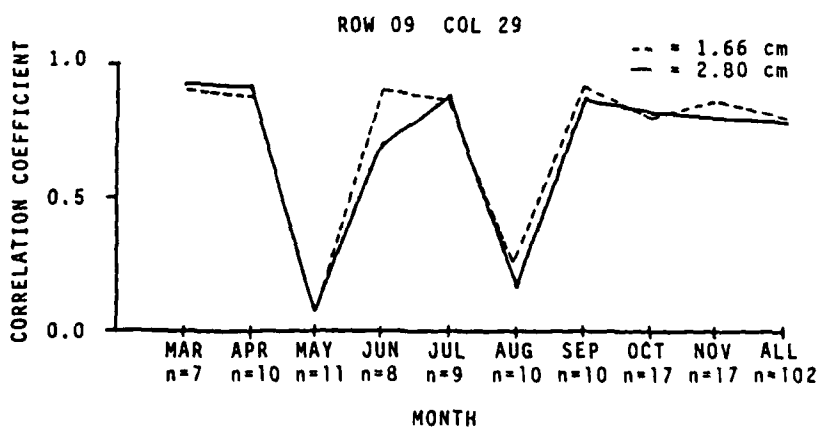


Figure 17b. Comparison of the correlation coefficients between the horizontally polarized normalized brightness temperature and API for row 09 col 29. The correlation coefficients are for both the 1.66 and 2.80 cm SMMR wavelengths.

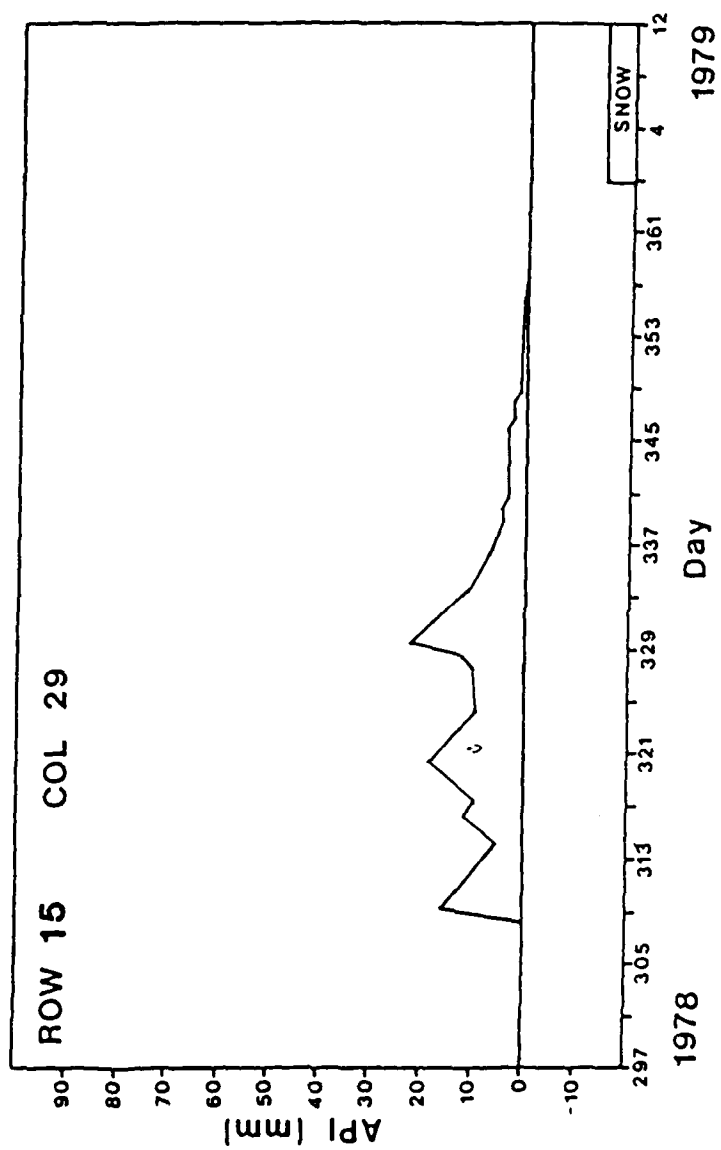


Figure 18a. Time series plots of API for row 15 col 29 between 23 Oct 1978 and 12 Jan 1979.

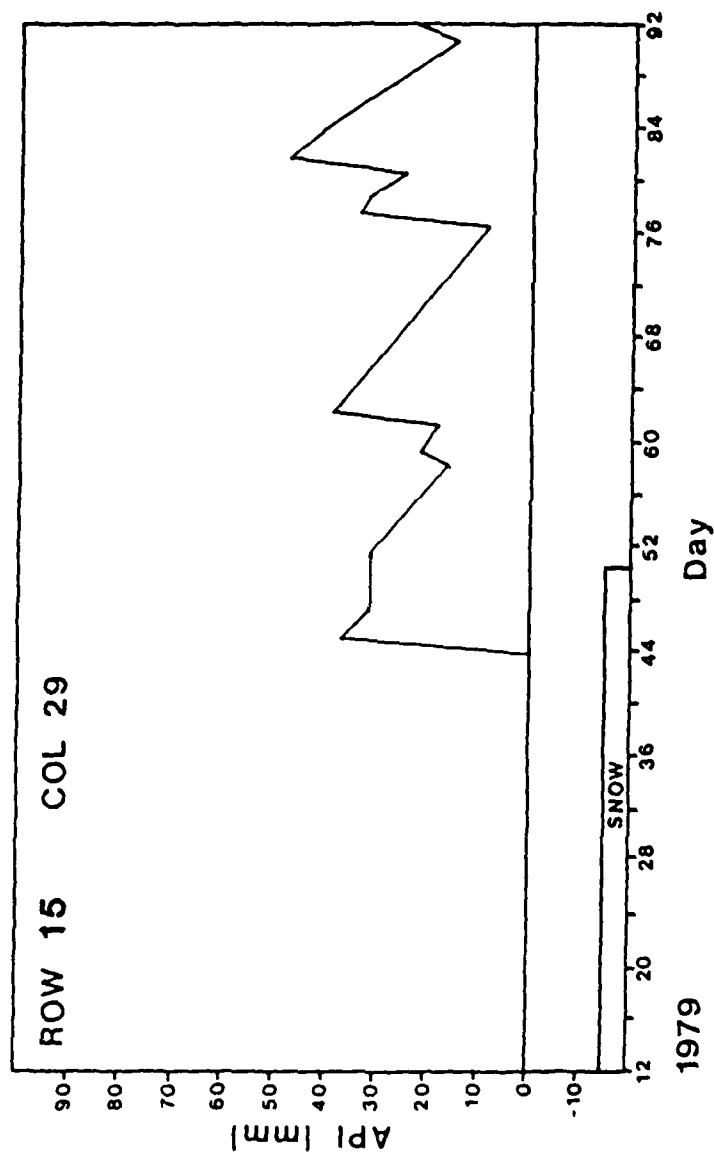


Figure 18b. Time series plots of API for row 15 col 29 between 12 Jan 1979 and 01 Apr 1979.

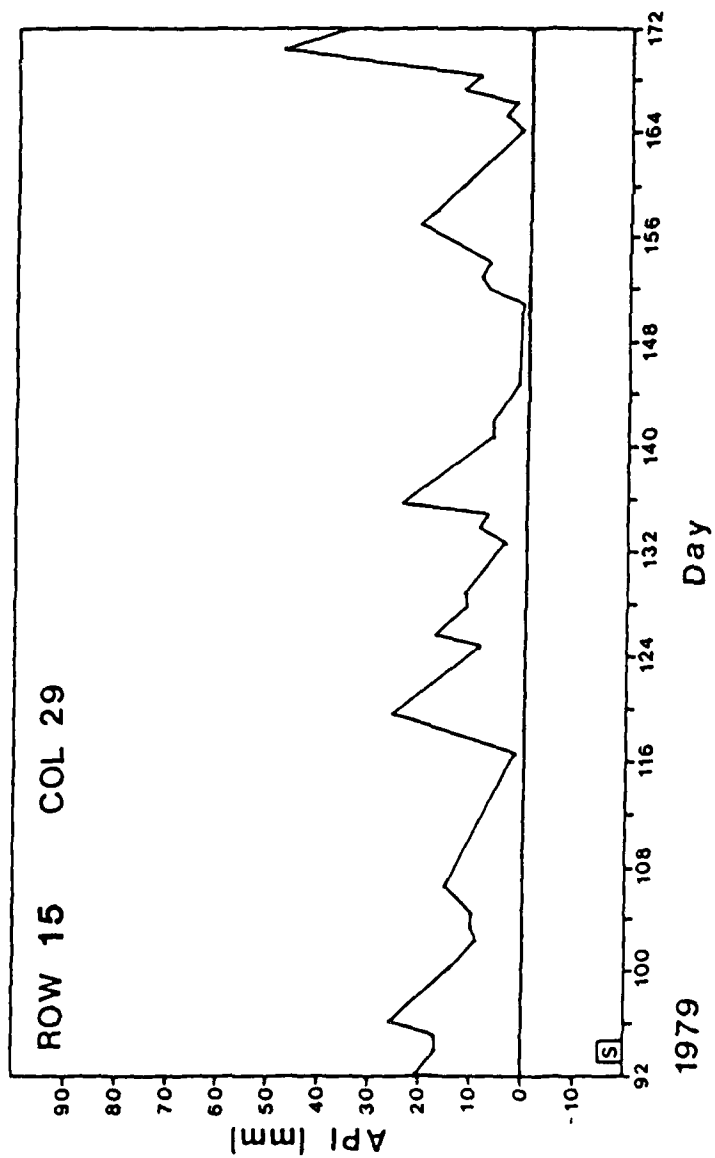


Figure 18c. Time series plots of API for row 15 col 29 between 01 Apr 1979 and 20 Jun 1979.

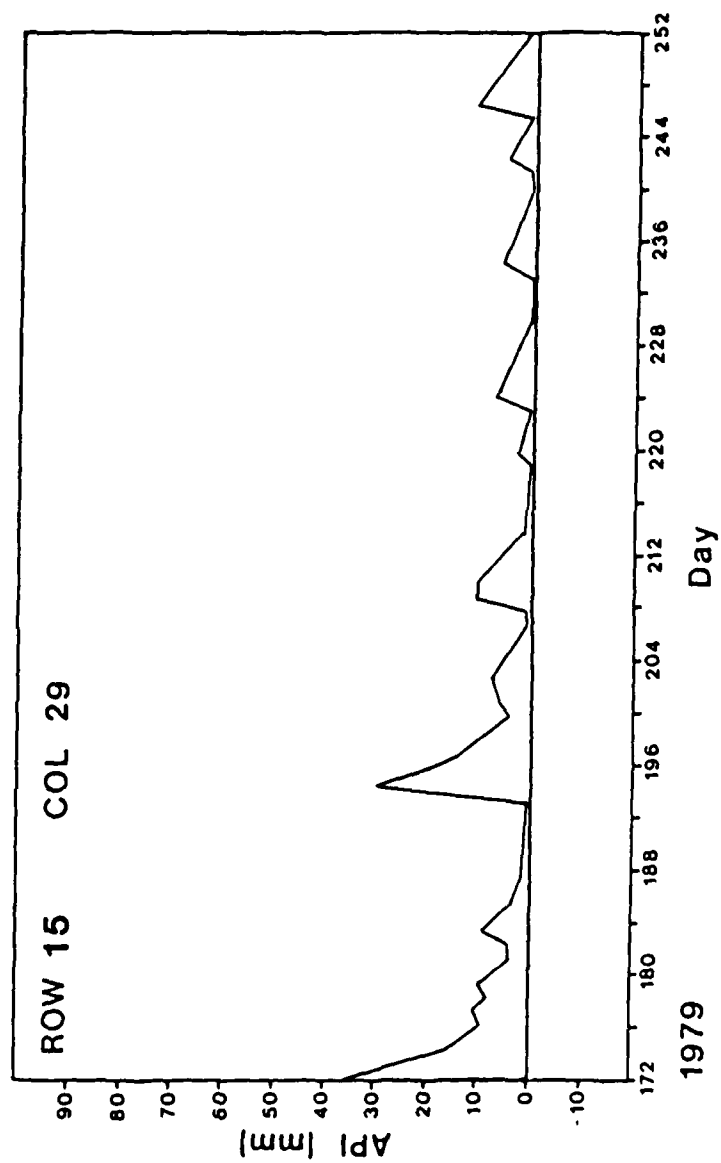


Figure 18d. Time series plots of API for row 15 col 29 between 20 Jun 1979 and 08 Sep 1979.

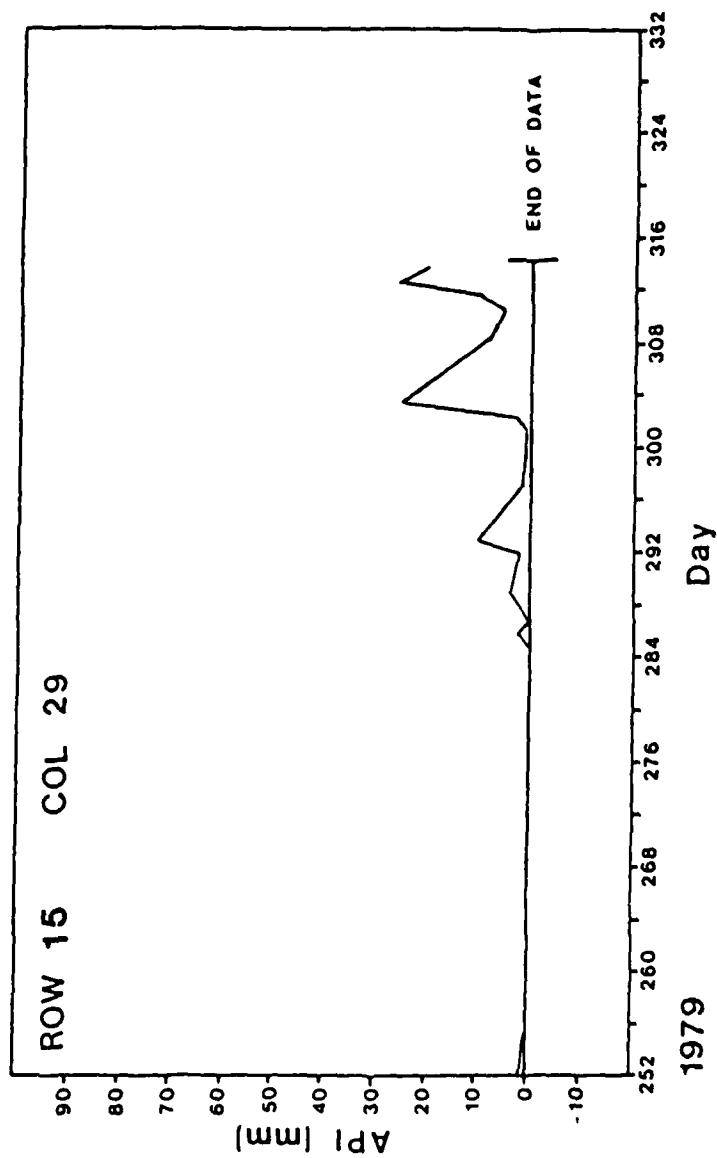


Figure 18e. Time series plots of API for row 15 col 29 between 08 Sep 1979 and 10 Nov 1979.

canopy. By May, the wheat had reached maturity, and the amount of the convective precipitation was less than either March or April. The large drop in the correlation coefficient, from > 0.85 to near 0.40 was due to the increasing reflection from the developing wheat canopy. The wheat harvest occurred in June and the amount of rainfall increased. The increase in bare soil observed by the SMMR sensor contributed to a large rise in the correlation coefficient, which increased to > 0.90 . The low precipitation combined with the effects of the miscellaneous vegetation present in the grid cell, primarily alfalfa hay (see Table 3), caused the correlation coefficient to remain near 0.60 for July and August. By October, as a consequence of the continued dry weather, the vegetative cover declined and the correlation coefficient increased to > 0.80 . By November, the amount of precipitation increased resulting in the development of the winter wheat canopy and a slight decrease of the correlation coefficient to approximately 0.75 . The months of December, January, and February are excluded since the observed brightness temperatures are not related to soil moisture when the soil surface is either frozen or covered with snow.

The monthly correlation coefficient between the horizontally polarized normalized brightness temperature transform and API for the 1.66 and 2.80 cm wavelengths for the mixed wheat and sorghum grid cell, row 09 column 29, is shown in Fig. 17b. The associated annual API trace is given in Figs. 19a-e. The correlation coefficients for March and April are extremely high (near 0.90) due to the predominance of bare soil, short vegetation, and abundant rainfall. By May, the wheat had reached maturity and the precipitation decreased, and the

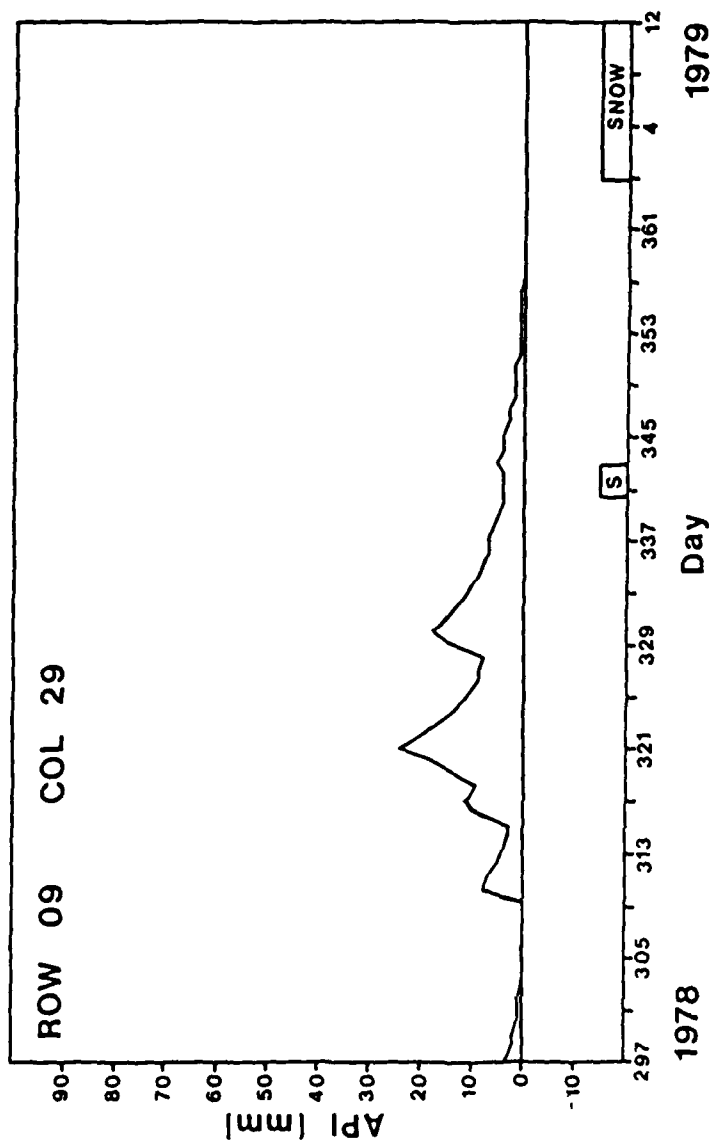


Figure 19a. Time series plots of API for row 09 col 29 between 23 Oct 1978 and 12 Jan 1979.

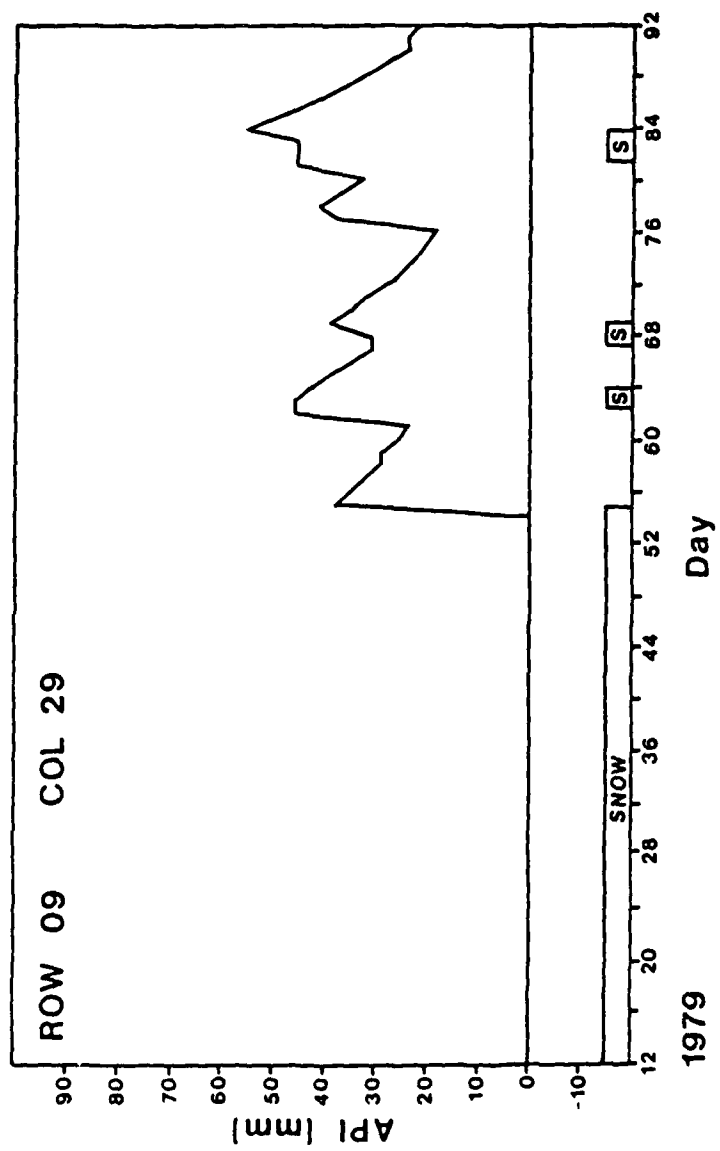


Figure 19b. Time series plots of API for row 09 col 29 between 12 Jan 1979 and 01 Apr 1979.

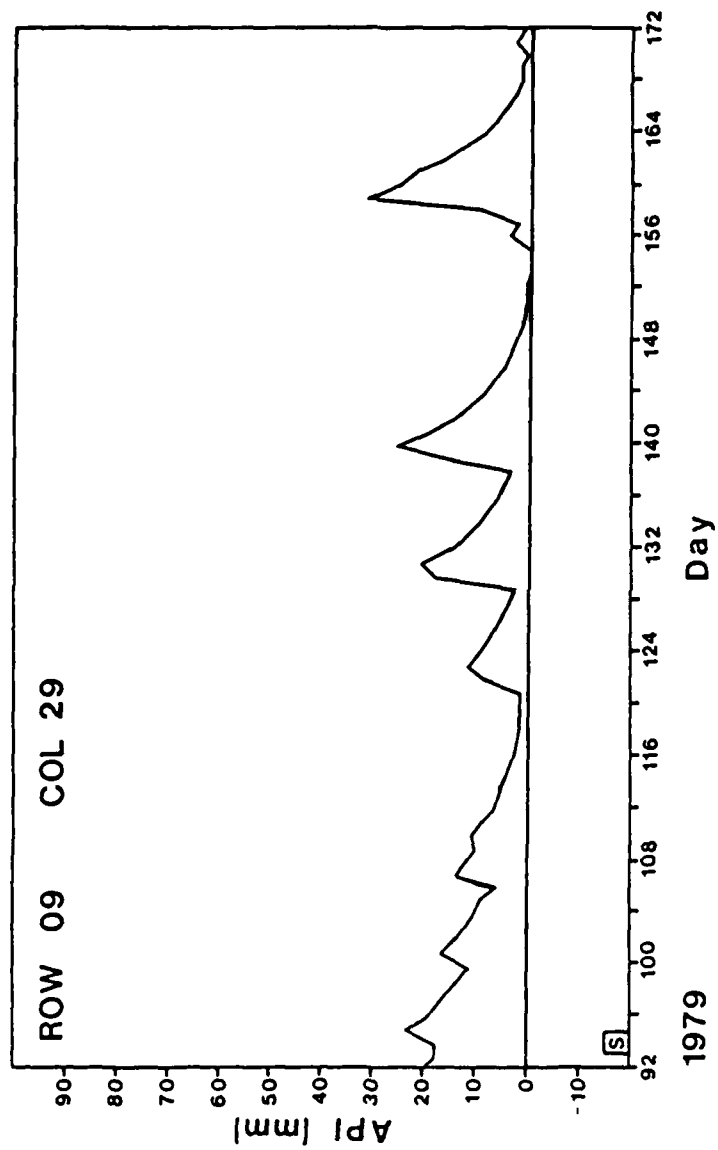


Figure 19c. Time series plots of API for row 09 col 29 between 01 Apr 1979 and 20 Jun 1979.

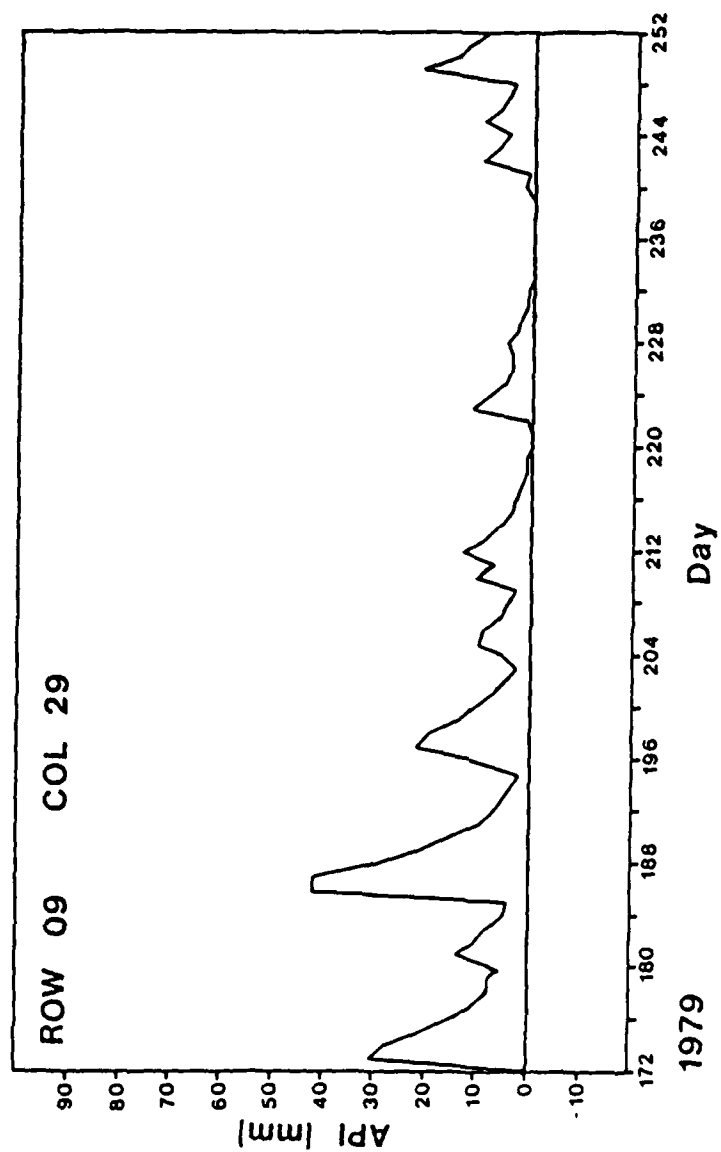


Figure 19d. Time series plots of API for row 09 col 29 between 20 Jun 1979 and 08 Sep 1979.

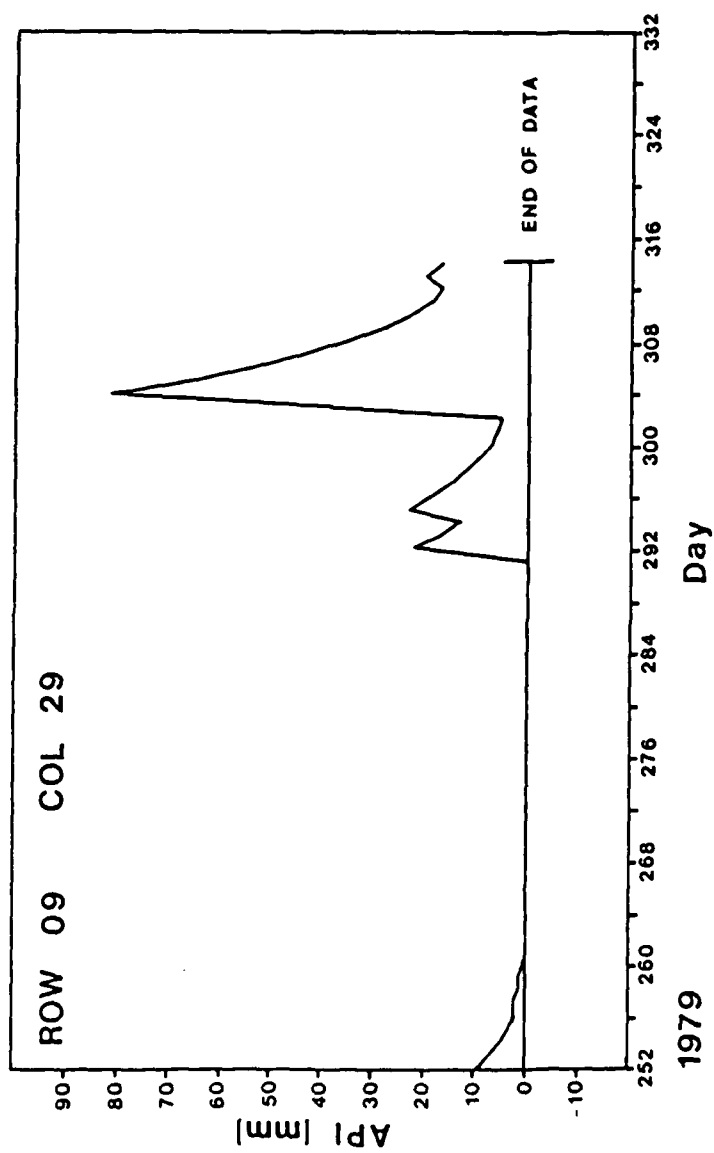


Figure 19e. Time series plots of API for row 09 col 29 between 08 Sep 1979 and 10 Nov 1979.

correlation coefficient plummeted to < 0.10 . In June, the winter wheat was harvested, with the increase in amount of bare soil seen by the SMMR sensor resulting in a increase in the correlation coefficient to > 0.90 for the 1.66 cm wavelength. August had a very low recorded precipitation amount and predominantly bare wheat fields, however, irrigation of the new seedbed and the maturing sorghum crop caused the correlation coefficient to drop to approximately 0.25. By September, the correlation coefficient had risen to approximately 0.90, and stayed between 0.80 and 0.90 through November. This increase was the result of the increased bare soil after the summer crops were harvested and the relatively poor condition of the wheat crop due to the dry soil. The correlation between the SMMR brightness temperatures and the API is significantly better over bare soil. With knowledge of the surface conditions, the changes observed in the correlation coefficients can be interpreted throughout the year. The correlation remains better over a uniform agricultural surface since there are fewer interfering factors, although the correlation coefficient for a mixed agricultural grid cell still reaches the extremely high levels seen in the predominantly wheat grid cell. The thickness and height of vegetation will strongly affect the correlation coefficient however, the type of vegetation in a mixed agricultural grid cell seems to be irrelevant.

Supporting Data

The brightness temperature correlation coefficient and the normalized brightness temperature correlation coefficient matrices for all five wavelengths and both polarizations for row 15 column 29, are given

AD-A145 419

MULTISPECTRAL PASSIVE MICROWAVE CORRELATIONS WITH AN
ANTECEDENT PRECIPITA..(U) AIR FORCE INST OF TECH
WRIGHT-PATTERSON AFB OH G D WILKE AUG 84

22

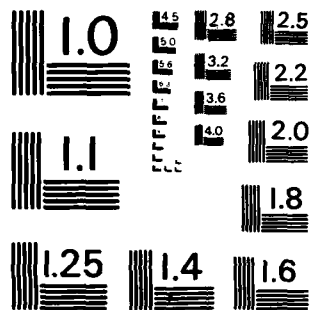
UNCLASSIFIED

AFIT/CI/NR-84-61T

F/G 14/2

NL

END
DATE
FILMED
10-84
DTIC



MICROCOPY RESOLUTION TEST CHART
NATIONAL BUREAU OF STANDARDS-1963-A

in Appendix C, Tables C-1 and C-2. The correlation coefficient between both the horizontally and vertically polarized brightness temperatures and API, for all 7 case study grid cells, is given in Appendix C, Tables C-3 and C-4. The correlation coefficient between the 1.66 cm wavelength transforms and API for both a Jan-Feb and Feb-Mar series are given in Appendix C, Tables C-5 and C-6.

CHAPTER V

SUMMARY AND CONCLUSIONS

Summary

The major purpose of this research was to find ways to estimate the API using multispectral dual polarized passive microwave data. Since the API is by definition strongly related to surface soil moisture, this investigation encompasses estimation of surface soil moisture. This investigation involved selecting and qualitatively analyzing case study days spanning the entire study area. Photographs of the recorded brightness temperatures for a selected case study day were taken to assist in a qualitative areal pattern recognition analysis of all 10 recorded channels of microwave data. A quantitative temporal analysis was accomplished using correlation coefficients between various brightness temperature transforms and API for the case study grid cells on a monthly, bi-monthly, and annual basis.

Conclusions

The brightness temperature range for all five wavelengths was larger in the horizontal polarized channel than the vertical channel. This allowed a more in-depth pattern recognition analysis. The coldest brightness temperature patterns corresponded to areas of maximum precipitation, rather than areas of maximum recorded rainfall.

The 0.81 cm wavelength was strongly attenuated by precipitating clouds and correlated well with atmospheric water vapor content. The resulting pattern on the 0.81 cm wavelength imagery indicated the

presence of clouds and surface moisture for areas where clouds did not attenuate the passive microwave signal. The relatively small brightness temperature range from the 1.36 cm wavelength resulted in a very uniform visual pattern on the brightness temperature imagery. Since this wavelength is in an atmospheric water vapor attenuation region, 1.36 cm data would be of value in detecting the presence of atmospheric water vapor, but is of limited usefulness for a soil moisture investigation. The 1.66 cm wavelength data provided increased pattern detail and responded better to the surface moisture conditions than the shorter wavelength data. The 2.80 cm wavelength data provided the most distinct high resolution brightness temperature pattern of all five available SMMR wavelengths. Since the horizontal polarized channel provided a larger brightness temperature range, the 2.80 horizontally polarized channel would be the best single SMMR channel to use for a surface soil moisture investigation. The 4.54 cm wavelength data responded very well to the surface moisture conditions, however the lower resolution reduced the value of this data for a small area soil moisture investigation.

The API effective precipitation exponent of 0.891 used to convert precipitation to effective precipitation (soil moisture component) worked well for this study area, although a value of 0.90 had essentially the same results. The topography and amount and intensity of the precipitation seemed to be the predominant factors to consider when optimizing an API effective precipitation exponent for a particular area.

The correlation coefficients between the horizontally polarized

normalized brightness temperature (T_h/T) and API for the months of April and September were very high and indicated little difference among the five SMMR wavelengths. The correlation coefficients for this transform over bare ground were near 0.90 for all six case study grid cells. The correlation coefficient between the polarization difference ($T_v - T_h$) transform and API had a larger range of values than the previous transform, and a slightly higher overall value among the five wavelengths for both April and September. The 2.80 cm wavelength had the highest correlation coefficient for all five wavelengths. The correlation coefficients between the normalized polarization difference $[T_v - T_h / 0.5(T_v + T_h)]$ and API were nearly identical to those from the polarization difference transform, with the 2.80 cm wavelength again having the highest correlation coefficient for all five wavelengths for the months of April and September. The correlation coefficients from the multiple linear regression performed on all three transforms were slightly higher than those from any of the individual transforms. The 2.80 cm wavelength again had the highest correlation coefficient, however this value was approximately the same as the value from either the polarization difference transform or the normalized polarization difference transform. This indicates that either one of these transforms could be used independently to estimate the API over bare soil without an estimation of the surface temperature.

Monthly changes in the correlation coefficients between the SMMR brightness temperatures and API can be interpreted throughout the year using supplementary surface observations. The correlation coefficients

are consistently higher over bare soil due to fewer interfering factors, such as the thickness and height of the vegetative cover.

Recommendations for Further Research

The API model can be improved upon by optimizing the effective precipitation exponent used in reducing precipitation to effective precipitation. By accounting for terrain, type and amount of vegetation, soil type and structure, and type and rate of precipitation, an improved effective precipitation exponent could be developed on a single grid cell basis. An improvement over the methodology used in this investigation would be to vary the exponent monthly by either grid cell or latitude. A two-layer model of the effective precipitation curve could be implemented also since the soil dry-down occurs in various stages depending on the available soil moisture.

Atmospheric effects were not specifically accounted for in this investigation. The 0.81 cm wavelength was shown to indicate the presence of precipitating clouds while the 1.36 cm band indicated atmospheric water vapor content. This information could be used to modify the response of the longer wavelengths when inferring surface soil moisture.

A study by Smith and Newton (1983) used simulated passive microwave data to drive a soil moisture model called CONSERVB. With the addition of measured soil moisture data, the usefulness of this model could be tested with multispectral dual polarized SMMR data, to determine whether the CONSERVB or API model correlates better with soil moisture.

The SSM/I sensor aboard the next DMSP satellite will contain similar wavelengths and polarizations as the SMMR sensor. The analysis methodology used in this investigation will be applicable to all future investigations involving this type of data. The conclusions drawn from this investigation should be used as a launching platform for analyzing future passive microwave data utilizing advanced statistical techniques.

REFERENCES

- Baier, W., and G.W. Robertson, 1966: A new versatile soil moisture budget. Can. J. Plant Sci., 46, 299-315.
- Batlivala, P., and F.T. Ulaby, 1977: Estimation of soil moisture with radar remote sensing. Proc. 11th International Symposium on Remote Sensing of Environment, Vol II, 1557-1566.
- Blanchard, B.J., M.J. McFarland, T.J. Schmugge, and E. Rhoades, 1980: Estimation of surface soil moisture with API algorithms and microwave emission. Water Resour. Bull., 17, 767-773.
- Blanchard, B.J., M.J. McFarland, S.W. Theis, and J.G. Richter, 1981: Correlation of spacecraft passive microwave system data with soil moisture indices (API). Final Rep. RSC-3622-4 under NASA contr. NSG-5193, Remote Sensing Center, Texas A&M Univ., 92 pp.
- Brooks, C.E.P., and N. Carruthers, 1953: Handbook of Statistical Methods in Meteorology. H. M. S. O., London, 412 pp.
- Burgy, R.H., 1974: An assessment of remote sensing applications in hydrologic engineering. Rep HEC-RN-4, Contr DACW05-74-C-0034, Burgy and Associates, Davis, CA. 61 pp.
- Burke, H.K., 1980: Evaluation of the effects of varying moisture contents on microwave emissions from agricultural fields. NASA CR-166679, Goddard Space Flight Center, Greenbelt, MD, 53 pp.
- Burke, H.K., and J.H. Ho, 1981: Analysis of soil moisture extraction algorithm using data from aircraft experiments. NASA CR-166719, Goddard Space Flight Center, Greenbelt, MD, 37 pp.
- Burke, W.J., and J.F. Paris, 1975: A radiative transfer model for microwave emissions from bare agricultural soils. NASA TMX-58166, Johnson Space Center, Houston, TX, 29 pp.
- Burke, W.J., T.J. Schmugge, and J.F. Paris, 1979: Comparison of 2.8- and 21-cm microwave radiometer observations over soils with emission model calculations. J. Geophys. Res., 84, 287-294.
- Chang, J., 1968: Climate and Agriculture - An Ecological Survey. Aldine Publishing Company, Chicago, IL, 304 pp.
- Choudhury, B.J., and B.J. Blanchard, 1981: A simulation study of the recession coefficient for antecedent precipitation index. NASA TM 83860, Goddard Space Flight Center, Greenbelt, MD, 25 pp.
- Choudhury, B.J., T.J. Schmugge, A. Chang, and R.W. Newton, 1979: Effect of surface roughness on the microwave emission from soils. J. Geophys. Res., 84, 5699-5706.

- Cihlar, J. and F.T. Ulaby, 1975: Microwave remote sensing of soil water content. Remote Sensing Lab. Tech. Rep. 264-6, University of Kansas Space Technology Center, Lawrence, Kansas. 183 pp.
- Derendinger, G.L., 1971: The relationship of evaporation in the falling rate stage to water diffusivity in soils. P.h.D. Dissertation, Dept. of Soil Physics, Texas A&M University, 103 pp.
- Eagleman, J.R., and W.C. Lin, 1976: Remote sensing of soil moisture by a 21-cm passive radiometer. J. Geophys. Res., 81, 3660-3666.
- Edgerton, A.T., F. Ruskey, D. Williams, A. Stogryn, G. Poe, D. Meeks, and O. Russell, 1971: Microwave emission characteristics of natural materials and the environment (a summary of six years research). Final Tech. Rep. 9016R-8, Aerojet-General Corp., El Monte, CA, 288 pp.
- Harder, P.H., 1984: Soil moisture estimation over the great plains with dual polarization 1.66 centimeter passive microwave data from Nimbus 7. P.h.D. Dissertation, Texas A&M University, 143 pp.
- Harder, P.H., and M.J. McFarland, 1984: Objective Analysis Software for the VAX 11/750. Tech. Memo in preparation, Remote Sensing Center, Texas A&M University, College Station, TX.
- Hardy, K.R., S.H. Cohen, L.K. Rogers, H.K. Burke, R.C. Leupold, and M.D. Smallwood, 1981: An evaluation of the spatial resolution of soil moisture information. NASA CR-166724, Goddard Space Flight Center, Greenbelt, MD, 83 pp.
- Hollinger, J.P., and R.C. Lo, 1983: SSM/I project summary report. NRL Memo Rep. 5055, Naval Research Laboratory, Washington, DC, 106 pp.
- Idso, S.B., R.D. Jackson, R.J. Reginato, B.A. Kimbal, and F.S. Nakayama, 1975a: The dependence of bare soil albedo on soil water content. J. Appl. Meteor., 14, 109-113.
- Idso, S.B., T.J. Schmugge, R.D. Jackson, and R.J. Reginato, 1975b: The utility of surface temperature measurements for the remote sensing of surface soil water status. J. Geophys. Res., 80, 3044-3049.
- Jackson, R.D., J. Cihlar, J.E. Estes, J.L. Heilman, A. Kakle, E.T. Kannemasu, J. Millard, J.C. Price, and C. Wiegard, 1978: Soil moisture estimation using reflected solar and emitted thermal radiation, Soil Moisture Workshop, NASA conf. publ. 2073, Nat. Oceanic & Atmos. Admin., Greenbelt, MD, 219 pp.
- Kirdyashev, K.P., A.A. Chukhlantsev, and A.M. Shutko, 1979: Microwave radiation of the earth's surface in the presence of a vegetative cover. Radiotekhnika i Elektronika, English trans. in Radio Eng. & Electronic Physics, 24, 37-44.

- Kohler, M.A., and R.K. Linsley, 1951: *Predicting the runoff from storm rainfall*, U.S. Weather Bureau Res. Pap. 34, cited in Linsley, et al. (1975).
- Linsley, R.K., Jr., M.A. Kohler, and J.L.H. Paulhus, 1975: Hydrology for Engineers, 2nd ed., McGraw-Hill, New York, 482 pp.
- Lintz, J.Jr., and D.S. Simonett, 1976: Remote Sensing of Environment, Addison-Wesley Publishing Company, Reading, MA., 694 pp.
- McFarland, M.J., 1976: The correlation of SKYLAB L-band brightness temperatures with antecedent precipitation. Preprints Conf. Hydrometeor., Fort Worth, TX, Amer. Meteor. Soc., 60-65.
- McFarland, M.J., 1982: Personal communication.
- McFarland, M.J., and B.J. Blanchard, 1977: Temporal correlations of antecedent precipitation with Nimbus 5 ESMR brightness temperatures. Preprints 2nd Conf. Hydrometeor., Toronto, Ont., Canada, Amer. Meteor. Soc., 311-315.
- McFarland, M.J., and P.H. Harder, 1982: Development of an early warning system of crop moisture conditions using passive microwave. Final rep. RSC-4659, NASA contr. NAS 9-16556, Remote Sensing Center, Texas A&M Univ., 111 pp.
- McFarland, M.J., and P.H. Harder, 1983: Crop moisture conditions assessment with passive microwave radiometry. Preprints International Geoscience and Remote Sensing Symposium, San Francisco, Aug 31 - Sep 2, 1983.
- Meneely, J.M., 1977: Application of the electrically scanning microwave radiometer (EMSR) to classification of the moisture condition of the ground. Earth Satellite Corporation, Washington, DC, Final Rep. under NASA contr. NAS 5-22328, 39 pp.
- Mo, T., and B.J. Choudhury, 1980. Diurnal variation of microwave brightness temperature of soils. Report under NASA contr. NAS 5-24350, CSC/TR-80/6003, Computer Sciences Corporation, Greenbelt, MD, 46 pp.
- Mo, T., T.J. Schmugge, and B.J. Choudhury, 1980: Calculations of the spectral nature of the microwave emission from soils. AgRISTARS rep. SM-GO-04018, NASA TM-82002, Goddard Space Flight Center, Greenbelt, MD, 66 pp.
- Newton, R.W., 1977: Microwave remote sensing and its application to soil moisture detection. Tech. Rep. RSC-81, Remote Sensing Center, Texas A&M Univ., 500 pp.
- Newton, R.W., 1980: Microwave soil moisture measurements and analysis. Final Rep. RSC-3058 under NASA contr. NAS 9-13904, Remote Sensing Center, Texas A&M Univ., 370 pp.

- Newton, R.W., B.V. Clark, J.F. Paris, and W.M. Pitchford, 1982: Orbiting passive microwave sensor simulation applied to soil moisture estimation. TEES-TR-43753-82, Remote Sensing Center, Texas A&M Univ., 208 pp.
- Njoku, E.G., and P.E. O'Neill, 1982: Multifrequency microwave radiometer measurements of soil moisture. IEEE Trans. Geosci. & Rem. Sens., GE-20, 468-475.
- Pandey, P.C., and R.K. Kakar, 1983: A two step linear statistical technique using leaps and bounds procedure for retrieval of geophysical parameters from microwave radiometric data. IEEE Trans. Geosci. & Rem. Sens., GE-21, 208-214.
- Penman, H.L., 1956: Evaporation: An introductory survey. Netherlands J. of Agric. Science, 4, 9-29.
- Poe, G.A., and A.T. Edgerton, 1971: Determination of soil moisture content with airborne microwave radiometry. Summary rep. 4006R-2, NOAA contr. 1-35378, Aerojet-General Corp., El Monte, CA, 61 pp.
- Rodgers, E., and H. Siddalingaiah, 1983: The utilization of Nimbus-7 SMMR measurements to delineate rainfall over land. J. Climate and Appl. Meteor., 22, 1753-1763.
- Rodgers, E., H. Siddalingaiah, A.T.C. Chang, and T. Wilheit, 1979: A statistical technique for determining rainfall over land employing Nimbus 6 ESMR measurements. J. Appl. Meteor., 18, 978-990.
- Saxton, K.E., and A.T. Lenz, 1967: Antecedent retention indexes predict soil moisture. Proc. ASCE J. Hyd. Div. 93, 223-241.
- Schmugge, T.J., 1978: Remote sensing of surface soil moisture. J. Appl. Meteor., 17, 1549-1557.
- Schmugge, T.J., 1980a: Microwave approaches in hydrology. Photogramm. Eng. & Rem. Sens., 46, 495-507.
- Schmugge, T.J., 1980b: Soil moisture sensing with microwave radiometers, 1980 Machine Processing of Remotely Sensed Data Symposium, 346-354.
- Schmugge, T.J., B.J. Blanchard, A. Anderson, and J.R. Wang, 1978: Soil moisture sensing with aircraft observations of the diurnal range of surface temperature. Water Resour. Bull., 14, 798-807.
- Schmugge, T.J., and B.J. Choudhury, 1981: A comparison of radiative transfer models for predicting the microwave emission from soils. Radio Sci., 16, 927-938.
- Schmugge, T.J., P. Gloersen, T. Wilheit, and F. Geiger, 1974: Remote sensing of soil moisture with microwave radiometers. J. Geophys. Res., 79, 317-323.

- Schmugge, T.J., T.J. Jackson, and H.L. McKim, 1979: Survey of methods for soil moisture determination. NASA TM 80587, Goddard Space Flight Center, Greenbelt, MD. 74 pp.
- Schmugge, T.J., T.J. Jackson, and H.L. McKim, 1980: Survey of methods for soil moisture determination. Water Resour. Res., 16, 961-979.
- Schmugge, T.J., J.M. Meneely, A. Rango, and R. Neff, 1977: Satellite microwave observations of soil moisture variations. Water Resour. Bull., 13, 265-281.
- Schmugge, T.J., T. Wilheit, W. Webster, Jr., and P. Gloersen, 1976: Remote sensing of soil moisture with microwave radiometers-II. NASA TN D-8321, Goddard Space Flight Center, Greenbelt, MD, 34 pp.
- Smith, M.R., and R.W. Newton, 1983: The prediction of root zone soil moisture with a water balance - microwave emission model. Tech. Rep. RSC-136 under NASA contr. NAG 5-31, Remote Sensing Center, Texas A&M Univ., 148 pp.
- Spencer, R.W., D.W. Martin, B.B. Hinton, and J.A. Weinman, 1983: Satellite microwave radiances correlated with radar rain rates over land. Nature, 304, 141-143.
- Stucky, B.E., 1975: Analysis of SKYLAB S193 apparent brightness temperatures in a thunderstorm environment. M.S. Thesis, Dept of Meteorology, Univ. of Okla., Norman, 59 pp.
- Theis, S.W., 1979: Surface soil moisture estimation with the Electrically Scanning Microwave Radiometer (ESMR). M.S. Thesis, Dept. of Meteorology, Texas A&M Univ., 45 pp.
- Theis, S.W., M.J. McFarland, W.D. Rosenthal, and C.L. Jones, 1982: Microwave remote sensing of soil moisture. NASA CR 166822, Goddard Space Flight Center, Greenbelt, MD, 131 pp.
- Ulaby, F.T., 1974: Radar measurement of soil moisture content. IEEE Trans. Antennas Propagat., AP-22, 257-265.
- Ulaby, F.T., and P.P. Batlivala, 1974: Optimum radar parameters for mapping soil moisture. IEEE Trans. Geosci. Elect., GS-14, 81-93.
- Ulaby, F.T., J. Cihlar, and R.K. Moore, 1974: Active microwave measurements of soil water content. Remote Sensing Environ., 3, 185-203.
- Ulaby, F.T., G. A. Bradley, M.C. Dobson, and J. E. Bare, 1977: Analysis of the active microwave response to soil moisture, part II, Vegetation Covered Ground, RSL Tech. Rep, Univ. of Kansas Center for Research, Inc.

- Ulaby, F.T., P. P. Batlivala, and M.C. Dobson, 1978: Microwave backscatter dependence on surface roughness, soil moisture and soil texture, I, Bare soil, IEEE Trans. Geosci. Elec., GS-16, 286-295.
- Van Bavel, C.H.M., and R. Lascano, 1980: CONSERVB - a numerical method to compute soil water content and temperature profiles under a bare surface. Tech. rep. RSC-134 under NASA contr. 9-13904, Remote Sensing Center, Texas A&M Univ., 73 pp.
- Wang, J.R., 1980: The dielectric properties of soil-water mixtures at microwave frequencies. Radio Sci., 15, 977-985.
- Wang, J.R., and B.J. Choudhury, 1981: Remote sensing of soil moisture content over bare field at 1.4 GHz frequency. J. Geophy. Res., 86, 5277-5282.
- Wang, J.R., J.E. McMurtrey, III, E.T. Engman, T.J. Jackson, T.J. Schmugge, W.I. Gould, W.S. Glazar, and J.E. Fuchs, 1981: Radiometric measurements over bare and vegetated fields at 1.4 GHz and 5 GHz frequencies. AgRISTARS Rep. SM-G1-04113, NASA TM-82151, Goddard Space Flight Center, Greenbelt, MD, 23 pp.
- Wang, J.R., and T.J. Schmugge, 1978: An empirical model for the complex dielectric permittivity of soils as a function of water content. NASA TM 79659, Goddard Space Flight Center, Greenbelt, MD, 35 pp.
- Wang, J.R., and T.J. Schmugge, 1980: An empirical model for the complex dielectric permittivity of soils as a function of water content. IEEE Trans. Geosci. Elec., GE-18, 288-295.
- Wang, J.R., T.J. Schmugge, J.E. McMurtrey, III, W.I. Gould, and W.S. Glazar, 1981: A multi-frequency radiometric measurement of soil moisture content over bare and vegetated fields. AgRISTARS rep. SM-G1-04178, NASA TM-83842, Goddard Space Flight Center, Greenbelt, MD, 16 pp.
- Wang, J.R., J.C. Shiue, S.L. Chuang, and M. Dombrowski, 1980a: Thermal microwave emissions from vegetated fields: a comparison between theory and experiment. NASA TM-80739, Goddard Space Flight Center, Greenbelt, MD, 27 pp.
- Wang, J.R., J.C. Shiue, and J.E. McMurtrey, III, 1980b: Microwave remote sensing of soil moisture content over bare and vegetated fields. Geophy. Res. Letters, 7, 801-804.
- Weger, E., 1960: Apparent sky temperatures in the microwave region. J. Meteor., 17, 159-165.
- Wilheit, T., 1978: Radiative transfer in a plane stratified dielectric. IEEE Trans. Geosci. Elec., GE-16, 138-143.

APPENDIX A
AREAL MAPS OF SMMR, CLIMATIC, AND API DATA

ORBITED SMMR BRIGHTNESS TEMPERATURES (minus 200) FROM FILE EN79130X, CHANNEL 1																																											
	1	2	3	4	5	6	7	8	9	10	11	12	13	14	15	16	17	18	19	20	21	22	23	24	25	26	27	28	29	30	31	32	33	34	35	36	37	38	39	40			
1	-99	-99	-99	-99	46	46	46	48	48	46	47	48	48	43	42	43	46	45	46	44	44	47	47	50	52	55	56	56	56	56	56	56	56	56	56	56	56	56	56	56	56	56	
2	-99	-99	-99	-99	46	46	47	49	49	47	49	49	49	43	43	43	43	43	43	46	46	46	48	48	47	50	52	53	57	58	59	59	59	59	59	59	59	59	59	59	59	59	
3	-99	-99	-99	-99	45	46	46	48	47	47	48	49	48	43	46	45	47	47	47	47	47	47	47	47	47	50	52	53	56	57	57	57	57	57	57	57	57	57	57	57	57	57	57
4	-99	-99	-99	-99	44	44	46	47	47	47	47	47	47	47	47	47	47	47	47	47	47	47	47	47	47	50	52	53	56	57	57	57	57	57	57	57	57	57	57	57	57	57	57
5	-99	-99	-99	-99	47	46	43	45	46	46	47	47	47	47	47	47	47	47	47	47	47	47	47	47	47	50	52	53	56	57	57	57	57	57	57	57	57	57	57	57	57	57	57
6	-99	-99	-99	-99	45	45	45	46	47	49	50	49	47	47	47	47	47	47	47	47	47	47	47	47	47	50	52	53	56	57	57	57	57	57	57	57	57	57	57	57	57	57	57
7	-99	-99	-99	-99	46	46	46	48	47	49	51	52	51	49	47	46	45	48	50	48	51	52	51	49	49	50	54	58	56	60	63	66	67	64	62	60	63	62	62	62	62	62	
8	-99	-99	-99	-99	46	46	46	48	47	48	50	52	52	52	52	52	52	52	52	52	52	52	52	52	52	52	52	52	52	52	52	52	52	52	52	52	52	52	52	52	52	52	52
9	-99	-99	-99	-99	46	46	48	50	50	52	52	52	52	52	52	52	52	52	52	52	52	52	52	52	52	52	52	52	52	52	52	52	52	52	52	52	52	52	52	52	52	52	52
10	-99	-99	-99	-99	44	44	45	46	49	51	53	53	52	46	44	45	47	49	51	52	51	49	46	43	36	37	46	53	56	59	61	61	64	66	66	64	63	64	66	67	66	66	
11	-99	-99	-99	-99	44	44	45	47	50	52	54	54	54	54	54	54	54	54	54	54	54	54	54	54	54	54	54	54	54	54	54	54	54	54	54	54	54	54	54	54	54	54	54
12	-99	-99	-99	-99	45	45	45	48	51	52	54	53	50	43	42	40	46	51	52	51	50	47	45	43	43	47	54	60	59	62	64	68	68	67	65	65	65	65	65	65	65	65	
13	-99	-99	-99	-99	44	44	44	46	48	50	51	51	48	43	39	39	47	50	50	49	49	48	43	41	28	26	43	59	63	64	67	69	68	68	67	67	67	67	67	67	67	67	
14	-99	-99	-99	-99	41	41	42	44	48	50	51	49	46	42	37	31	38	48	52	51	53	50	48	43	42	30	13	43	63	65	68	69	68	67	67	67	67	67	67	67	67	67	
15	-99	-99	-99	-99	43	41	40	44	46	48	50	46	43	40	33	28	27	34	54	53	50	45	44	42	30	13	43	63	65	68	69	68	67	67	67	67	67	67	67	67	67	67	
16	-99	-99	-99	-99	44	44	44	46	48	50	46	43	40	33	28	27	34	54	53	50	45	44	42	30	13	43	63	65	68	69	68	67	67	67	67	67	67	67	67	67	67	67	
17	-99	-99	-99	-99	48	48	49	51	50	49	48	46	46	47	51	53	54	55	53	51	47	43	37	33	33	45	58	67	69	68	69	70	68	68	69	70	67	67	67	67	67	67	
18	-99	-99	-99	-99	50	50	51	52	50	49	47	45	47	48	49	49	52	53	52	52	49	46	35	32	39	48	59	66	69	68	67	66	65	65	65	65	65	65	65	65	65	65	
19	-99	-99	-99	-99	50	50	51	51	50	50	49	47	45	47	48	49	49	52	53	52	52	49	46	35	32	39	48	59	66	69	68	67	66	65	65	65	65	65	65	65	65	65	
20	-99	-99	-99	-99	51	51	51	50	50	49	47	45	47	48	49	49	52	53	52	52	49	46	35	32	39	48	59	66	69	68	67	66	65	65	65	65	65	65	65	65	65	65	
21	-99	-99	-99	-99	51	51	51	50	50	49	47	45	47	48	49	49	52	53	52	52	49	46	35	32	39	48	59	66	69	68	67	66	65	65	65	65	65	65	65	65	65	65	
22	-99	-99	-99	-99	51	51	51	50	50	49	47	45	47	48	49	49	52	53	52	52	49	46	35	32	39	48	59	66	69	68	67	66	65	65	65	65	65	65	65	65	65	65	
23	-99	-99	-99	-99	51	51	51	50	50	49	47	45	47	48	49	49	52	53	52	52	49	46	35	32	39	48	59	66	69	68	67	66	65	65	65	65	65	65	65	65	65	65	
24	-99	-99	-99	-99	51	51	51	50	50	49	47	45	47	48	49	49	52	53	52	52	49	46	35	32	39	48	59	66	69	68	67	66	65	65	65	65	65	65	65	65	65	65	
25	-99	-99	-99	-99	51	51	51	50	50	49	47	45	47	48	49	49	52	53	52	52	49	46	35	32	39	48	59	66	69	68	67	66	65	65	65	65	65	65	65	65	65	65	
26	-99	-99	-99	-99	51	51	51	50	50	49	47	45	47	48	49	49	52	53	52	52	49	46	35	32	39	48	59	66	69	68	67	66	65	65	65	65	65	65	65	65	65	65	
27	-99	-99	-99	-99	51	51	51	50	50	49	47	45	47	48	49	49	52	53	52	52	49	46	35	32	39	48	59	66	69	68	67	66	65	65	65	65	65	65	65	65	65	65	
28	-99	-99	-99	-99	51	51	51	50	50	49	47	45	47	48	49	49	52	53	52	52	49	46	35	32	39	48	59	66	69	68	67	66	65	65	65	65	65	65	65	65	65	65	
29	-99	-99	-99	-99	51	51	51	50	50	49	47	45	47	48	49	49	52	53	52	52	49	46	35	32	39	48	59	66	69	68	67	66	65	65	65	65	65	65	65	65	65	65	
30	-99	-99	-99	-99	51	51	51	50	50	49	47	45	47	48	49	49	52	53	52	52	49	46	35	32	39	48	59	66	69	68	67	66	65	65	65	65	65	65	65	65	65	65	
31	-99	-99	-99	-99	51	51	51	50	50	49	47	45	47	48	49	49	52	53	52	52	49	46	35	32	39	48	59	66	69	68	67	66	65	65	65	65	65	65	65	65	65	65	
32	-99	-99	-99	-99	51	51	51	50	50	49	47	45	47	48	49	49	52	53	52	52	49	46	35	32	39	48	59	66	69	68	67	66	65	65	65	65	65	65	65	65	65	65	
33	-99	-99	-99	-99	51	51	51	50	50	49	47	45	47	48	49	49	52	53	52	52	49	46	35	32	39	48	59	66	69	68	67	66	65	65	65	65	65	65	65	65	65	65	
34	-99	-99	-99	-99	51	51	51	50	50	49	47	45	47	48	49	49	52	53	52	52	49	46	35	32	39	48	59	66	69	68	67	66	65	65	65	65	65	65	65	65	65	65	
35	-99	-99	-99	-99	51	51	51	50	50	49	47	45	47	48	49	49	52	53	52	52	49	46	35	32	39	48	59	66	69	68	67	66	65	65	65	65	65	65	65	65	65	65	

Figure A-1. Areal map of the 10 May 1979 SMMR brightness temperatures (K) for the study area for the 0.81 cm horizontally polarized wavelength.

ORRIDDED SPWR BRIGHTNESS TEMPERATURES (minus 200) FROM FILE SN79130X, CHANNEL 2.

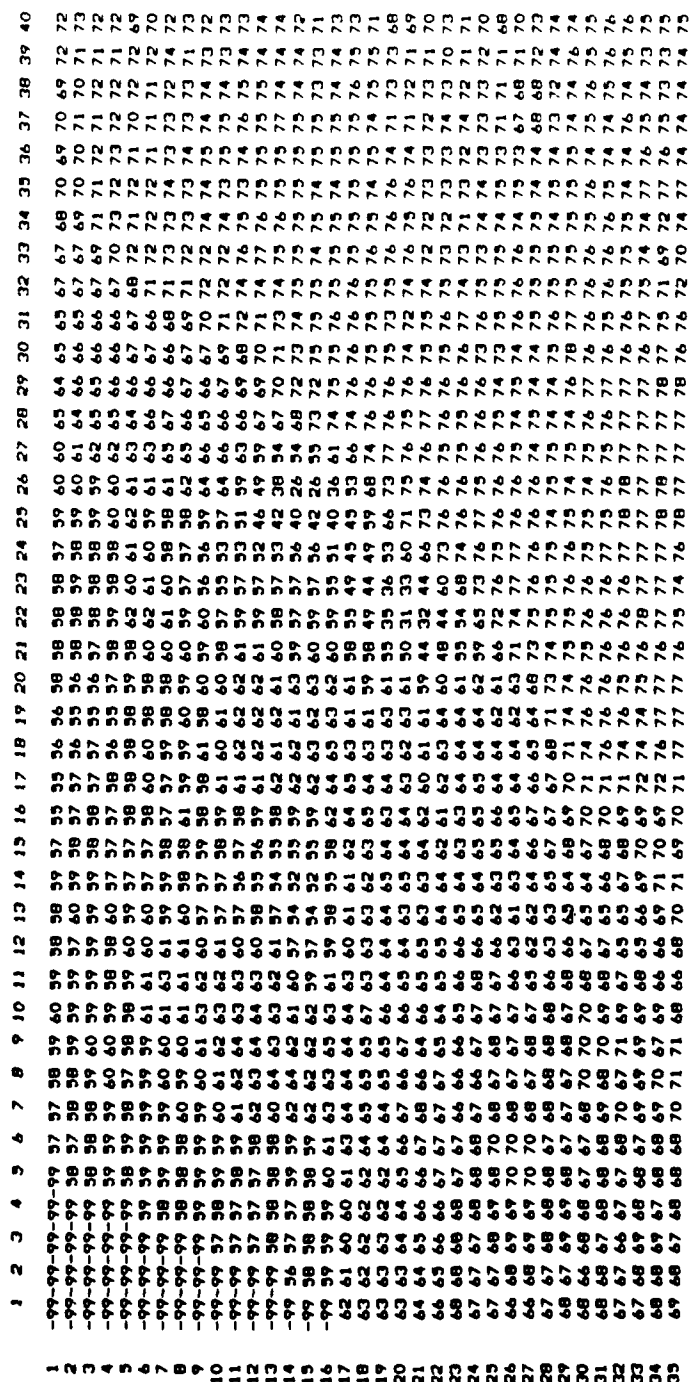


Figure A-2. Areal map of the 10 May 1979 SNWR brightness temperatures (K) for the study area for the 0.81 cm vertically polarized wavelength.

GRIDDED SMMR BRIGHTNESS TEMPERATURES (minus 200) FROM FILE SN79130X. CHANNEL 3:

1	-99	-99	-99	-99	-99	48	48	47	47	46	46	47	46	44	41	40	43	44	42	42	43	43	44	46	49	51	55	55	55	55	56	58	60	62	61	60	62	63	63
2	-99	-99	-99	-99	-99	47	47	48	48	47	47	46	45	42	43	46	46	45	46	46	47	46	49	50	55	57	56	56	58	59	61	63	62	63	64	63	64	63	
3	-99	-99	-99	-99	-99	46	46	47	47	46	45	47	46	43	44	46	48	48	47	48	48	49	50	51	52	58	58	58	60	60	62	63	63	63	63	63	64	64	
4	-99	-99	-99	-99	-99	47	47	46	46	47	46	45	44	43	43	45	49	49	48	48	47	49	50	51	50	53	54	59	59	61	63	63	63	63	63	64	64		
5	-99	-99	-99	-99	-99	47	47	48	48	46	47	46	44	43	43	45	46	47	49	49	50	51	50	53	54	59	59	61	63	63	63	63	63	63	63	63	63		
6	-99	-99	-99	-99	-99	45	45	45	47	48	48	45	43	42	44	45	46	48	49	50	51	52	53	53	56	58	59	60	61	63	66	65	63	63	62	62	61		
7	-99	-99	-99	-99	-99	48	47	48	49	50	52	50	47	46	44	42	43	43	46	47	50	51	52	52	58	58	60	62	63	67	67	67	67	67	67	67	67		
8	-99	-99	-99	-99	-99	48	48	49	50	54	53	51	49	46	45	44	42	42	47	48	50	51	51	56	59	61	61	63	64	66	66	66	66	66	66	66	66		
9	-99	-99	-99	-99	-99	49	49	51	52	54	53	51	48	45	42	43	44	48	49	50	51	51	56	61	61	62	64	64	68	67	66	65	65	65	65	65	66		
10	-99	-99	-99	-99	-99	49	49	51	52	54	53	51	48	45	42	43	44	48	49	50	51	51	56	61	61	62	64	64	68	67	66	65	65	65	65	65	66		
11	-99	-99	-99	-99	-99	46	47	48	50	51	53	54	50	45	42	43	47	48	49	50	52	50	52	53	57	62	62	63	63	65	65	65	65	65	65	65	65	66	
12	-99	-99	-99	-99	-99	42	43	46	50	52	52	51	51	49	44	42	41	46	51	52	51	52	50	54	56	57	58	61	63	65	66	67	67	67	67	67	67	67	
13	-99	-99	-99	-99	-99	42	42	43	47	51	51	50	49	46	42	38	37	44	45	50	51	51	50	50	51	52	63	63	66	66	68	68	67	67	67	67	67	67	
14	-99	-99	-99	-99	-99	41	42	43	46	50	49	46	42	38	34	36	43	47	51	52	54	53	52	49	48	52	63	64	66	66	68	68	67	67	67	67	67	67	
15	-99	-99	-99	-99	-99	41	42	43	46	49	49	46	40	39	35	39	43	49	52	54	56	53	52	49	48	52	63	64	66	66	68	68	67	67	67	67	67	67	
16	-99	-99	-99	-99	-99	43	46	48	49	49	48	47	43	40	38	44	45	52	53	53	52	52	52	48	57	64	65	66	66	68	68	67	67	67	67	67	67	67	
17	-99	-99	-99	-99	-99	47	47	47	49	50	48	46	44	43	47	48	55	53	53	53	52	53	53	54	66	67	68	69	68	68	67	67	67	67	67	67	67	67	
18	-99	-99	-99	-99	-99	47	47	47	49	50	49	47	46	48	48	51	52	56	59	54	53	52	51	53	57	58	66	67	69	68	68	67	67	67	67	67	67	67	
19	-99	-99	-99	-99	-99	48	48	52	53	50	51	49	50	50	50	50	52	53	53	52	51	49	49	54	59	62	66	67	69	68	68	68	67	67	67	67	67	67	
20	-99	-99	-99	-99	-99	52	52	52	53	54	52	53	50	51	53	51	50	50	48	47	51	48	47	59	61	66	67	69	68	68	68	67	67	67	67	67	67		
21	54	53	53	53	53	54	53	53	54	52	51	50	51	50	50	47	52	52	49	49	49	49	49	63	69	71	71	68	68	68	68	67	67	67	67	67	67		
22	53	53	53	54	56	55	54	55	56	55	54	52	52	52	50	47	55	54	52	54	56	56	70	71	69	68	68	68	68	67	67	67	67	67	67	67	67		
23	53	53	53	57	57	57	54	54	53	56	56	53	51	53	53	52	51	54	55	56	56	61	67	68	70	70	67	68	67	66	66	66	66	66	66	66	66		
24	54	54	55	55	56	55	54	55	56	56	56	53	52	53	54	55	55	56	57	57	56	60	69	67	67	68	67	66	67	66	67	66	67	66	67	66	67		
25	54	53	53	55	56	56	55	57	58	56	55	53	52	53	54	55	56	60	60	60	60	69	67	67	68	67	66	67	66	67	66	67	66	67	66	67	66		
26	54	54	54	56	57	57	56	56	55	53	53	48	51	52	53	54	56	57	59	63	64	68	69	67	67	67	66	66	66	66	66	66	66	66	66	66	66		
27	54	54	54	56	57	57	56	56	55	54	50	47	52	54	54	54	54	54	54	54	54	54	68	68	67	67	67	66	66	66	66	66	66	66	66	66	66		
28	54	54	54	56	57	57	56	56	55	54	50	47	52	54	54	54	54	54	54	54	54	54	68	68	67	67	67	66	66	66	66	66	66	66	66	66	66		
29	56	55	56	55	53	53	56	58	57	56	54	53	58	59	62	62	66	66	68	68	68	68	68	67	67	67	67	67	67	67	67	67	67	67	67	67	67		
30	55	55	55	55	55	56	57	58	57	56	54	53	58	61	63	64	67	68	68	68	68	68	68	68	67	67	67	67	67	67	67	67	67	67	67	67	67		
31	55	55	54	56	55	55	56	57	58	56	55	54	57	58	62	63	66	67	68	68	68	68	68	68	68	67	67	67	67	67	67	67	67	67	67	67			
32	55	54	54	55	56	57	57	58	58	54	53	54	58	58	64	67	67	67	68	68	68	68	68	68	68	67	67	67	67	67	67	67	67	67	67	67			
33	55	54	56	56	56	58	59	57	52	53	53	53	60	61	63	63	69	69	68	68	68	68	68	68	68	67	67	67	67	67	67	67	67	67	67	67			
34	55	54	57	57	56	59	59	60	56	52	53	57	60	62	63	66	68	68	68	68	68	68	68	68	68	67	67	67	67	67	67	67	67	67	67	67	67		
35	56	56	57	55	56	59	59	58	55	52	56	57	60	62	64	65	67	68	68	67	68	67	69	69	71	71	70	68	65	63	62	63	62	63	62	63	62		

Figure A-3. Areal map of the 10 May 1979 SMMR brightness temperatures (K) for the study area for the 1.36 cm horizontally polarized wavelength.

GRIDDED SMMR BRIGHTNESS TEMPERATURES (minus 200) FROM FILE SN79130X. CHANNEL 4.

1	1	2	3	4	5	6	7	8	9	10	11	12	13	14	15	16	17	18	19	20	21	22	23	24	25	26	27	28	29	30	31	32	33	34	35	36	37	38	39	40
1	-99	-99	-99	-99	-99	51	51	50	50	51	48	49	52	52	50	50	49	51	53	53	53	52	53	53	55	55	57	57	60	61	63	63	63	65	68	67	68	68	70	71
2	-99	-99	-99	-99	-99	51	51	50	49	49	49	54	52	51	50	50	49	50	51	53	54	55	56	57	57	60	61	62	63	64	64	66	67	69	70	70	70	70	70	71
3	-99	-99	-99	-99	-99	51	51	49	48	50	52	54	52	50	49	51	51	54	53	54	55	56	58	58	62	63	63	62	66	67	67	70	70	69	69	69	70	70	71	
4	-99	-99	-99	-99	-99	48	49	50	51	49	51	52	53	50	49	52	52	54	55	56	56	55	56	59	59	63	63	63	65	68	69	70	70	69	69	69	69	69	70	
5	-99	-99	-99	-99	-99	49	48	49	50	51	54	52	51	50	49	52	53	54	54	55	56	59	60	64	64	66	67	68	69	70	71	69	69	69	69	69	69	69		
6	-99	-99	-99	-99	-99	49	49	48	51	53	54	53	51	51	51	52	56	55	54	56	57	58	60	61	64	65	67	69	70	71	72	69	68	69	69	69	69	69		
7	-99	-99	-99	-99	-99	49	49	51	52	54	55	53	51	52	54	52	51	54	55	57	58	58	59	60	62	63	64	65	67	68	71	71	71	71	71	71	71	71	71	
8	-99	-99	-99	-99	-99	50	50	50	51	52	57	57	54	49	50	52	50	53	53	57	58	58	59	60	63	63	63	65	66	69	70	72	72	71	71	71	71	71	71	
9	-99	-99	-99	-99	-99	47	48	48	47	52	57	57	54	49	49	52	52	54	56	57	58	59	60	63	63	63	65	66	69	70	72	72	71	71	71	71	71	71	71	
10	-99	-99	-99	-99	-99	48	48	47	46	52	53	57	58	53	49	51	53	53	56	57	58	59	60	61	64	65	67	68	69	70	72	73	73	73	73	73	73	73	71	
11	-99	-99	-99	-99	-99	52	51	49	48	54	56	58	57	54	52	51	53	53	56	57	58	59	60	62	65	67	68	69	70	72	73	73	73	73	73	73	73	73	71	
12	-99	-99	-99	-99	-99	51	51	51	53	58	57	55	52	50	51	52	54	55	58	57	58	58	59	60	62	65	67	68	69	70	72	72	72	72	72	72	72	72	71	
13	-99	-99	-99	-99	-99	46	47	48	49	51	56	59	57	55	49	49	51	53	53	57	58	58	59	60	62	65	67	68	69	70	72	72	72	72	72	72	72	72	71	
14	-99	-99	-99	-99	-99	46	46	46	47	51	56	56	57	58	56	47	48	51	54	56	57	58	58	59	60	62	65	67	68	69	70	72	72	72	72	72	72	72	70	
15	-99	-99	-99	-99	-99	45	46	47	54	56	57	57	58	55	48	49	50	56	57	58	58	59	60	62	65	67	68	69	70	72	72	72	72	72	72	72	72	72	70	
16	-99	-99	-99	-99	-99	46	46	50	56	59	60	59	56	54	52	51	58	58	59	59	59	60	60	62	65	67	68	69	70	72	72	72	72	72	72	72	72	72	70	
17	-99	-99	-99	-99	-99	50	49	51	52	55	56	59	60	58	56	53	56	59	60	60	60	60	60	62	65	67	68	69	70	72	72	72	72	72	72	72	72	72	70	
18	-99	-99	-99	-99	-99	52	52	53	54	57	60	61	59	58	58	60	61	60	59	58	59	60	60	62	65	67	68	69	70	72	72	72	72	72	72	72	72	72	71	
19	-99	-99	-99	-99	-99	50	50	50	50	59	60	61	59	58	58	60	60	60	60	60	60	60	62	65	67	68	69	70	72	72	72	72	72	72	72	72	72	72	71	
20	-99	-99	-99	-99	-99	53	53	53	53	57	60	60	62	58	58	60	60	60	60	60	60	60	62	65	67	68	69	70	72	72	72	72	72	72	72	72	72	72	71	
21	-99	-99	-99	-99	-99	58	58	58	58	59	61	60	63	63	60	60	60	60	60	60	60	60	62	65	67	68	69	70	72	72	72	72	72	72	72	72	72	72	71	
22	-99	-99	-99	-99	-99	59	59	60	61	60	63	60	62	62	60	60	60	60	60	60	60	60	62	65	67	68	69	70	72	72	72	72	72	72	72	72	72	72	71	
23	-99	-99	-99	-99	-99	62	62	61	60	63	62	63	61	61	62	62	62	62	62	62	62	62	64	67	68	69	70	72	72	72	72	72	72	72	72	72	72	72	71	
24	-99	-99	-99	-99	-99	63	64	64	63	64	63	63	62	61	61	61	61	61	61	61	61	62	65	67	68	69	70	72	72	72	72	72	72	72	72	72	72	72	71	
25	-99	-99	-99	-99	-99	64	64	64	64	64	64	64	63	62	60	61	62	62	62	62	62	62	64	67	68	69	70	72	72	72	72	72	72	72	72	72	72	71		
26	-99	-99	-99	-99	-99	62	63	64	64	64	64	64	64	64	64	64	64	64	64	64	64	64	66	69	70	72	72	72	72	72	72	72	72	72	72	72	72	72	71	
27	-99	-99	-99	-99	-99	61	63	63	63	64	64	64	64	64	64	64	64	64	64	64	64	64	66	69	70	72	72	72	72	72	72	72	72	72	72	72	72	72	71	
28	-99	-99	-99	-99	-99	63	63	63	63	64	64	64	64	64	64	64	64	64	64	64	64	64	66	69	70	72	72	72	72	72	72	72	72	72	72	72	72	72	71	
29	-99	-99	-99	-99	-99	62	62	61	62	62	64	64	63	63	63	63	63	63	63	63	63	63	65	68	69	70	72	72	72	72	72	72	72	72	72	72	72	72	71	
30	-99	-99	-99	-99	-99	62	62	62	62	63	64	64	63	63	63	63	63	63	63	63	63	63	65	68	69	70	72	72	72	72	72	72	72	72	72	72	72	72	71	
31	-99	-99	-99	-99	-99	61	61	61	61	62	62	64	63	63	63	63	63	63	63	63	63	63	65	68	69	70	72	72	72	72	72	72	72	72	72	72	72	72	71	
32	-99	-99	-99	-99	-99	61	61	61	61	62	62	64	63	63	63	63	63	63	63	63	63	63	65	68	69	70	72	72	72	72	72	72	72	72	72	72	72	72	71	
33	-99	-99	-99	-99	-99	62	62	62	62	63	64	64	63	63	63	63	63	63	63	63	63	63	65	68	69	70	72	72	72	72	72	72	72	72	72	72	72	72	71	
34	-99	-99	-99	-99	-99	62	62	61	61	62	62	64	63	63	63	63	63	63	63	63	63	63	65	68	69	70	72	72	72	72	72	72	72	72	72	72	72	72	71	
35	-99	-99	-99	-99	-99	62	62	63	63	63	63	63	63	63	63	63	63	63	63	63	63	63	65	68	69	70	72	72	72	72	72	72	72	72	72	72	72	72	71	

Figure A-4. Areal map of the 10 May 1979 SMMR brightness temperatures (K) for the study area for the 1.36 cm vertically polarized wavelength.

ORRIDDED SMMR BRIGHTNESS TEMPERATURES (minus 200) FROM FILE 6N79130X, CHANNEL 8:

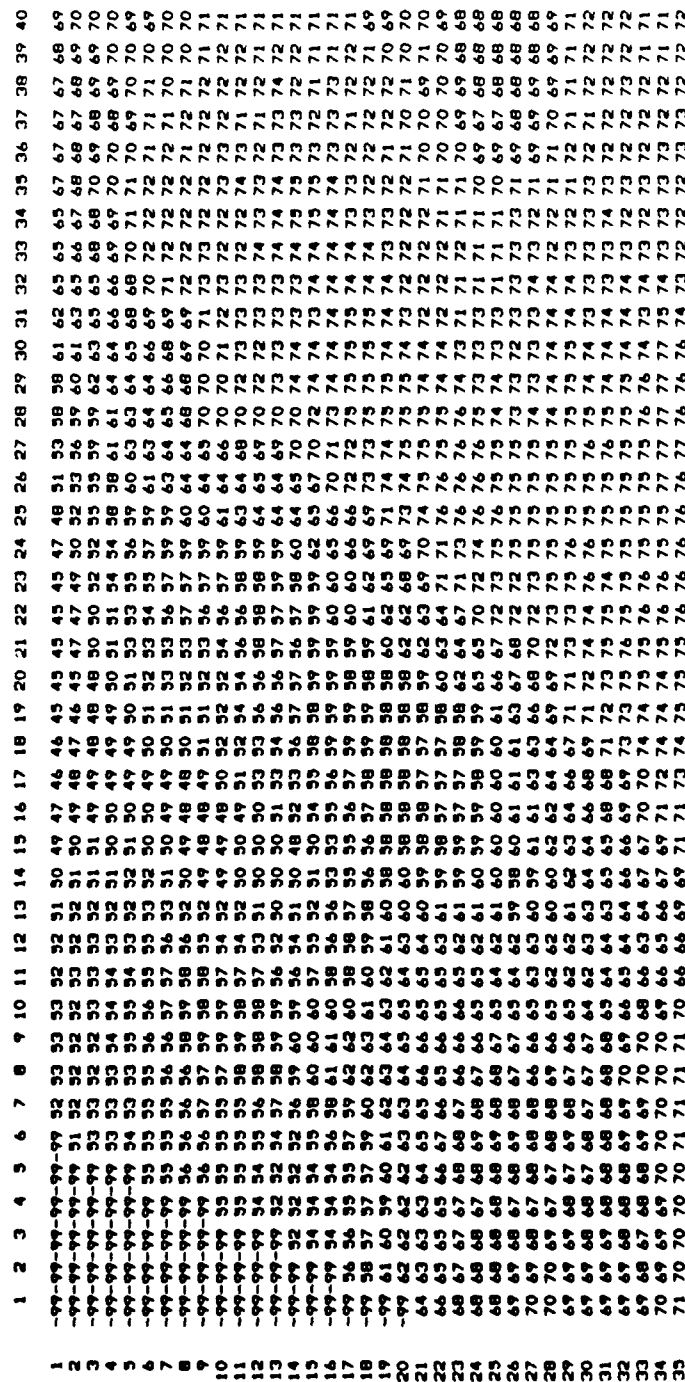


Figure A-8. Areal map of the 10 May 1979 SMMR brightness temperatures (K) for the study area for the 2.80 cm vertically polarized wavelength.

ORRDED SMMR BRIGHTNESS TEMPERATURES (minus 200) FROM FILE SN79130X, CHANNEL 10

1	-99	-99	-99	-99	-99	52	52	52	51	51	51	50	50	47	45	45	43	43	43	43	45	45	45	47	57	56	55	56	65	64	64	67	70	70	74	74
2	-99	-99	-99	-99	-99	53	53	52	51	51	51	51	46	46	45	44	44	47	47	47	46	46	46	55	58	58	58	63	66	66	69	69	70	75	75	
3	-99	-99	-99	-99	-99	52	52	52	53	52	51	51	48	48	45	45	44	50	49	50	49	49	59	59	59	59	67	67	67	71	71	70	75	75		
4	-99	-99	-99	-99	-99	53	53	52	53	53	52	51	50	49	47	46	45	52	52	51	61	61	61	60	60	68	68	68	68	71	71	73	74	75		
5	-99	-99	-99	-99	-99	53	53	53	54	53	53	52	50	49	47	46	45	48	47	48	53	53	53	63	63	62	62	68	68	69	71	71	74	74		
6	-99	-99	-99	-99	-99	52	52	52	54	54	53	53	48	48	48	48	48	48	48	52	54	54	54	64	64	63	62	68	68	71	72	72	74	74		
7	-99	-99	-99	-99	-99	53	53	53	53	53	53	53	53	49	49	49	48	48	48	53	53	53	64	64	63	63	69	69	69	73	73	74	74	75		
8	-99	-99	-99	-99	-99	53	53	53	53	53	53	53	53	49	49	49	48	48	48	53	53	53	64	64	63	63	69	69	69	73	73	74	74	75		
9	-99	-99	-99	-99	-99	53	53	53	53	53	53	53	53	49	49	49	48	48	48	53	53	53	64	64	63	63	69	69	69	73	73	74	74	75		
10	-99	-99	-99	-99	-99	53	53	53	53	53	53	53	53	49	49	49	48	48	48	53	53	53	64	64	63	63	69	69	69	73	73	74	74	75		
11	-99	-99	-99	-99	-99	53	53	53	53	53	53	53	53	49	49	49	48	48	48	53	53	53	64	64	63	63	69	69	69	73	73	74	74	75		
12	-99	-99	-99	-99	-99	53	53	53	53	53	53	53	53	49	49	49	48	48	48	53	53	53	64	64	63	63	69	69	69	73	73	74	74	75		
13	-99	-99	-99	-99	-99	53	53	53	53	53	53	53	53	49	49	49	48	48	48	53	53	53	64	64	63	63	69	69	69	73	73	74	74	75		
14	-99	-99	-99	-99	-99	53	53	53	53	53	53	53	53	49	49	49	48	48	48	53	53	53	64	64	63	63	69	69	69	73	73	74	74	75		
15	-99	-99	-99	-99	-99	53	53	53	53	53	53	53	53	49	49	49	48	48	48	53	53	53	64	64	63	63	69	69	69	73	73	74	74	75		
16	-99	-99	-99	-99	-99	53	53	53	53	53	53	53	53	49	49	49	48	48	48	53	53	53	64	64	63	63	69	69	69	73	73	74	74	75		
17	-99	-99	-99	-99	-99	53	53	53	53	53	53	53	53	49	49	49	48	48	48	53	53	53	64	64	63	63	69	69	69	73	73	74	74	75		
18	-99	-99	-99	-99	-99	53	53	53	53	53	53	53	53	49	49	49	48	48	48	53	53	53	64	64	63	63	69	69	69	73	73	74	74	75		
19	-99	-99	-99	-99	-99	53	53	53	53	53	53	53	53	49	49	49	48	48	48	53	53	53	64	64	63	63	69	69	69	73	73	74	74	75		
20	-99	-99	-99	-99	-99	53	53	53	53	53	53	53	53	49	49	49	48	48	48	53	53	53	64	64	63	63	69	69	69	73	73	74	74	75		
21	-99	-99	-99	-99	-99	53	53	53	53	53	53	53	53	49	49	49	48	48	48	53	53	53	64	64	63	63	69	69	69	73	73	74	74	75		
22	-99	-99	-99	-99	-99	53	53	53	53	53	53	53	53	49	49	49	48	48	48	53	53	53	64	64	63	63	69	69	69	73	73	74	74	75		
23	-99	-99	-99	-99	-99	53	53	53	53	53	53	53	53	49	49	49	48	48	48	53	53	53	64	64	63	63	69	69	69	73	73	74	74	75		
24	-99	-99	-99	-99	-99	53	53	53	53	53	53	53	53	49	49	49	48	48	48	53	53	53	64	64	63	63	69	69	69	73	73	74	74	75		
25	-99	-99	-99	-99	-99	53	53	53	53	53	53	53	53	49	49	49	48	48	48	53	53	53	64	64	63	63	69	69	69	73	73	74	74	75		
26	-99	-99	-99	-99	-99	53	53	53	53	53	53	53	53	49	49	49	48	48	48	53	53	53	64	64	63	63	69	69	69	73	73	74	74	75		
27	-99	-99	-99	-99	-99	53	53	53	53	53	53	53	53	49	49	49	48	48	48	53	53	53	64	64	63	63	69	69	69	73	73	74	74	75		
28	-99	-99	-99	-99	-99	53	53	53	53	53	53	53	53	49	49	49	48	48	48	53	53	53	64	64	63	63	69	69	69	73	73	74	74	75		
29	-99	-99	-99	-99	-99	53	53	53	53	53	53	53	53	49	49	49	48	48	48	53	53	53	64	64	63	63	69	69	69	73	73	74	74	75		
30	-99	-99	-99	-99	-99	53	53	53	53	53	53	53	53	49	49	49	48	48	48	53	53	53	64	64	63	63	69	69	69	73	73	74	74	75		
31	-99	-99	-99	-99	-99	53	53	53	53	53	53	53	53	49	49	49	48	48	48	53	53	53	64	64	63	63	69	69	69	73	73	74	74	75		
32	-99	-99	-99	-99	-99	53	53	53	53	53	53	53	53	49	49	49	48	48	48	53	53	53	64	64	63	63	69	69	69	73	73	74	74	75		
33	-99	-99	-99	-99	-99	53	53	53	53	53	53	53	53	49	49	49	48	48	48	53	53	53	64	64	63	63	69	69	69	73	73	74	74	75		
34	-99	-99	-99	-99	-99	53	53	53	53	53	53	53	53	49	49	49	48	48	48	53	53	53	64	64	63	63	69	69	69	73	73	74	74	75		
35	-99	-99	-99	-99	-99	53	53	53	53	53	53	53	53	49	49	49	48	48	48	53	53	53	64	64	63	63	69	69	69	73	73	74	74	75		

Figure A-10. Areal map of the 10 May 1979 SMMR brightness temperatures (K) for the study area for the 4.54 cm vertically polarized wavelength.

ORIGDED CLIMATIC DATA FROM FILE 8C79130V, CHANNEL 1:

CHANNEL 1-TMAX(C), 2-TMIN(C), 3=PRECIP(mm), 4=SNOWFALL(cm), 5=SNOWDEPTH(cm)

1	2	3	4	5	6	7	8	9	10	11	12	13	14	15	16	17	18	19	20	21	22	23	24	25	26	27	28	29	30	31	32	33	34	35	36	37	38	39	40		
6	6	5	4	4	5	6	6	7	8	8	8	8	8	8	8	9	9	10	10	9	8	9	9	9	9	9	9	9	10	11	12	13	15	22	25	26	26	27	26	26	26
2	3	4	4	4	5	6	7	8	8	8	8	8	8	8	8	9	10	10	10	10	10	10	10	10	10	10	10	10	10	10	10	10	10	10	10	10	10	10	10	10	10
3	4	4	3	3	4	4	6	7	8	8	8	8	8	8	8	9	10	10	11	11	11	11	10	10	10	10	10	10	10	10	10	10	10	10	10	10	10	10	10	10	10
4	4	4	3	3	4	4	6	7	8	8	8	8	8	8	8	9	10	10	10	11	11	11	10	10	10	10	10	10	10	10	10	10	10	10	10	10	10	10	10	10	10
5	4	4	3	3	4	5	7	8	8	9	10	10	10	10	10	10	10	10	10	11	11	11	11	10	10	10	10	10	10	10	10	10	10	10	10	10	10	10	10	10	10
6	5	4	4	4	7	9	9	9	10	11	11	11	10	10	10	10	10	10	10	11	11	11	11	10	10	10	10	10	10	10	10	10	10	10	10	10	10	10	10	10	10
7	6	5	6	13	14	12	10	9	10	11	11	11	11	10	10	10	10	10	10	11	11	11	11	11	10	10	10	10	10	10	10	10	10	10	10	10	10	10	10	10	10
8	6	6	10	15	15	14	12	10	11	11	10	10	11	12	12	11	11	12	12	11	11	11	11	11	12	13	14	16	18	20	20	21	22	23	24	25	26	27	28	28	28
9	7	8	10	14	15	14	12	10	11	11	10	10	11	12	12	12	11	11	12	12	11	11	11	11	12	13	14	16	18	20	20	21	22	22	22	22	24	25	27	28	28
10	8	10	12	14	14	14	13	12	11	11	11	11	11	11	12	12	12	12	12	12	12	12	12	12	12	12	12	12	12	12	12	12	12	12	12	12	12	12	12	12	12
11	9	10	10	11	13	14	14	14	13	13	12	12	12	11	11	12	12	12	12	12	12	12	12	12	12	12	12	12	12	12	12	12	12	12	12	12	12	12	12	12	12
12	9	10	10	11	13	12	14	14	14	13	13	13	13	13	13	12	12	12	12	12	12	12	12	12	12	12	12	12	12	12	12	12	12	12	12	12	12	12	12	12	12
13	9	10	10	11	11	12	14	14	14	14	14	14	14	14	14	14	14	14	14	14	14	14	14	14	14	14	14	14	14	14	14	14	14	14	14	14	14	14	14	14	14
14	9	11	11	11	11	11	12	14	14	14	14	14	14	14	14	14	14	14	14	14	14	14	14	14	14	14	14	14	14	14	14	14	14	14	14	14	14	14	14	14	14
15	4	8	11	11	11	11	12	14	14	14	14	14	14	14	14	14	14	14	14	14	14	14	14	14	14	14	14	14	14	14	14	14	14	14	14	14	14	14	14	14	14
16	8	9	10	12	12	13	15	17	15	15	15	15	15	15	15	15	15	15	15	15	15	15	15	15	15	15	15	15	15	15	15	15	15	15	15	15	15	15	15	15	15
17	9	10	11	14	19	20	21	21	17	16	16	16	16	16	16	16	16	16	16	16	16	16	16	16	16	16	16	16	16	16	16	16	16	16	16	16	16	16	16	16	16
18	10	10	11	12	19	22	22	21	17	16	16	16	16	16	16	16	16	16	16	16	16	16	16	16	16	16	16	16	16	16	16	16	16	16	16	16	16	16	16	16	16
19	10	11	11	15	21	21	19	17	16	16	16	16	16	16	16	16	16	16	16	16	16	16	16	16	16	16	16	16	16	16	16	16	16	16	16	16	16	16	16	16	16
20	10	10	11	13	18	18	18	17	19	21	22	23	22	24	24	24	24	24	24	24	24	24	24	24	24	24	24	24	24	24	24	24	24	24	24	24	24	24	24	24	24
21	10	11	12	13	14	15	16	18	19	20	22	23	24	24	24	24	24	24	24	24	24	24	24	24	24	24	24	24	24	24	24	24	24	24	24	24	24	24	24	24	24
22	13	14	16	15	15	16	20	22	22	22	22	22	22	22	22	22	22	22	22	22	22	22	22	22	22	22	22	22	22	22	22	22	22	22	22	22	22	22	22	22	22
23	16	17	18	17	18	16	16	16	16	16	16	16	16	16	16	16	16	16	16	16	16	16	16	16	16	16	16	16	16	16	16	16	16	16	16	16	16	16	16	16	
24	17	18	19	21	22	19	21	23	23	23	23	23	23	23	23	23	23	23	23	23	23	23	23	23	23	23	23	23	23	23	23	23	23	23	23	23	23	23	23	23	23
25	20	19	20	22	19	17	18	20	22	22	22	22	22	22	22	22	22	22	22	22	22	22	22	22	22	22	22	22	22	22	22	22	22	22	22	22	22	22	22	22	22
26	21	20	22	22	19	17	18	19	20	20	20	19	19	19	19	19	19	19	19	19	19	19	19	19	19	19	19	19	19	19	19	19	19	19	19	19	19	19	19	19	19
27	21	21	21	18	17	17	17	18	18	18	18	18	18	18	18	18	18	18	18	18	18	18	18	18	18	18	18	18	18	18	18	18	18	18	18	18	18	18	18	18	18
28	21	22	23	22	19	18	18	18	18	18	18	18	18	18	18	18	18	18	18	18	18	18	18	18	18	18	18	18	18	18	18	18	18	18	18	18	18	18	18	18	18
29	20	22	24	22	20	19	18	18	20	19	18	18	18	18	18	18	18	18	18	18	18	18	18	18	18	18	18	18	18	18	18	18	18	18	18	18	18	18	18	18	18
30	20	22	23	21	20	19	20	20	20	20	20	20	20	20	20	20	20	20	20	20	20	20	20	20	20	20	20	20	20	20	20	20	20	20	20	20	20	20	20	20	20
31	22	24	25	22	21	20	20	20	20	20	20	20	20	20	20	20	20	20	20	20	20	20	20	20	20	20	20	20	20	20	20	20	20	20	20	20	20	20	20	20	20
32	24	26	27	25	21	20	20	20	20	20	20	20	20	20	20	20	20	20	20	20	20	20	20	20	20	20	20	20	20	20	20	20	20	20	20	20	20	20	20	20	20
33	24	26	28	28	23	20	20	20	20	20	20	20	20	20	20	20	20	20	20	20	20	20	20	20	20	20	20	20	20	20	20	20	20	20	20	20	20	20	20	20	20
34	23	24	28	28	27	21	20	22	22	22	22	22	22	22	22	22	22	22	22	22	22	22	22	22	22	22	22	22	22	22	22	22	22	22	22	22	22	22	22	22	22
35	26	28	30	30	29	26	26	24	23	23	23	23	23	23	23	23	23	23	23	23	23	23	23	23	23	23	23	23	23	23	23	23	23	23	23	23	23	23	23	23	23

Figure A-11. Areal map of the 10 May 1979 maximum temperatures (C) for the study area.

ORIPDED CLIMATIC DATA FROM FILE SC79130V, CHANNEL 3:

CHANNEL 1=THAX(C), 2=THIN(C), 3=PRECIP(mm), 4=SNOWFALL(cm), 5=SNOWDEPTH(cm)

1	2	3	4	5	6	7	8	9	10	11	12	13	14	15	16	17	18	19	20	21	22	23	24	25	26	27	28	29	30	31	32	33	34	35	36	37	38	39	40			
1	10	10	4	3	6	10	10	9	6	3	2	2	1	2	7	10	17	19	16	19	27	31	28	14	6	2	2	2	3	4	5	4	2	1	1	2	4	4	4	4		
2	10	7	3	9	11	11	11	8	3	2	2	1	2	9	13	14	18	22	29	36	32	24	10	2	2	1	3	4	5	4	4	3	1	0	0	3	5	4	4	5		
3	4	1	2	8	11	11	10	9	8	2	1	1	3	9	14	13	18	31	40	37	24	12	5	2	2	2	2	4	6	6	4	4	2	0	0	2	3	4	5	5		
4	1	1	2	8	11	11	9	5	4	1	0	0	2	4	8	14	19	27	39	47	38	22	9	3	2	3	6	9	10	10	9	7	3	0	0	1	0	2	4	3		
5	2	1	1	7	11	11	9	5	3	1	0	0	2	4	9	16	21	29	36	45	32	19	7	2	4	6	8	12	15	13	11	7	3	1	1	1	1	1	2	1		
6	3	2	4	9	9	9	8	4	1	0	0	2	7	11	15	19	26	34	34	22	10	4	3	6	9	12	15	19	17	12	6	3	3	2	1	0	0	0	0			
7	6	3	3	4	3	3	7	8	4	1	0	1	5	10	9	8	16	32	33	22	13	5	3	5	8	12	16	20	24	21	12	4	3	2	1	0	0	0	0			
8	18	8	5	5	3	1	2	4	2	0	0	1	7	11	10	7	17	35	26	15	8	5	6	7	9	13	21	26	26	19	10	5	3	2	0	0	0	0	0			
9	18	16	9	6	3	0	0	0	0	0	0	1	7	14	16	14	19	27	20	13	7	5	6	7	7	16	29	31	22	15	9	5	4	3	1	0	0	0	0			
10	16	13	7	5	2	0	0	0	0	0	0	1	10	18	24	28	21	17	15	5	4	5	6	10	18	32	31	22	15	9	5	3	1	0	0	0	0	0	1			
11	15	10	6	4	0	0	0	0	0	0	1	2	8	15	21	27	21	14	8	3	3	4	4	9	14	23	31	32	27	16	7	5	1	0	0	0	0	0	0			
12	23	12	10	2	0	0	0	0	0	0	1	2	4	10	12	17	13	6	3	2	3	7	10	11	24	28	33	34	29	16	9	5	1	0	0	0	0	0	0			
13	24	16	12	11	9	8	5	0	0	0	0	1	8	10	9	7	5	2	2	4	9	18	24	31	34	40	32	23	18	12	7	1	0	0	0	1	0	0	0	0		
14	16	14	10	9	7	9	5	0	0	0	0	2	13	15	12	5	3	2	4	5	13	32	42	40	43	49	33	19	12	5	2	0	0	0	0	0	0	0	0	0		
15	13	9	6	7	9	8	3	0	0	0	0	1	9	13	9	5	3	2	3	8	13	40	54	52	50	53	47	28	13	5	2	0	0	0	0	0	0	0	0	0		
16	9	6	6	6	5	2	0	0	0	0	0	2	4	5	5	4	2	5	12	32	76	80	60	50	35	21	13	7	2	1	0	0	0	0	0	0	0	0	0	0	0	
17	6	5	6	5	3	3	2	0	0	0	0	1	2	3	6	10	19	32	46	87	99	82	63	28	8	6	7	5	1	1	0	0	0	0	0	0	0	0	0	0	0	
18	4	2	1	1	2	1	1	0	0	0	0	0	0	1	5	18	23	33	56	80	123	113	72	55	20	7	3	3	2	2	2	1	0	0	0	0	0	0	0	0	0	
19	2	1	0	0	0	0	0	0	0	0	0	0	0	4	20	20	23	42	88	112	114	91	58	38	11	6	2	0	1	4	3	0	0	0	1	4	2	0	0	0	0	
20	0	0	0	0	0	0	0	0	0	0	0	0	0	9	20	20	22	46	93	97	81	58	42	16	7	5	1	0	1	4	3	0	0	0	1	4	2	0	0	0	0	
21	0	0	0	0	0	0	0	0	0	0	0	0	0	2	20	20	24	37	52	63	48	37	21	7	6	3	0	0	0	0	2	1	0	0	0	0	3	6	4	1	0	0
22	0	0	0	0	0	0	0	0	0	0	0	0	0	0	17	22	41	48	51	45	36	29	16	4	3	1	0	0	0	0	0	0	0	0	0	0	1	4	2	0	0	0
23	0	0	0	0	0	0	0	0	0	0	0	0	0	0	10	20	28	40	48	36	28	23	15	4	2	1	0	0	0	0	0	0	0	0	0	0	0	0	0	0	0	
24	0	0	0	1	1	0	0	0	0	0	0	0	0	0	8	12	13	14	16	18	17	11	7	2	1	1	0	0	0	0	0	0	0	0	0	0	0	0	0	0	0	0
25	0	0	0	1	1	0	0	0	0	0	0	0	0	1	5	11	12	12	13	12	5	3	1	0	0	0	0	0	0	0	0	0	0	0	0	0	0	0	0	0	0	0
26	0	0	0	0	0	0	0	0	0	0	0	0	0	0	0	3	10	10	9	7	4	3	1	0	0	0	0	0	0	0	0	0	0	0	0	0	0	0	0	0	0	0
27	0	0	0	0	0	0	0	0	0	0	0	0	0	0	0	0	2	9	10	8	5	3	3	2	1	1	3	3	0	0	0	0	0	0	0	0	0	0	0	0	0	0
28	0	0	0	0	0	0	0	0	0	0	0	0	0	0	0	0	0	0	0	1	4	6	3	1	2	2	2	1	2	4	3	0	0	0	0	0	0	0	0	0	0	
29	0	0	0	0	0	0	0	0	0	0	0	1	2	1	0	0	0	0	0	1	0	0	1	1	2	1	1	2	1	1	2	1	0	0	0	0	0	0	0	0	0	0
30	0	0	0	0	0	0	0	0	0	0	1	3	6	3	1	0	0	0	0	0	0	0	0	1	2	3	0	0	0	0	0	0	0	0	0	0	0	0	0	0	0	0
31	0	0	0	0	0	0	0	0	0	0	0	1	5	6	3	1	0	0	0	0	0	0	0	0	1	3	3	0	0	0	0	0	0	0	0	0	0	0	0	0	0	0
32	0	0	0	0	0	0	0	0	0	0	0	2	6	4	1	0	0	0	0	0	0	0	0	0	1	2	2	1	0	0	0	0	0	0	0	0	0	0	0	0	0	0
33	0	0	0	0	0	0	0	0	0	0	1	7	8	5	1	0	0	0	0	0	0	0	0	0	1	1	1	0	0	0	0	0	0	0	0	0	0	0	0	0	0	0
34	0	0	0	0	0	0	0	0	0	0	0	4	7	5	3	0	0	0	0	0	0	0	0	0	1	1	1	0	0	0	0	0	0	0	0	0	0	0	0	0	0	0
35	0	0	0	0	0	0	0	0	0	0	2	3	2	1	0	0	0	0	0	0	0	0	0	0	0	0	0	0	0	0	0	0	0	0	0	0	0	0	0	0	0	0

Figure A-13. Areal map of the 10 May 1979 precipitation (mm) for the study area.

GRIDDED CLIMATIC DATA FROM FILE BC79130V, CHANNEL 4:

CHANNEL 1=THMAX(C), 2=THMIN(C), 3=PRECIP(mm), 4=SNOWFALL(cm), 5=SNOWDEPTH(cm)

1	2	3	4	5	6	7	8	9	10	11	12	13	14	15	16	17	18	19	20	21	22	23	24	25	26	27	28	29	30	31	32	33	34	35	36	37	38	39	40
5	5	3	3	3	3	13	9	4	2	1	0	0	0	0	0	0	0	0	0	0	0	0	0	0	0	0	0	0	0	0	0	0	0	0	0	0	0	0	0
5	3	0	0	3	10	9	4	2	1	0	0	0	0	0	0	0	0	0	0	0	0	0	0	0	0	0	0	0	0	0	0	0	0	0	0	0	0	0	0
3	2	0	0	0	4	11	9	4	2	1	0	0	0	0	0	0	0	0	0	0	0	0	0	0	0	0	0	0	0	0	0	0	0	0	0	0	0	0	0
4	0	0	0	0	0	5	12	8	1	0	0	0	0	0	0	0	0	0	0	0	0	0	0	0	0	0	0	0	0	0	0	0	0	0	0	0	0	0	0
6	0	0	0	0	0	4	5	1	0	0	0	0	0	0	0	0	0	0	0	0	0	0	0	0	0	0	0	0	0	0	0	0	0	0	0	0	0	0	0
7	1	0	0	0	0	0	0	0	0	0	0	0	0	0	0	0	0	0	0	0	0	0	0	0	0	0	0	0	0	0	0	0	0	0	0	0	0	0	0
8	7	1	0	0	0	0	0	0	0	0	0	0	0	0	0	0	0	0	0	0	0	0	0	0	0	0	0	0	0	0	0	0	0	0	0	0	0	0	0
9	4	1	0	0	0	0	0	0	0	0	0	0	0	0	0	0	0	0	0	0	0	0	0	0	0	0	0	0	0	0	0	0	0	0	0	0	0	0	0
10	1	0	0	0	0	0	0	0	0	0	0	0	0	0	0	0	0	0	0	0	0	0	0	0	0	0	0	0	0	0	0	0	0	0	0	0	0	0	0
11	2	0	0	0	0	0	0	0	0	0	0	0	0	0	0	0	0	0	0	0	0	0	0	0	0	0	0	0	0	0	0	0	0	0	0	0	0	0	0
12	10	2	0	0	0	0	0	0	0	0	0	0	0	0	0	0	0	0	0	0	0	0	0	0	0	0	0	0	0	0	0	0	0	0	0	0	0	0	0
13	14	5	0	0	0	0	0	0	0	0	0	0	0	0	0	0	0	0	0	0	0	0	0	0	0	0	0	0	0	0	0	0	0	0	0	0	0	0	0
14	11	8	1	0	1	0	0	0	0	0	0	0	0	0	0	0	0	0	0	0	0	0	0	0	0	0	0	0	0	0	0	0	0	0	0	0	0	0	0
15	10	4	0	0	0	0	0	0	0	0	0	0	0	0	0	0	0	0	0	0	0	0	0	0	0	0	0	0	0	0	0	0	0	0	0	0	0	0	0
16	4	1	0	0	0	0	0	0	0	0	0	0	0	0	0	0	0	0	0	0	0	0	0	0	0	0	0	0	0	0	0	0	0	0	0	0	0	0	0
17	0	0	0	0	0	0	0	0	0	0	0	0	0	0	0	0	0	0	0	0	0	0	0	0	0	0	0	0	0	0	0	0	0	0	0	0	0	0	0
18	0	0	0	0	0	0	0	0	0	0	0	0	0	0	0	0	0	0	0	0	0	0	0	0	0	0	0	0	0	0	0	0	0	0	0	0	0	0	0
19	0	0	0	0	0	0	0	0	0	0	0	0	0	0	0	0	0	0	0	0	0	0	0	0	0	0	0	0	0	0	0	0	0	0	0	0	0	0	0
20	0	0	0	0	0	0	0	0	0	0	0	0	0	0	0	0	0	0	0	0	0	0	0	0	0	0	0	0	0	0	0	0	0	0	0	0	0	0	0
21	0	0	0	0	0	0	0	0	0	0	0	0	0	0	0	0	0	0	0	0	0	0	0	0	0	0	0	0	0	0	0	0	0	0	0	0	0	0	0
22	0	0	0	0	0	0	0	0	0	0	0	0	0	0	0	0	0	0	0	0	0	0	0	0	0	0	0	0	0	0	0	0	0	0	0	0	0	0	0
23	0	0	0	0	0	0	0	0	0	0	0	0	0	0	0	0	0	0	0	0	0	0	0	0	0	0	0	0	0	0	0	0	0	0	0	0	0	0	0
24	0	0	0	0	0	0	0	0	0	0	0	0	0	0	0	0	0	0	0	0	0	0	0	0	0	0	0	0	0	0	0	0	0	0	0	0	0	0	0
25	0	0	0	0	0	0	0	0	0	0	0	0	0	0	0	0	0	0	0	0	0	0	0	0	0	0	0	0	0	0	0	0	0	0	0	0	0	0	0
26	0	0	0	0	0	0	0	0	0	0	0	0	0	0	0	0	0	0	0	0	0	0	0	0	0	0	0	0	0	0	0	0	0	0	0	0	0	0	0
27	0	0	0	0	0	0	0	0	0	0	0	0	0	0	0	0	0	0	0	0	0	0	0	0	0	0	0	0	0	0	0	0	0	0	0	0	0	0	0
28	0	0	0	0	0	0	0	0	0	0	0	0	0	0	0	0	0	0	0	0	0	0	0	0	0	0	0	0	0	0	0	0	0	0	0	0	0	0	0
29	0	0	0	0	0	0	0	0	0	0	0	0	0	0	0	0	0	0	0	0	0	0	0	0	0	0	0	0	0	0	0	0	0	0	0	0	0	0	0
30	0	0	0	0	0	0	0	0	0	0	0	0	0	0	0	0	0	0	0	0	0	0	0	0	0	0	0	0	0	0	0	0	0	0	0	0	0	0	0
31	0	0	0	0	0	0	0	0	0	0	0	0	0	0	0	0	0	0	0	0	0	0	0	0	0	0	0	0	0	0	0	0	0	0	0	0	0	0	0
32	0	0	0	0	0	0	0	0	0	0	0	0	0	0	0	0	0	0	0	0	0	0	0	0	0	0	0	0	0	0	0	0	0	0	0	0	0	0	0
33	0	0	0	0	0	0	0	0	0	0	0	0	0	0	0	0	0	0	0	0	0	0	0	0	0	0	0	0	0	0	0	0	0	0	0	0	0	0	0
34	0	0	0	0	0	0	0	0	0	0	0	0	0	0	0	0	0	0	0	0	0	0	0	0	0	0	0	0	0	0	0	0	0	0	0	0	0	0	0
35	0	0	0	0	0	0	0	0	0	0	0	0	0	0	0	0	0	0	0	0	0	0	0	0	0	0	0	0	0	0	0	0	0	0	0	0	0	0	0

Figure A-14. Areal map of the 10 May 1979 snowfall (cm) for the study area.

GRIDDED CLIMATIC DATA FROM FILE SC79130V, CHANNEL 3:
 CHANNEL 1=TMX(C), 2=TMN(C), 3=PRECIP(mm), 4=SNOWFALL(cm), 5=SNOWDEPTH(cm)

	1	2	3	4	5	6	7	8	9	10	11	12	13	14	15	16	17	18	19	20	21	22	23	24	25	26	27	28	29	30	31	32	33	34	35	36	37	38	39	40		
1	5	5	7	10	6	1	2	2	1	0	0	0	0	0	0	0	0	0	0	0	0	0	0	0	0	0	0	0	0	0	0	0	0	0	0	0	0	0	0	0	0	
2	5	5	3	1	2	6	5	4	2	0	0	0	0	0	0	0	0	0	0	0	0	0	0	0	0	0	0	0	0	0	0	0	0	0	0	0	0	0	0	0	0	0
3	6	5	3	1	2	7	6	3	3	0	0	0	0	0	0	0	0	0	0	0	0	0	0	0	0	0	0	0	0	0	0	0	0	0	0	0	0	0	0	0	0	0
4	6	5	4	1	3	8	6	1	1	0	0	0	0	0	0	0	0	0	0	0	0	0	0	0	0	0	0	0	0	0	0	0	0	0	0	0	0	0	0	0	0	0
5	4	6	4	2	3	8	5	1	0	0	0	0	0	0	0	0	0	0	0	0	0	0	0	0	0	0	0	0	0	0	0	0	0	0	0	0	0	0	0	0	0	0
6	1	2	1	1	3	3	1	0	0	0	0	0	0	0	0	0	0	0	0	0	0	0	0	0	0	0	0	0	0	0	0	0	0	0	0	0	0	0	0	0	0	0
7	0	0	0	0	0	0	0	0	0	0	0	0	0	0	0	0	0	0	0	0	0	0	0	0	0	0	0	0	0	0	0	0	0	0	0	0	0	0	0	0	0	0
8	0	0	0	0	0	0	0	0	0	0	0	0	0	0	0	0	0	0	0	0	0	0	0	0	0	0	0	0	0	0	0	0	0	0	0	0	0	0	0	0	0	0
9	0	0	0	0	0	0	0	0	0	0	0	0	0	0	0	0	0	0	0	0	0	0	0	0	0	0	0	0	0	0	0	0	0	0	0	0	0	0	0	0	0	0
10	1	0	0	0	0	0	0	0	0	0	0	0	0	0	0	0	0	0	0	0	0	0	0	0	0	0	0	0	0	0	0	0	0	0	0	0	0	0	0	0	0	0
11	1	0	0	0	0	0	0	0	0	0	0	0	0	0	0	0	0	0	0	0	0	0	0	0	0	0	0	0	0	0	0	0	0	0	0	0	0	0	0	0	0	0
12	4	1	0	0	0	0	0	0	0	0	0	0	0	0	0	0	0	0	0	0	0	0	0	0	0	0	0	0	0	0	0	0	0	0	0	0	0	0	0	0	0	0
13	4	2	0	0	0	0	0	0	0	0	0	0	0	0	0	0	0	0	0	0	0	0	0	0	0	0	0	0	0	0	0	0	0	0	0	0	0	0	0	0	0	0
14	7	2	0	0	0	0	0	0	0	0	0	0	0	0	0	0	0	0	0	0	0	0	0	0	0	0	0	0	0	0	0	0	0	0	0	0	0	0	0	0	0	0
15	4	0	0	0	0	0	0	0	0	0	0	0	0	0	0	0	0	0	0	0	0	0	0	0	0	0	0	0	0	0	0	0	0	0	0	0	0	0	0	0	0	0
16	4	0	0	0	0	0	0	0	0	0	0	0	0	0	0	0	0	0	0	0	0	0	0	0	0	0	0	0	0	0	0	0	0	0	0	0	0	0	0	0	0	0
17	0	0	0	0	0	0	0	0	0	0	0	0	0	0	0	0	0	0	0	0	0	0	0	0	0	0	0	0	0	0	0	0	0	0	0	0	0	0	0	0	0	0
18	0	0	0	0	0	0	0	0	0	0	0	0	0	0	0	0	0	0	0	0	0	0	0	0	0	0	0	0	0	0	0	0	0	0	0	0	0	0	0	0	0	0
19	0	0	0	0	0	0	0	0	0	0	0	0	0	0	0	0	0	0	0	0	0	0	0	0	0	0	0	0	0	0	0	0	0	0	0	0	0	0	0	0	0	0
20	0	0	0	0	0	0	0	0	0	0	0	0	0	0	0	0	0	0	0	0	0	0	0	0	0	0	0	0	0	0	0	0	0	0	0	0	0	0	0	0	0	0
21	0	0	0	0	0	0	0	0	0	0	0	0	0	0	0	0	0	0	0	0	0	0	0	0	0	0	0	0	0	0	0	0	0	0	0	0	0	0	0	0	0	0
22	0	0	0	0	0	0	0	0	0	0	0	0	0	0	0	0	0	0	0	0	0	0	0	0	0	0	0	0	0	0	0	0	0	0	0	0	0	0	0	0	0	0
23	0	0	0	0	0	0	0	0	0	0	0	0	0	0	0	0	0	0	0	0	0	0	0	0	0	0	0	0	0	0	0	0	0	0	0	0	0	0	0	0	0	0
24	0	0	0	0	0	0	0	0	0	0	0	0	0	0	0	0	0	0	0	0	0	0	0	0	0	0	0	0	0	0	0	0	0	0	0	0	0	0	0	0	0	0
25	0	0	0	0	0	0	0	0	0	0	0	0	0	0	0	0	0	0	0	0	0	0	0	0	0	0	0	0	0	0	0	0	0	0	0	0	0	0	0	0	0	0
26	0	0	0	0	0	0	0	0	0	0	0	0	0	0	0	0	0	0	0	0	0	0	0	0	0	0	0	0	0	0	0	0	0	0	0	0	0	0	0	0	0	0
27	0	0	0	0	0	0	0	0	0	0	0	0	0	0	0	0	0	0	0	0	0	0	0	0	0	0	0	0	0	0	0	0	0	0	0	0	0	0	0	0	0	0
28	0	0	0	0	0	0	0	0	0	0	0	0	0	0	0	0	0	0	0	0	0	0	0	0	0	0	0	0	0	0	0	0	0	0	0	0	0	0	0	0	0	0
29	0	0	0	0	0	0	0	0	0	0	0	0	0	0	0	0	0	0	0	0	0	0	0	0	0	0	0	0	0	0	0	0	0	0	0	0	0	0	0	0	0	0
30	0	0	0	0	0	0	0	0	0	0	0	0	0	0	0	0	0	0	0	0	0	0	0	0	0	0	0	0	0	0	0	0	0	0	0	0	0	0	0	0	0	0
31	0	0	0	0	0	0	0	0	0	0	0	0	0	0	0	0	0	0	0	0	0	0	0	0	0	0	0	0	0	0	0	0	0	0	0	0	0	0	0	0	0	0
32	0	0	0	0	0	0	0	0	0	0	0	0	0	0	0	0	0	0	0	0	0	0	0	0	0	0	0	0	0	0	0	0	0	0	0	0	0	0	0	0	0	0
33	0	0	0	0	0	0	0	0	0	0	0	0	0	0	0	0	0	0	0	0	0	0	0	0	0	0	0	0	0	0	0	0	0	0	0	0	0	0	0	0	0	0
34	0	0	0	0	0	0	0	0	0	0	0	0	0	0	0	0	0	0	0	0	0	0	0	0	0	0	0	0	0	0	0	0	0	0	0	0	0	0	0	0	0	0
35	0	0	0	0	0	0	0	0	0	0	0	0	0	0	0	0	0	0	0	0	0	0	0	0	0	0	0	0	0	0	0	0	0	0	0	0	0	0	0	0	0	0

Figure A-15. Areal map of the 10 May 1979 snowdepth (cm) for the study area.

GRIDDED API (mm) FROM FILE SA791301

1	2	3	4	5	6	7	8	9	10	11	12	13	14	15	16	17	18	19	20	21	22	23	24	25	26	27	28	29	30	31	32	33	34	35	36	37	38	39	40	
5	6	17	20	16	22	11	6	5	6	5	5	4	6	11	13	20	23	28	33	36	38	31	18	10	6	7	9	9	10	10	8	7	6	7	9	9	9	9	9	
2	6	8	11	10	18	10	5	5	7	5	7	5	5	7	14	16	18	22	27	32	33	29	12	5	4	6	8	10	9	10	9	7	6	5	7	9	9	10	11	
3	13	14	14	11	17	12	7	4	5	8	7	6	8	10	14	17	22	30	33	30	21	12	6	4	5	7	11	11	11	10	9	7	6	4	6	7	9	11	12	
4	21	15	14	11	16	12	7	3	7	10	8	7	9	11	13	16	20	26	31	34	27	17	9	5	9	7	11	14	14	13	12	9	6	3	3	6	9	8	11	10
5	13	15	14	11	17	10	6	5	7	7	7	4	7	10	12	15	18	21	28	31	23	15	9	5	9	11	12	14	16	14	12	9	6	4	4	6	7	8	9	7
6	14	9	11	10	13	9	2	8	5	2	2	3	5	9	11	13	17	20	25	24	17	12	9	8	11	13	14	15	17	15	12	8	6	6	5	6	7	7	6	5
7	15	15	15	12	5	3	7	8	4	2	1	3	6	9	10	10	16	30	33	21	15	11	10	11	12	14	16	18	20	18	12	7	7	6	5	5	5	5	5	
8	18	16	13	9	5	2	2	4	2	1	0	1	7	10	10	16	30	33	21	15	11	10	11	12	14	16	18	20	18	12	7	7	6	5	5	5	5	5	5	
9	17	16	12	8	5	1	0	0	0	0	1	6	12	14	18	27	19	14	11	9	9	11	10	15	22	23	18	14	11	9	8	7	5	4	5	5	5	4	5	
10	6	16	13	10	5	3	2	2	1	1	1	1	10	17	20	22	19	16	13	9	8	8	9	10	12	16	24	25	20	16	13	10	7	5	4	5	5	5	6	
11	7	15	13	12	4	4	3	2	1	2	3	3	11	21	24	19	16	13	11	9	8	8	9	14	21	27	29	27	20	14	11	6	5	3	6	5	4	5		
12	7	10	17	17	7	4	3	1	2	2	3	3	11	20	22	20	16	13	14	13	11	13	13	22	26	31	32	29	20	15	12	8	7	6	6	6	6	7	8	10
13	12	18	15	13	13	16	16	9	5	9	23	23	22	10	9	10	11	10	15	25	32	33	40	46	33	21	16	12	9	7	6	7	8	9	10	10	11	10	11	10
14	15	18	16	15	14	14	16	19	16	13	7	7	18	23	18	10	8	10	12	15	32	39	38	48	44	29	17	10	8	6	6	6	7	8	9	11	11	10	11	10
15	17	15	16	15	11	9	15	19	16	13	7	5	9	14	12	11	10	11	14	16	27	33	35	43	38	35	24	18	12	8	7	6	5	6	6	8	10	10	9	
16	10	11	15	13	6	4	9	14	13	7	8	9	10	10	12	14	24	41	60	46	58	49	29	16	13	13	13	12	9	10	8	7	7	8	9	10	9	9	9	9
17	8	7	7	6	6	7	7	7	8	5	7	9	9	13	22	25	32	47	61	81	75	54	46	25	16	12	11	10	11	10	10	11	11	11	11	11	11	11	11	11
18	6	5	4	4	5	6	5	4	4	4	4	4	14	23	25	26	39	65	75	75	64	48	38	22	18	14	11	11	12	12	11	10	12	13	14	12	12	12	12	12
19	3	4	4	4	5	6	5	4	4	4	4	4	14	23	25	30	56	71	70	56	46	40	26	20	19	16	15	13	14	12	11	12	15	20	16	13	14	14	14	
20	3	3	4	5	5	4	3	3	3	3	3	4	7	25	26	37	58	61	54	38	32	25	19	19	18	16	17	17	19	18	15	13	15	18	22	20	18	18	16	
21	2	3	3	4	5	4	3	2	1	1	3	4	4	22	27	47	53	53	41	30	27	21	15	15	13	12	14	15	17	18	20	21	20	18	16	18	22	21	19	17
22	1	3	3	3	3	3	3	2	1	1	2	3	4	4	15	22	28	36	41	33	27	24	20	15	13	12	14	15	18	21	22	23	22	19	19	18	19	17	14	
23	1	3	3	3	3	3	2	1	1	3	3	3	3	11	14	15	16	19	24	23	17	14	12	10	10	13	14	15	18	21	22	23	22	19	19	18	19	17	14	
24	2	3	3	3	3	3	2	1	1	2	3	3	3	2	3	8	14	15	16	19	19	12	10	10	11	14	15	16	18	17	15	12	12	13	12	10	9	10	9	10
25	2	2	1	1	2	2	2	2	1	1	2	2	1	2	2	6	14	15	15	13	10	9	12	13	14	15	15	16	16	17	13	10	9	10	10	9	8	7	9	
26	2	2	1	1	2	2	2	2	1	1	2	2	1	2	2	2	9	13	14	13	12	10	10	12	13	16	18	15	15	13	10	8	8	8	8	7	7	8	7	9
27	3	3	2	2	2	2	2	2	1	1	1	1	1	2	2	3	6	10	11	9	9	11	12	11	13	16	15	12	12	11	9	9	7	7	7	7	7	7	9	
28	3	3	2	2	2	2	2	2	2	2	2	2	3	3	4	5	7	7	7	8	8	9	10	9	8	9	10	8	7	7	7	7	7	7	7	7	7	9		
29	3	3	2	2	2	2	2	2	2	2	2	2	3	3	3	5	6	6	7	8	8	9	10	9	8	9	10	8	7	7	7	7	6	6	6	5	5	9		
30	1	2	2	2	2	2	2	2	2	2	2	2	3	3	3	5	6	6	7	9	9	8	8	7	5	4	3	2	2	2	2	3	6	4	4	3	3	6	6	
31	0	1	2	2	2	2	2	2	2	2	2	2	3	3	3	5	6	6	7	9	9	8	8	7	5	4	3	2	2	2	2	3	6	4	4	3	3	6	6	
32	1	1	1	2	2	2	3	4	5	7	7	5	2	0	2	4	4	4	4	4	5	6	6	5	4	4	2	2	1	2	2	2	3	1	1	1	5	6	7	8
33	1	1	1	1	2	2	3	4	5	7	7	5	2	0	2	4	4	4	4	4	5	6	6	5	4	4	2	2	1	2	2	2	1	1	1	5	6	7	8	
34	1	1	1	1	1	1	4	4	4	4	4	4	4	4	4	4	4	4	4	5	5	5	4	3	3	3	3	4	2	2	2	2	2	2	2	5	11	8	7	10
35	1	1	1	1	1	1	1	4	4	4	4	4	3	3	3	3	5	4	4	4	5	9	8	5	3	3	3	3	3	4	2	2	2	3	4	10	19	14	13	14

Figure A-16. Areal map of the 10 May 1979 Antecedent Precipitation Index values (mm) for the study area.

APPENDIX B
MONTHLY CORRELATION COEFFICIENTS

TABLE B-1
CORRELATION COEFFICIENT ($\times 1000$) BETWEEN THE 1.66 CM TRANSFORMS
AND API FOR ROW 15 COL 29 BETWEEN 25 OCT 1978 AND 10 NOV 1979

DEPLETION COEFFICIENT TRANSFORM		MONTH											
		MAR	APR	MAY	JUN	JUL	AUG	SEP	OCT	NOV	ALL		
0.850	Th/T	-747	-886	-444	-695	-534	-670	-876	-921	-745	-755		
	Tv-Th	724	697	278	220	258	632	910	873	610	673		
	$[(Tv-Th)/0.5(Tv+Th)]$	742	714	322	199	266	611	916	896	631	695		
	M.L. Reg on All 3	776	891	631	834	590	773	923	964	822	774		
0.891	Th/T	-764	-879	-436	-723	-579	-588	-882	-924	-744	-761		
	Tv-Th	739	692	286	219	300	574	917	880	620	679		
	$[(Tv-Th)/0.5(Tv+Th)]$	755	709	332	202	313	549	923	902	641	702		
	M.L. Reg on All 3	792	884	651	861	632	737	929	966	818	782		
0.900	Th/T	-768	-871	-452	-715	-579	-588	-882	-923	-732	-764		
	Tv-Th	745	666	289	226	300	574	917	876	603	682		
	$[(Tv-Th)/0.5(Tv+Th)]$	762	685	333	206	313	549	923	899	625	705		
	M.L. Reg on All 3	797	876	638	852	632	737	929	965	807	785		
0.950	Th/T	-749	-890	-452	-746	-502	-530	-868	-922	-743	-770		
	Tv-Th	732	709	290	245	201	515	915	873	628	690		
	$[(Tv-Th)/0.5(Tv+Th)]$	750	727	335	225	214	486	920	897	650	713		
	M.L. Reg on All 3	783	897	646	881	592	724	922	967	819	790		

TABLE B-2
CORRELATION COEFFICIENT (x1000) BETWEEN ALL TRANSFORMS AND
API FOR ROW 03 COL 27 BETWEEN 25 OCT 1978 AND 10 NOV 1979

WAVE- LENGTH (cm)	TRANSFORM	MONTH											
		MAR	APR	MAY	JUN	JUL	AUG	SEP	OCT	NOV	ALL		
0.81	Th/T	-774	-912	-887	-823	-754	-546	-059	-857	-547	-822		
	Tv-Th	675	933	809	597	480	329	340	751	730	758		
	[(Tv-Th)/0.5(Tv+Th)]	742	926	820	601	499	341	310	793	766	777		
	M.L. Reg on All 3	868	941	928	907	793	574	433	941	858	855		
1.36	Th/T	-679	-882	-916	-868	-353	-723	-136	-780	-674	-793		
	Tv-Th	699	784	694	717	037	138	483	531	474	655		
	[(Tv-Th)/0.5(Tv+Th)]	720	784	704	722	015	133	464	599	558	681		
	M.L. Reg on All 3	786	894	920	889	831	729	546	967	921	826		
1.66	Th/T	-827	-904	-933	-943	-745	-770	-199	-863	-794	-844		
	Tv-Th	679	819	931	869	457	479	035	806	786	783		
	[(Tv-Th)/0.5(Tv+Th)]	769	844	927	871	482	496	032	854	808	806		
	M.L. Reg on All 3	857	912	955	954	790	787	227	981	923	873		
2.80	Th/T	-649	-887	-889	-980	-737	-754	-344	-823	-728	-821		
	Tv-Th	104	916	869	923	465	424	661	700	625	739		
	[(Tv-Th)/0.5(Tv+Th)]	334	924	884	935	510	426	717	781	692	772		
	M.L. Reg on All 3	924	925	907	982	842	777	782	984	906	867		
4.54	Th/T	-459	-867	-900	-958	-784	-859	-553	-741	-696	-787		
	Tv-Th	276	807	895	944	497	700	769	670	540	720		
	[(Tv-Th)/0.5(Tv+Th)]	433	854	902	945	549	699	726	738	623	754		
	M.L. Reg on All 3	757	940	915	972	891	868	817	978	898	840		

TABLE B-3
CORRELATION COEFFICIENT (x1000) BETWEEN ALL TRANSFORMS AND
API FOR ROW 09 COL 21 BETWEEN 25 OCT 1978 AND 10 NOV 1979

WAVE- LENGTH (cm)	TRANSFORM	MONTH											
		MAR	APR	MAY	JUN	JUL	AUG	SEP	OCT	NOV	ALL		
0.81	Th/T	-807	-898	-888	-358	-728	-386	-398	-917	-430	-851		
	Tv-Th	835	883	656	420	830	530	503	891	532	845		
	[(Tv-Th)/0.5(Tv+Th)]	849	877	669	393	833	516	484	909	541	854		
	M.L. Reg on All 3	928	919	899	508	863	722	662	990	656	882		
1.36	Th/T	-621	-962	-952	-222	-799	-505	-174	-853	-450	-847		
	Tv-Th	586	844	791	093	948	038	107	626	372	725		
	[(Tv-Th)/0.5(Tv+Th)]	609	859	818	090	955	043	146	680	411	747		
	M.L. Reg on All 3	684	969	962	381	975	703	513	981	765	866		
1.66	Th/T	-680	-965	-904	-155	-815	-545	-479	-941	-667	-872		
	Tv-Th	584	934	892	072	896	021	705	943	592	813		
	[(Tv-Th)/0.5(Tv+Th)]	603	935	893	076	896	032	674	960	618	828		
	M.L. Reg on All 3	692	969	928	264	906	632	801	996	804	888		
2.80	Th/T	-710	-949	-857	-401	-813	-596	-390	-919	-688	-881		
	Tv-Th	683	982	823	344	884	577	760	961	660	892		
	[(Tv-Th)/0.5(Tv+Th)]	710	980	879	324	893	582	748	977	690	902		
	M.L. Reg on All 3	754	983	902	444	945	614	863	997	831	912		
4.54	Th/T	-545	-966	-846	-728	-896	-400	-284	-778	-666	-841		
	Tv-Th	048	941	609	761	910	112	296	719	605	764		
	[(Tv-Th)/0.5(Tv+Th)]	132	970	745	768	923	136	359	803	640	820		
	M.L. Reg on All 3	914	984	879	804	985	544	829	980	847	888		

TABLE B-4

CORRELATION COEFFICIENT (x1000) BETWEEN ALL TRANSFORMS AND
API FOR ROW 09 COL 29 BETWEEN 25 OCT 1978 AND 10 NOV 1979

WAVE- LENGTH (cm)	TRANSFORM	MONTH											
		MAR	APR	MAY	JUN	JUL	AUG	SEP	OCT	NOV	ALL		
0.81	Th/T	-854	-873	-255	-634	-832	-148	-907	-851	-659	-777		
	Tv-Th	744	882	439	445	724	243	805	803	713	738		
	[(Tv-Th)/0.5(Tv+Th)]	741	878	456	461	781	268	793	820	733	750		
	M.L. Reg on All 3	866	929	633	684	973	352	938	893	855	810		
1.36	Th/T	-833	-931	259	-423	-764	-348	-856	-816	-754	-767		
	Tv-Th	726	721	-369	287	274	314	841	653	645	649		
	[(Tv-Th)/0.5(Tv+Th)]	720	740	-336	298	308	331	849	679	677	669		
	M.L. Reg on All 3	1000	952	602	584	930	647	917	852	881	783		
1.66	Th/T	-894	-868	-028	-899	-871	-251	-927	-819	-868	-814		
	Tv-Th	880	705	677	943	735	147	672	685	800	750		
	[(Tv-Th)/0.5(Tv+Th)]	855	734	698	938	755	176	661	722	816	763		
	M.L. Reg on All 3	991	880	747	952	937	430	929	872	900	820		
2.80	Th/T	-925	-909	-069	-692	-868	-167	-874	-827	-809	-791		
	Tv-Th	889	965	236	427	491	188	949	735	664	725		
	[(Tv-Th)/0.5(Tv+Th)]	887	964	251	458	580	265	937	776	724	751		
	M.L. Reg on All 3	953	966	453	889	988	506	964	942	951	827		
4.54	Th/T	-926	-911	-027	-718	-918	-405	-828	-780	-802	-760		
	Tv-Th	943	845	044	488	800	549	907	650	752	685		
	[(Tv-Th)/0.5(Tv+Th)]	960	899	090	532	853	562	903	699	796	719		
	M.L. Reg on All 3	963	960	440	889	961	642	933	943	955	800		

TABLE B-5
CORRELATION COEFFICIENT ($\times 1000$) BETWEEN ALL TRANSFORMS AND
API FOR ROW 15 COL 29 BETWEEN 25 OCT 1978 AND 10 NOV 1979

WAVE- LENGTH (cm)	TRANSFORM	MONTH											
		MAR	APR	MAY	JUN	JUL	AUG	SEP	OCT	NOV	ALL		
0.81	Th/T	-707	-917	-358	-701	-539	-579	-586	-874	-518	-701		
	Tv-Th	835	889	655	621	607	180	602	847	583	687		
	$[(Tv-Th)/0.5(Tv+Th)]$	836	894	693	585	602	168	579	866	605	702		
	M.L. Reg on All 3	842	917	769	908	610	625	733	952	731	744		
1.36	Th/T	-717	-873	-353	-752	-440	-659	-946	-842	-645	-748		
	Tv-Th	716	593	182	333	098	506	675	629	623	674		
	$[(Tv-Th)/0.5(Tv+Th)]$	727	607	223	318	112	498	686	675	632	688		
	M.L. Reg on All 3	758	893	652	894	538	690	970	959	671	757		
1.66	Th/T	-764	-879	-436	-723	-579	-588	-882	-924	-744	-761		
	Tv-Th	739	692	286	219	300	574	917	880	620	679		
	$[(Tv-Th)/0.5(Tv+Th)]$	755	709	332	202	313	549	923	902	641	702		
	M.L. Reg on All 3	792	884	651	861	632	737	929	966	818	782		
2.80	Th/T	-757	-874	-420	-925	-626	-597	-833	-929	-770	-765		
	Tv-Th	753	946	564	900	678	519	965	942	630	757		
	$[(Tv-Th)/0.5(Tv+Th)]$	777	940	606	899	666	497	969	961	664	771		
	M.L. Reg on All 3	800	949	704	926	699	606	971	990	864	790		
4.54	Th/T	-762	-867	-321	-925	-493	-112	-661	-622	-782	-726		
	Tv-Th	679	845	269	906	670	235	698	381	696	629		
	$[(Tv-Th)/0.5(Tv+Th)]$	707	895	308	894	638	234	723	447	723	688		
	M.L. Reg on All 3	888	951	659	939	764	258	917	901	840	801		

TABLE B-6
CORRELATION COEFFICIENT (x1000) BETWEEN ALL TRANSFORMS AND
API FOR ROW 18 COL 27 BETWEEN 25 OCT 1978 AND 10 NOV 1979

WAVE- LENGTH (cm)	TRANSFORM	MONTH											
		MAR	APR	MAY	JUN	JUL	AUG	SEP	OCT	NOV	ALL		
0.81	Th/T	-785	-641	-234	-526	-756	-922	-963	-875	-693	-677		
	Tv-Th	806	585	110	485	662	780	939	848	655	616		
	[(Tv-Th)/0.5(Tv+Th)]	799	599	177	478	675	788	947	865	676	629		
	M.L. Reg on All 3	822	696	690	656	797	927	978	955	810	702		
1.36	Th/T	-790	-798	-323	-404	-838	-941	-970	-850	-652	-703		
	Tv-Th	633	716	-077	215	458	631	964	540	586	584		
	[(Tv-Th)/0.5(Tv+Th)]	650	729	-039	221	487	643	969	587	613	599		
	M.L. Reg on All 3	833	847	818	630	842	967	996	974	753	712		
1.66	Th/T	-780	-874	-607	-155	-785	-940	-942	-938	-726	-734		
	Tv-Th	739	770	419	128	752	752	939	689	670	669		
	[(Tv-Th)/0.5(Tv+Th)]	739	764	486	124	753	769	948	753	684	687		
	M.L. Reg on All 3	781	916	839	157	787	972	973	992	756	741		
2.80	Th/T	-821	-888	-535	-325	-793	-966	-925	-934	-746	-750		
	Tv-Th	850	939	541	301	781	893	961	963	718	732		
	[(Tv-Th)/0.5(Tv+Th)]	843	936	621	307	783	885	963	976	733	742		
	M.L. Reg on All 3	851	943	784	364	803	973	964	995	783	759		
4.54	Th/T	-730	-915	-480	-810	-721	-759	-915	-775	-647	-755		
	Tv-Th	518	886	402	751	525	903	908	549	511	613		
	[(Tv-Th)/0.5(Tv+Th)]	570	885	463	776	566	910	915	634	553	658		
	M.L. Reg on All 3	889	918	664	905	776	919	942	978	759	772		

TABLE B-7

CORRELATION COEFFICIENT (x1000) BETWEEN ALL TRANSFORMS AND
API FOR ROW 21 COL 14 BETWEEN 25 OCT 1978 AND 10 NOV 1979

WAVE- LENGTH (cm)	TRANSFORM	MONTH											
		MAR	APR	MAY	JUN	JUL	AUG	SEP	OCT	NOV	ALL		
0.81	Th/T	-789	-423	-835	-590	-593	-411	-869	-261	-761	-562		
	Tv-Th	669	750	447	576	305	502	749	160	846	428		
	[(Tv-Th)/0.5(Tv+Th)]	688	739	466	634	331	483	760	245	855	438		
	M.L. Reg on All 3	846	791	843	812	611	551	915	571	868	567		
1.36	Th/T	-822	-564	-783	-619	-543	-440	-824	-535	-754	-500		
	Tv-Th	753	885	236	205	275	-058	374	699	395	259		
	[(Tv-Th)/0.5(Tv+Th)]	761	143	299	231	278	-059	395	720	447	275		
	M.L. Reg on All 3	843	706	816	728	597	526	894	804	831	535		
1.66	Th/T	-864	-453	-901	-692	-730	-576	-918	-299	-888	-633		
	Tv-Th	734	450	769	367	719	645	886	495	879	584		
	[(Tv-Th)/0.5(Tv+Th)]	741	473	765	428	711	623	889	548	891	587		
	M.L. Reg on All 3	866	555	905	847	754	688	946	632	919	638		
2.80	Th/T	-866	-582	-802	-820	-582	-649	-860	-219	-867	-623		
	Tv-Th	795	778	469	568	382	761	955	647	872	569		
	[(Tv-Th)/0.5(Tv+Th)]	797	773	522	662	417	761	948	676	892	575		
	M.L. Reg on All 3	867	783	838	958	938	776	965	713	926	626		
4.54	Th/T	-875	-557	-794	-826	-630	-706	-717	-273	-874	-657		
	Tv-Th	743	460	538	391	584	836	561	576	872	608		
	[(Tv-Th)/0.5(Tv+Th)]	766	501	594	532	602	830	722	630	907	622		
	M.L. Reg on All 3	899	671	863	979	702	862	922	697	952	661		

TABLE B-8

CORRELATION COEFFICIENT ($\times 1000$) BETWEEN ALL TRANSFORMS AND
API FOR ROW 29 COL 22 BETWEEN 25 OCT 1978 AND 10 NOV 1979

WAVE- LENGTH (cm)	TRANSFORM	MONTH											
		MAR	APR	MAY	JUN	JUL	AUG	SEP	OCT	NOV	ALL		
0.81	Th/T	-745	-855	-415	-968	-930	-839	-926	-602	-782	-663		
	Tv-Th	742	789	484	922	761	729	786	546	864	635		
	[(Tv-Th)/0.5(Tv+Th)]	740	757	548	926	791	747	733	561	874	642		
	M.L. Reg on All 3	813	927	824	977	935	848	961	689	893	690		
1.36	Th/T	-759	-856	-559	-966	-740	-855	-953	-581	-802	-675		
	Tv-Th	654	674	453	894	247	505	712	258	910	534		
	[(Tv-Th)/0.5(Tv+Th)]	670	673	521	909	214	517	689	285	915	548		
	M.L. Reg on All 3	788	899	880	994	971	884	957	741	917	681		
1.66	Th/T	-734	-856	-633	-983	-671	-887	-862	-682	-826	-704		
	Tv-Th	928	703	375	936	087	818	410	742	779	620		
	[(Tv-Th)/0.5(Tv+Th)]	899	726	463	933	139	820	397	747	806	635		
	M.L. Reg on All 3	948	931	922	992	954	903	977	771	894	713		
2.80	Th/T	-694	-751	-626	-893	-762	-924	-881	-795	-786	-709		
	Tv-Th	842	700	454	960	516	767	867	880	889	688		
	[(Tv-Th)/0.5(Tv+Th)]	815	711	534	973	562	781	852	888	902	701		
	M.L. Reg on All 3	874	769	907	991	911	944	933	919	935	733		
4.54	Th/T	-634	-558	-661	-875	-746	-948	-908	-882	-783	-708		
	Tv-Th	791	573	628	951	344	867	554	390	249	524		
	[(Tv-Th)/0.5(Tv+Th)]	777	579	687	948	432	881	545	500	387	600		
	M.L. Reg on All 3	843	594	902	954	924	955	921	969	934	755		

APPENDIX C
BI-MONTHLY AND ANNUAL CORRELATION COEFFICIENTS

TABLE C-1

BRIGHTNESS TEMPERATURE CORRELATION COEFFICIENT MATRIX
FOR ROW 15 COL 29 BETWEEN 25 OCT 1978 AND 10 NOV 1979

HORIZONTAL POLARIZATION WAVELENGTH (cm)					
	0.81	1.36	1.66	2.80	4.54
0.81	1.00	0.99	0.97	0.92	0.80
1.36		1.00	0.99	0.95	0.84
1.66			1.00	0.98	0.87
2.80				1.00	0.92
4.54					1.00

VERTICAL POLARIZATION WAVELENGTH (cm)					
	0.81	1.36	1.66	2.80	4.54
0.81	1.00				
1.36	0.98	1.00			
1.66	0.97	0.99	1.00		
2.80	0.94	0.97	0.99	1.00	
4.54	0.89	0.95	0.96	0.98	1.00

TABLE C-2

NORMALIZED BRIGHTNESS TEMPERATURE CORRELATION COEFFICIENT
MATRIX FOR ROW 15 COL 29 BETWEEN 25 OCT 1978 AND 10 NOV 1979

HORIZONTAL POLARIZATION					
WAVELENGTH (cm)					
	0.81	1.36	1.66	2.80	4.54
-----	-----	-----	-----	-----	-----
0.81	1.00	0.95	0.93	0.81	0.59
1.36		1.00	0.97	0.89	0.69
1.66			1.00	0.95	0.76
2.80				1.00	0.86
4.54					1.00

VERTICAL POLARIZATION					
WAVELENGTH (cm)					
	0.81	1.36	1.66	2.80	4.54
-----	-----	-----	-----	-----	-----
0.81	1.00				
1.36	0.87	1.00			
1.66	0.87	0.95	1.00		
2.80	0.81	0.92	0.96	1.00	
4.54	0.75	0.90	0.92	0.96	1.00

TABLE C-3

CORRELATION COEFFICIENT (x1000) BETWEEN THE HORIZONTALLY
POLARIZED NORMALIZED BRIGHTNESS TEMPERATURE AND API
BETWEEN 25 OCT 1978 AND 10 NOV 1979

<u>GRID CELL</u>	<u>DATA</u>	<u>CHANNEL</u>				
		<u>0.81H</u>	<u>1.35H</u>	<u>1.66H</u>	<u>2.80H</u>	<u>4.54H</u>
R03 C27	Night/Day	-768	-771	-816	-800	-794
	Night	-715	-802	-811	-843	-875
	Day	-848	-789	-840	-821	-775
R09 C21	Night/Day	-809	-830	-861	-861	-840
	Night	-819	-828	-863	-881	-895
	Day	-847	-876	-885	-901	-834
R09 C29	Night/Day	-748	-782	-800	-780	-747
	Night	-701	-796	-787	-785	-758
	Day	-831	-799	-830	-826	-790
R15 C29	Night/Day	-749	-764	-758	-763	-734
	Night	-701	-756	-717	-749	-766
	Day	-806	-787	-802	-816	-742
R18 C27	Night/Day	-678	-719	-736	-736	-752
	Night	-600	-707	-685	-685	-734
	Day	-771	-760	-787	-807	-787
R21 C14	Night/Day	-523	-479	-613	-616	-661
	Night	-586	-552	-676	-697	-761
	Day	-534	-495	-615	-639	-670
R29 C22	Night/Day	-647	-660	-693	-708	-720
	Night	-658	-678	-687	-763	-747
	Day	-679	-672	-716	-712	-758

TABLE C-4

CORRELATION COEFFICIENT ($\times 1000$) BETWEEN THE VERTICALLY
POLARIZED NORMALIZED BRIGHTNESS TEMPERATURE AND API
BETWEEN 25 OCT 1978 AND 10 NOV 1979

<u>GRID</u> <u>CELL</u>	<u>DATA</u>	<u>CHANNEL</u>				
		<u>0.81V</u>	<u>1.35V</u>	<u>1.66V</u>	<u>2.80V</u>	<u>4.54V</u>
R03 C27	Night/Day	-418	-585	-658	-696	-723
	Night	-212	-500	-576	-689	-781
	Day	-686	-759	-804	-829	-794
R09 C21	Night/Day	-534	-594	-713	-698	-733
	Night	-487	-539	-679	-709	-804
	Day	-709	-751	-834	-823	-739
R09 C29	Night/Day	-384	-540	-617	-652	-681
	Night	-295	-501	-546	-651	-698
	Day	-641	-733	-788	-812	-779
R15 C29	Night/Day	-499	-579	-674	-659	-656
	Night	-526	-548	-700	-748	-767
	Day	-655	-758	-762	-753	-735
R18 C27	Night/Day	-518	-584	-613	-621	-652
	Night	-462	-534	-544	-566	-660
	Day	-692	-734	-739	-756	-724
R21 C14	Night/Day	-410	-505	-505	-516	-575
	Night	-554	-745	-676	-709	-754
	Day	-454	-494	-525	-560	-587
R29 C22	Night/Day	-359	-446	-519	-562	-479
	Night	-458	-582	-639	-708	-581
	Day	-414	-456	-497	-568	-646

TABLE C-5

CORRELATION COEFFICIENT ($\times 1000$) BETWEEN THE 1.66 CM
TRANSFORMS AND API FOR A JAN-FEB SERIES BETWEEN
25 OCT 1978 AND 10 NOV 1979

<u>GRID CELL</u>	<u>TRANSFORM</u>	<u>MONTHS</u>					
		<u>ALL</u>	<u>MAR- APR</u>	<u>MAY- JUN</u>	<u>JUL- AUG</u>	<u>SEP- OCT</u>	<u>NOV- DEC</u>
R03 C27	Th/T	-844	-892	-905	-806	-848	-733
	Tv-Th	783	856	803	605	735	735
	$[(Tv-Th)/0.5(Tv+Th)]$	806	881	795	616	786	759
	M.L. Reg on All 3	873	919	913	806	953	885
R09 C21	Th/T	-872	-912	-722	-829	-919	-499
	Tv-Th	813	823	615	835	886	538
	$[(Tv-Th)/0.5(Tv+Th)]$	828	824	649	837	910	570
	M.L. Reg on All 3	888	921	740	853	979	718
R09 C29	Th/T	-814	-956	-347	-812	-819	-849
	Tv-Th	750	930	760	718	697	802
	$[(Tv-Th)/0.5(Tv+Th)]$	763	931	778	734	728	819
	M.L. Reg on All 3	820	957	810	858	859	888
R15 C29	Th/T	-761	-915	-504	-526	-926	-659
	Tv-Th	679	851	174	381	872	584
	$[(Tv-Th)/0.5(Tv+Th)]$	702	866	220	380	898	610
	M.L. Reg on All 3	782	925	607	529	956	773
R18 C27	Th/T	-734	-921	-461	-753	-946	-692
	Tv-Th	669	854	315	730	788	680
	$[(Tv-Th)/0.5(Tv+Th)]$	687	859	387	732	827	694
	M.L. Reg on All 3	741	927	781	755	989	740
R21 C14	Th/T	-633	-708	-812	-649	-597	-825
	Tv-Th	584	635	652	681	500	881
	$[(Tv-Th)/0.5(Tv+Th)]$	587	657	676	673	505	892
	M.L. Reg on All 3	638	748	821	698	630	907
R29 C22	Th/T	-704	-633	-704	-789	-700	-667
	Tv-Th	620	612	571	466	647	713
	$[(Tv-Th)/0.5(Tv+Th)]$	635	606	631	497	663	739
	M.L. Reg on All 3	713	681	861	842	757	795

TABLE C-6

CORRELATION COEFFICIENT (x1000) BETWEEN THE 1.66 CM
TRANSFORMS AND API FOR A FEB-MAR SERIES BETWEEN
25 OCT 1978 AND 10 NOV 1979

<u>GRID</u> <u>CELL</u>	<u>TRANSFORM</u>	<u>MONTHS</u>					
		<u>ALL</u>	<u>FEB-</u> <u>MAR</u>	<u>APR-</u> <u>MAY</u>	<u>JUN-</u> <u>JUL</u>	<u>AUG-</u> <u>SEP</u>	<u>OCT-</u> <u>NOV</u>
R03 C27	Th/T	-844		-813	-734	-728	-800
	Tv-Th	783		704	631	376	735
	$[(Tv-Th)/0.5(Tv+Th)]$	806		731	651	381	770
	M.L. Reg on All 3	873		849	765	730	891
R09 C21	Th/T	-872		-896	-790	-640	-868
	Tv-Th	813		836	811	297	802
	$[(Tv-Th)/0.5(Tv+Th)]$	828		841	819	300	832
	M.L. Reg on All 3	888		897	841	643	951
R09 C29	Th/T	-814		-220	-823	-689	-808
	Tv-Th	750		374	810	547	674
	$[(Tv-Th)/0.5(Tv+Th)]$	763		386	822	548	703
	M.L. Reg on All 3	820		431	866	781	854
R15 C29	Th/T	-761	-744	-442	-422	-799	-836
	Tv-Th	679	728	263	208	755	739
	$[(Tv-Th)/0.5(Tv+Th)]$	702	753	290	202	757	762
	M.L. Reg on All 3	782	787	502	463	811	878
R18 C27	Th/T	-734	-666	-558	-804	-939	-855
	Tv-Th	669	611	475	767	894	715
	$[(Tv-Th)/0.5(Tv+Th)]$	687	622	503	774	902	749
	M.L. Reg on All 3	741	671	634	806	942	872
R21 C14	Th/T	-633	-649	-728	-683	-651	-842
	Tv-Th	584	558	456	538	658	856
	$[(Tv-Th)/0.5(Tv+Th)]$	587	578	480	565	637	866
	M.L. Reg on All 3	638	681	791	781	708	890
R29 C22	Th/T	-704	-694	-686	-796	-887	-732
	Tv-Th	620	853	479	487	708	755
	$[(Tv-Th)/0.5(Tv+Th)]$	635	845	548	523	722	762
	M.L. Reg on All 3	713	854	792	796	891	780

VITA

Gregory Delfin Wilke was born and raised in Southern Minnesota. He received his B. G. S. and M. S. degree's in Geography from the University of Nebraska Omaha, in 1976 and 1977 respectively. He was awarded a commission in the USAF in May 1977, and entered the Basic Meteorology Program at Texas A&M University in January 1978. Upon completion of the program in December 1978, he was assigned to Kapaun A. S. Germany and served as a Forecast Center Team Chief at the European Forecast Unit. He was reassigned to Texas A&M University in September 1981 to pursue an M. S. degree in Meteorology. His permanent address is Route 1, Lewisville, Minnesota.

